NOAA Technical Report NOS 80

Circulation and Hydrodynamics of the Lower Cape Fear River, North Carolina

Rockville, Maryland
August 1979

U.S. DEPARTMENT OF COMMERCE
National Oceanic and Atmospheric Administration
National Ocean Survey

NOAA TECHNICAL REPORTS

National Ocean Survey Series

...vey (NOS) provides charts and related information for the safe navigation of ...e. The survey also furnishes other Earth science data--from geodetic, hydro-..., gravimetric, and astronomic surveys, observations, investigations, and mea-...ife and property and to meet the needs of engineering, scientific, defense, ...ial interests.

... reports deal with new practices and techniques, the views expressed are those of the authors ... necessarily represent final survey policy. NOS series NOAA Technical Reports is a continuation of, and retains the consecutive numbering sequence of, the former series, Environmental Science Services Administration (ESSA) Technical Reports Coast and Geodetic Survey (C&GS), and the earlier series, C&GS Technical Bulletins.

Microfiche for the following reports is available from the National Technical Information Service (NTIS), U.S. Department of Commerce, Sills Bldg., 5285 Port Royal Road, Springfield, VA 22161. (NTIS accession numbers given in parentheses.) Write to source for price.

NOAA TECHNICAL REPORTS

NOS 41 A user's guide to a computer program for harmonic analysis of data at tidal frequencies. R. E. Dennis and E. E. Long, July 1971. (COM-71-50606)

NOS 42 Computational procedures for the determination of a simple layer model of the geopotential from Doppler Observations. Bertold U. Witte, April 1971. (COM-71-50400)

NOS 43 Phase correction for sun-reflecting spherical satellite. Erwin Schmid, August 1971. (COM-72-50080)

NOS 44 The determination of focal mechanisms using P- and S-wave data. William H. Dillinger, Allen J. Pope, and Samuel T. Harding, July 1971. (COM-71-50392)

NOS 45 Pacific SEAMAP 1961-70 Data for Area 15524-10: Longitude 155°W to 165°W, Latitude 24°N to 30°N, bathymetry, magnetics, and gravity. J. J. Dowling, E. E. Chiburis, P. Dehlinger, and M. J. Yellin, January 1972. (COM-72-51029)

NOS 46 Pacific SEAMAP 1961-70 Data for Area 15530-10: Longitude 155°W to 165°W, Latitude 30°N to 36°N, bathymetry, magnetics, and gravity. J. J. Dowling, E. F. Chiburis, P. Dehlinger, and M. J. Yellin, January 1972. (COM-73-50145)

NOS 47 Pacific SEAMAP 1961-70 Data for Area 15248-14: Longitude 152°W to 166°W, Latitude 48°N to 54°N, bathymetry, magnetics, and gravity. J. J. Dowling, E. F. Chiburis, P. Dehlinger, and M. J. Yellin, April 1972. (COM-72-51030)

NOS 48 Pacific SEAMAP 1961-70 Data for Area 16648-14: Longitude 166°W to 180°, Latitude 48°N to 54°N, bathymetry, magnetics, and gravity. J. J. Dowling, E. F. Chiburis, P. Dehlinger, and M. J. Yellin, April 1972. (COM-72-51028)

NOS 49 Pacific SEAMAP 1961-70 Data for Areas 16530-10 and 17530-10: Longitude 165°W to 180°, Latitude 30°N to 36°N, bathymetry, magnetics, and gravity. E. F. Chiburis, J. J. Dowling, P. Dehlinger, and M. J. Yellin, July 1972. (COM-73-50173)

NOS 50 Pacific SEAMAP 1961-70 Data for Areas 16524-10 and 17524-10: Longitude 165°W to 180°, Latitude 24°N to 30°N, bathymetry, magnetics, and gravity. E. F. Chiburis, J. J. Dowling, P. Dehlinger, and M. J. Yellin, July 1972. (COM-73-50172)

NOS 51 Pacific SEAMAP 1961-70 Data for Areas 15636-12, 15642-12, 16836-12, and 16842-12: Longitude 156°W to 180°, Latitude 36°N to 48°N, bathymetry, magnetics, and gravity. E. F. Chiburis, J. J. Dowling, P. Dehlinger, and M. J. Yellin, July 1972. (COM-73-50280)

NOS 52 Pacific SEAMAP 1961-70 data evaluation summary. P. Dehlinger, E. F. Chiburis, and J. J. Dowling, July 1972. (COM-73-50110)

NOS 53 Grid calibration by coordinate transfer. Lawrence Fritz, December 1972. (COM-73-50240)

NOS 54 A cross-coupling computer for the Oceanographer's Askania Gravity Meter. Carl A. Pearson and Thomas E. Brown, February 1973. (COM-73-50317)

(Continued on inside back cover)

NOAA Technical Report NOS 80

Circulation and Hydrodynamics of the Lower Cape Fear River, North Carolina

Joseph M. Welch
Bruce B. Parker

Office of Oceanography
Circulatory Surveys Branch
Rockville, Md.
August 1979

U.S. DEPARTMENT OF COMMERCE
Juanita M. Kreps, Secretary

National Oceanic and Atmospheric Administration
Richard A. Frank, Administrator

National Ocean Survey
Rear Admiral Allen L. Powell, Director

Mention of a commercial company or product does not constitute an endorsement by NOAA/National Ocean Survey. Use for publicity or advertising purposes of information from this publication concerning proprietary products is not authorized.

CONTENTS

FIGURES

FIGURES (Continued)

TABLES

CIRCULATION AND HYDRODYNAMICS OF THE LOWER CAPE FEAR RIVER, NORTH CAROLINA

Joseph M. Welch
Bruce B. Parker
Office of Oceanography
National Ocean Survey, NOAA
Rockville, Maryland

ABSTRACT.—The results from the harmonic analysis of the data from tide and current stations in the lower Cape Fear River are presented in the form of tables, cotidal and corange charts, and charts illustrating the relationships among various harmonic constituents. Salinity and temperature data are presented in the form of contours of longitudinal transects and time series stations covering full tidal cycles. Instrumentation, data products, and the various methods of analysis are described. The implications from the results of the various methods of analysis of the circulation and hydrodynamics of the lower Cape Fear River are discussed.

A simple one-dimensional model is presented to help describe the tidal hydrodynamics of a long narrow estuary. The nontidal rise and fall of the water surface of the river as a result of the meteorological forces of wind and barometric pressure is discussed. NOS historical data, a physical description of the area, and approximate values of transport through several cross sections are given.

It has been concluded that the tidal wave in the Cape Fear River is close to being a pure damped progressive wave with a partial reflection in the narrowing channel around Wilmington, N.C. The considerable amount of dredging that has taken place in the past 100 years has resulted in significant physical parameter changes. The flow regime in the Cape Fear River is the result of gravitational effects caused by salinity intrusion, freshwater river flow, the river bathymetry, and channel structure. Salinity data indicate that the river changes from being partially mixed vertically to well mixed vertically as one progresses up the river.

1. INTRODUCTION

1.1. Significance of the Cape Fear River

The area covered by the Cape Fear River Circulatory Survey includes those sections of the Cape Fear and Brunswick Rivers from about 1 nautical mile (nmi) north of Wilmington, N.C., south to the mouth of the Cape Fear River, a distance of about 28 nmi. The study also includes those sections of the Atlantic Intracoastal Waterway (AIWW) contiguous to the Cape Fear River. To better understand the importance of the Cape Fear River and its value to North Carolina, this introduction will include facts about the entire Cape Fear River system, a distance of 198 miles (mi). Figure 1 shows the entire Cape Fear River basin, and figure 2 shows the area covered by the circulatory survey, designated as OPR–500–FE–76, Cape Fear, North Carolina.

Major uses of the river basin include sources of domestic and industrial water supplies; bathing, boating, and other forms of recreation; fish, shellfish, and wildlife propagation; commercial fishing; agriculture, including stock watering and irrigation; electric power production; disposal of sewage and industrial wastes; and navigation (Anonymous, 1957).

As of 1957, the basin had 25 public surface water supplies serving a population of about 380,000 with a rate of consumption of 39.3 million gallons a day (MGD), and 35 communities consuming an average of 9.3 MGD from groundwater sources. Records show that industries used 19.1 MGD from surface supplies

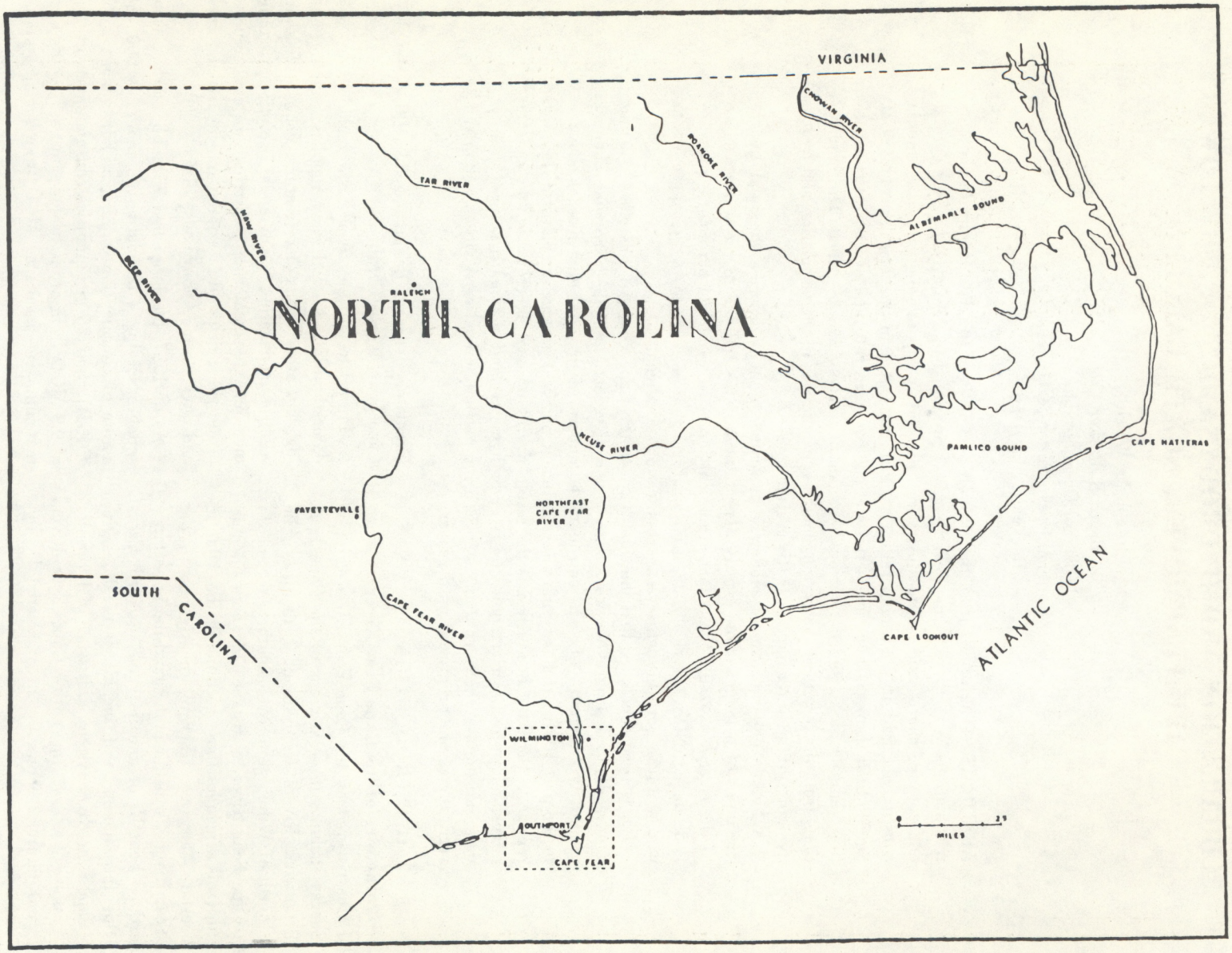

FIGURE 1.—Cape Fear River basin.

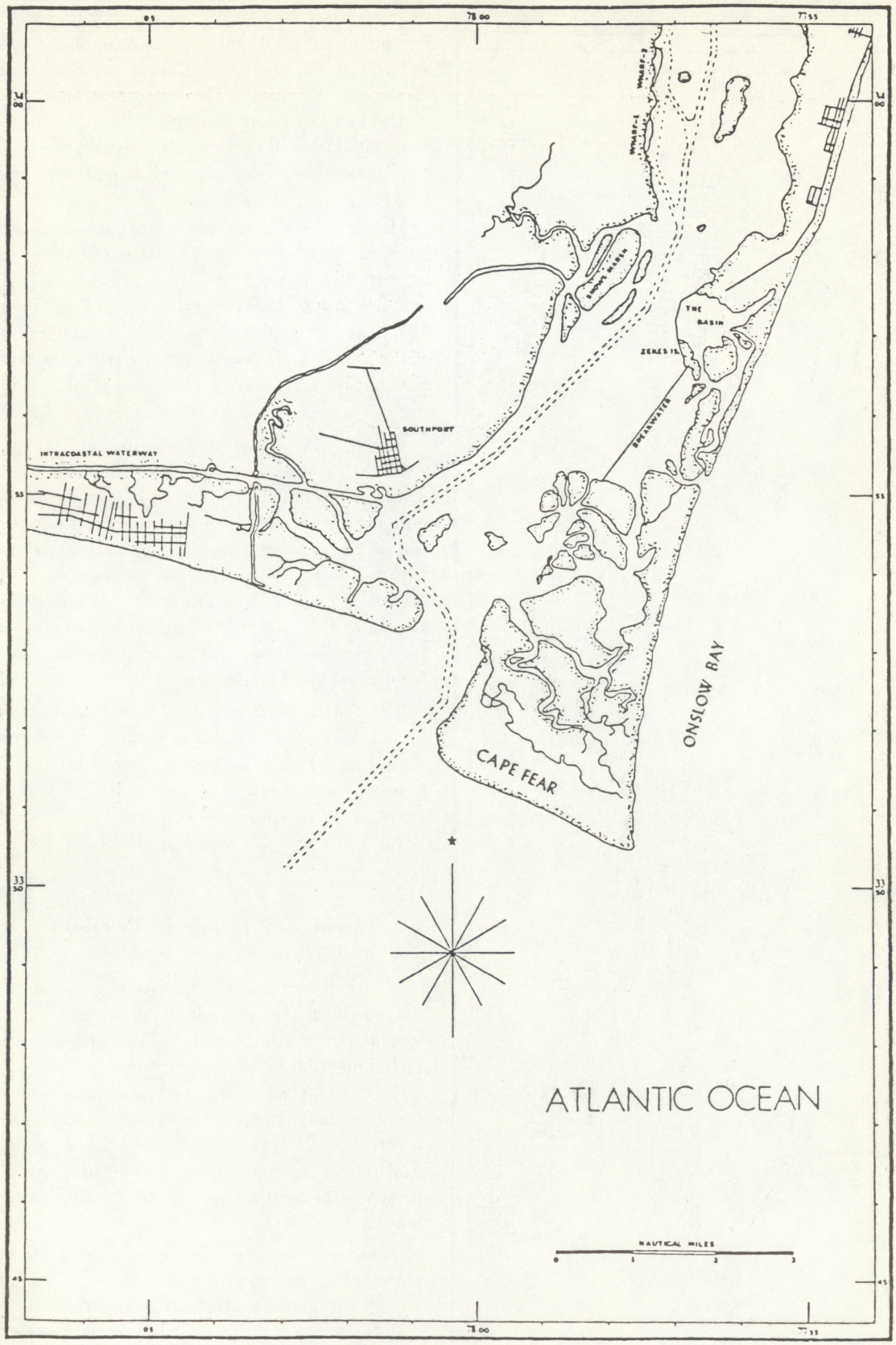

FIGURE 2.—General Survey area.

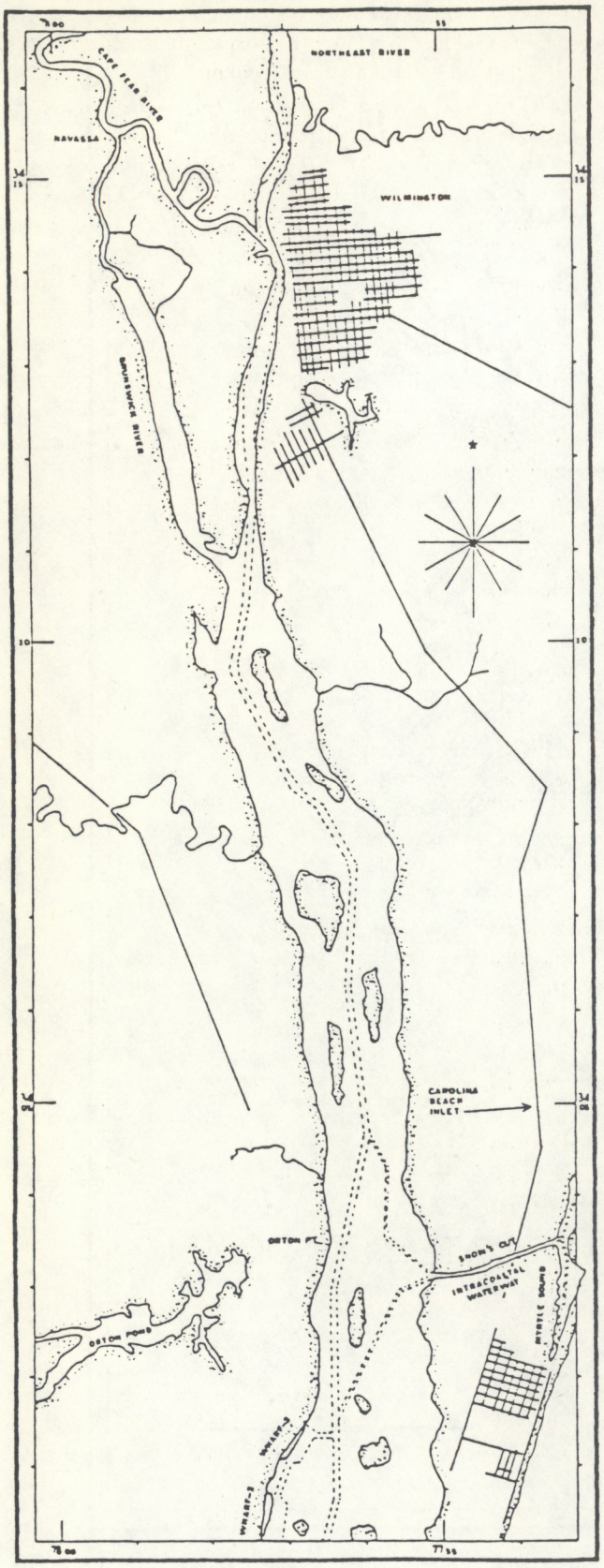

FIGURE 2.—Continued.

and about 1.0 MGD from ground supplies for process water. There were 143 significant sources of pollution throughout the basin. The rate of population growth and industrialization within the basin in the past 20 years indicates that these figures represent only a small part of the demand which is placed on the basin today.

The Cape Fear River Basin is the most industrialized basin in North Carolina. The largest concentrations of industry are on the Haw River, the upper Deep River, and the lower sections of the Cape Fear River (the area covered by this survey). The discharge of partially treated sewage and industrial wastes reportedly has damaged the waters in the areas of heavy industrialization and population (Anonymous, 1957).

The Military Ocean Terminal at Sunny Point (MOTSU), on the west bank of the Cape Fear River about 10 mi north of the river's mouth, is a strategic military port from which ordinance and munitions are shipped all over the world. The Carolina Power and Light Company (CP&L) has recently completed the construction of a nuclear-powered electricity generating plant that will be cooled with water taken from the Cape Fear River in the vicinity of Snows Marsh, 5 mi north of the river entrance.

The estuaries of coastal North Carolina represent one of the State's most valuable natural resources. The Cape Fear River, which opens directly into the Atlantic Ocean, is a dynamic estuarine system. A better understanding of the physical properties of the Cape Fear River will help man to better use this priceless water resource.

1.2. Circulatory Survey, Its Purposes and Its Benefits

A circulatory survey consists of the acquisition of tide, tidal current, salinity, and temperature data at specified depths and locations. Atmospheric parameters including wind speed and direction, sea level pressure, and air temperature are used in conjunction with the survey data to provide an accurate three-dimensional description of water movement in the survey area. Theoretical insight based on the processed data is presented to help clarify the description of the water movement.

Tides are the vertical movement of water resulting from the periodic astronomic-forcing functions. Sea level is a function of the astronomic tides, meteorological forces, and river runoff. Currents are the horizontal movement of water resulting from astronomic forces, winds, density gradients, and river runoff. The

salinity and temperature measurements are used to determine salinity intrusion, density structure, and mixing processes. The meteorological measurements are used to correlate nonperiodic water movement with the forcing functions of wind and atmospheric pressure.

Throughout this report, tables and figures will depict available data on station locations, instrumentation, time periods of occupation, and other pertinent information. Explanations will be given on how to acquire these data and what formats are available to enable the general public, other government agencies, and scientific institutions to obtain these data.

The purposes of the survey are to update tide and tidal current prediction data, redefine and update tidal datums for land movement and shoreline boundary determination, and provide input for all phases of coastal zone management. The data are also applicable to pollution problems, navigation, and coastal engineering. The survey results will provide a valuable foundation for basic oceanographic research in the lower Cape Fear River.

1.3. Physical Characteristics of the Cape Fear River

The Cape Fear River originates in the Piedmont Province of North Carolina at the junction of the Deep and Haw Rivers. It flows southwest through the Coastal Plain Province past Wilmington to the Atlantic Ocean, a distance of about 198 mi. At Wilmington, the Cape Fear River joins the Northeast Cape Fear River (fig. 1).

The Cape Fear River has a drainage area of more than 9,000 mi^2, over a third of which lies in the Piedmont Province. Clay, formed by the *in situ* weathering of underlying rock formations, characterizes the Piedmont Province. The drainage area of the Coastal Plain Province is characterized by low lying sandy terrain and a lower proportion of clay than is found in the Piedmont Province. The Northeast Cape Fear River has a drainage area of over 1,700 mi^2 and is in the Coastal Plain Province. River discharge rates and freshwater inflow vary from month to month and from year to year.

A detailed physical description of the Cape Fear River will be given only for that portion covered by this report. The lower Cape Fear contains many islands, tidal flats, and spoil areas. The principle feature of the study area is the dredged ship channel that runs from across the outer river bar to Fayetteville, N.C., about 100 mi upriver from Wilmington. The channel, which can be seen in figure 2, is not a natural channel. The U.S. Army Corps of Engineers has dredged and maintained the channel.

The project width and depth (at mean low water, MLW) for the channel from across the bar to Southport are 500 feet (ft) and 40 ft respectively. The project width and depth from Southport to the junction of the southern end of the Brunswick River and the Cape Fear River are 400 ft and 38 ft respectively. There is no maintained channel in the Brunswick River. The project dimensions from where the southern end of the Brunswick River and the Cape Fear River join, to the junction of the Cape Fear River and Northwest Cape Fear River are from 300 to 1,100 ft wide and 38 ft deep. From Wilmington to Navassa, the junction of the Cape Fear River and the northern end of the Brunswick River, the project dimensions are 160 ft wide and 11 ft deep. In the Northeast Cape Fear River, from Wilmington to the end of the project, the channel width varies from 200 to 800 ft and the depth varies from 25 to 32 ft. The Atlantic Intracoastal Waterway, which crosses the Cape Fear, has a project depth of 12 ft. Recent surveys have shown that the project dimensions are reasonably close, the differences being a result of natural shoaling processes that are periodically corrected through dredging. Table 1 is a chronological history of navigation-related developments for the lower Cape Fear River (U.S. Army Corps of Engineers, 1976).

The average width of the lower Cape Fear is from 1 to 2.5 mi up to the point where the southern end of the Brunswick River joins the Cape Fear River. The Brunswick River is about 0.30 mi across for the lower two-thirds and 0.06 mi across for the upper third. The Cape Fear River from the southern end of the Brunswick River to the junction of the Northeast Cape Fear River at Wilmington ranges in width from 0.10 mi to 0.30 mi. The Northeast Cape Fear River has a width of 0.15 mi within the survey area. From Wilmington to Navassa, the river width is about 0.10 mi.

Figure 3 shows the locations of the cross sections shown in figure 4. The obvious feature in each of the cross sections is the ship channel. This report will show that the water movement in the study area is concentrated along this main channel. Other physical features of the study area that have to be considered are the complex channel structure around MOTSU (Wharfs 1, 2, and 3); the Intracoastal Waterway west of Southport and at Snows Cut, which joins the Cape Fear River and Myrtle Sound; and the intake canal for CP&L's nuclear-powered electricity generating plant located west of Snows Marsh.

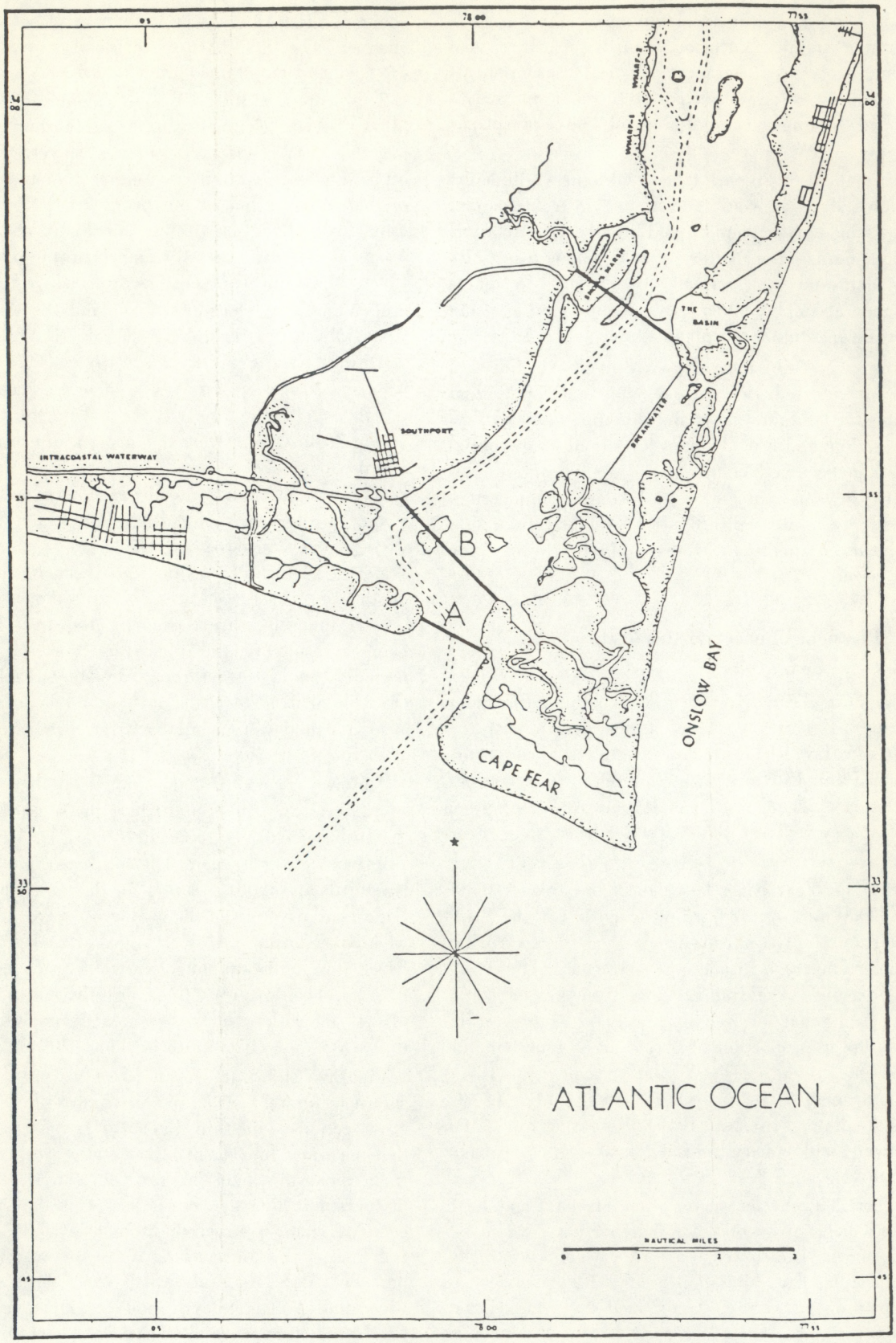

FIGURE 3.—Cross section locations.

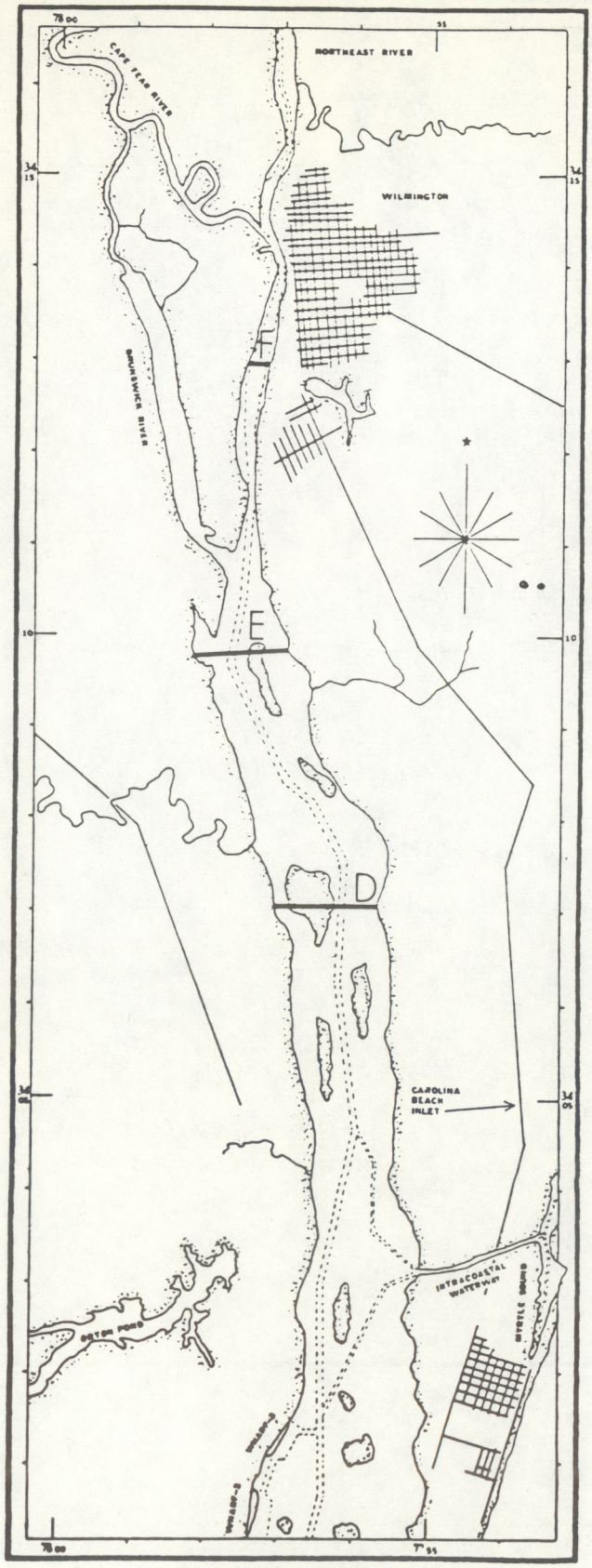

FIGURE 3.—Continued.

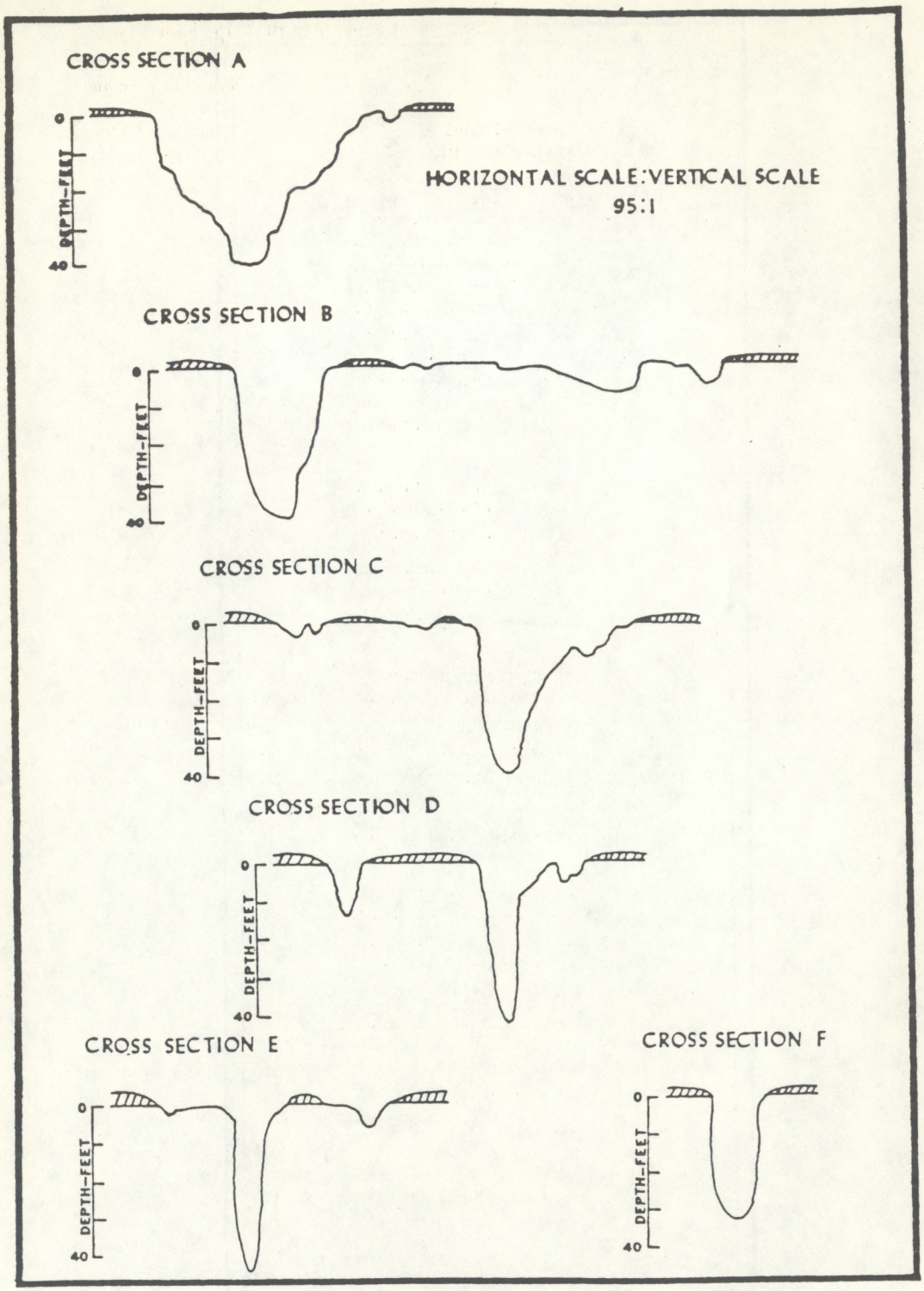

FIGURE 4.—Cross section bottom profiles.

TABLE 1.—Chronology of navigational developments in the Cape Fear River

Date Work Completed	Description of Work in Lower Cape Fear River	Ocean Entrance and River Channel, Depth and Width (Low Water Datum)
		Feet
1829–1889	Several engineering works undertaken to increase the depths of the lower Cape Fear River for navigation. Improvements included: (a) construction of contraction jetties in the 8-mile river reach immediately below Wilmington; (b) closure of New Inlet through the construction of New Inlet Dam; and (c) dredging of the river channel shoals. River's navigation channel between the ocean entrance and Wilmington developed to a depth of 16 feet and a width of 270 feet by 1889.	16 by 270 river channel (by 1889)
1907	River channel dimensions increased to a depth of 20 feet and width of 270 feet by dredging. Mooring basin excavated at Wilmington.	20 by 270 river channel
1913	Ocean entrance channel dredged to a depth of 26 feet and width of 400 feet. River channel dredged to a depth of 26 feet and width of 300 feet to Wilmington.	26 by 400 ocean entrance 26 by 300 river channel
1916	Anchorage basin dredged at Wilmington, having a length of about 2,000 feet, a width of about 1,000 feet, and a depth of 26 feet.	26 by 400 ocean entrance 26 by 300 river entrance
1926	Ocean entrance channel dredged to a depth of 30 feet and a bottom width of 400 feet.	30 by 400 ocean entrance 26 by 300 river channel
1930	Excavation of Snows Cut connected at Atlantic Intracoastal Waterway (AIWW) with Cape Fear River.	30 by 400 ocean entrance 26 by 300 river channel
1932	River channel dimensions increased by dredging to a depth of 30 feet and bottom width of 300 feet. A turning basin having a width of about 600 feet excavated at Wilmington. Work accomplished between 1931 and 1932.	30 by 400 ocean entrance 30 by 300 river channel
1948	River channel extended 1.25 miles north of Wilmington for the Hilton railroad bridge to an upstream point in the Northeast Cape Fear River. Extension had channel depth of 25 feet and bottom width of 200 feet. Work accomplished in winter of 1948.	30 by 400 ocean entrance 30 by 300 river channel to Hilton Bridge 25 by 200 river channel above Hilton Bridge
1949	Ocean entrance and river channel dimensions increased to a depth of 32 feet and bottom width of 400 feet. Work accomplished between 1947 and 1949.	32 by 400 ocean entrance 32 by 400 river channel to Wilmington
1952	Carolina Beach Inlet opened through barrier beach by earth-moving equipment and explosives. Work accomplished summer 1952.	32 by 400 ocean entrance 32 by 400 river channel
1955	Navigation facilities dredged at Military Ocean Terminal Sunny Point. Basins dredged to a width of 800 feet and depth of 34 feet. Entrance channels dredged to a width of 300 feet and depth of 34 feet. Work accomplished between 1953 and 1955.	32 by 400 ocean entrance 32 by 400 river channel to Wilmington

TABLE 1—Continued

Date Work Completed	Description of Work in Lower Cape Fear River	Ocean Entrance and River Channel, Depth and Width (Low Water Datum)
		Feet
1958	Ocean entrance dimensions increased to depth of 35 feet and bottom width of 400 feet. River channel dimensions to Wilmington increased to a depth of 34 feet and bottom width of 400 feet. Work accomplished between 1956 and 1958.	35 by 400 ocean entrance 34 by 400 river channel to Wilmington
1970	River channel dimension increased to a depth of 38 feet and bottom width of 400 feet. Work accomplished between 1965 and 1970.	35 by 400 ocean entrance 38 by 400 river channel to Wilmington
1971	Ocean entrance channel dimensions increased to a depth of 40 feet and width of 500 feet. Work accomplished between 1970 and 1973.	40 by 500 ocean entrance 38 by 400 river channel

Source: 1976. U.S. Army Corps of Engineers, Wilmington District, N.C.

2. TIDE DATA, DESCRIPTION AND ANALYSIS

2.1. Locations of Tide Gages and Installation Information

Personnel from the Wilmington District of the U.S. Army Corps of Engineers installed the tide gages between Zekes Island and Orton Point. A National Ocean Survey (NOS) tide party from the National Oceanic and Atmospheric Administration's (NOAA) Atlantic Marine Center (AMC) in Norfolk, Va., installed the control tide station at Wilmington. Personnel from the NOAA Ship FERREL put in the remaining gages.

Prior to each station installation, a reconnaissance of the proposed site was made to determine if the site was feasible and to recover any historic bench marks that might have been in the area. During the gage installation, additional bench marks were put in to bring the total for each gage to a minimum of five. Differential levels were run between the bench marks and tide staff during gage installation and removal to ascertain if there had been any staff movement and to establish reliable tidal datums.

For the purpose of this report, tide stations will be designated by the letter "*T*" followed by a two-digit number, for example T–00. Figure 5 shows the locations of the tide stations occupied during this study. Table 2 gives the following information for each station: circulatory study station number, geographic location, latitude and longitude, NOS station number, dates of occupation, and type of gage. Each station was occupied for a minimum of 29 days; and two stations, Wilmington (T–11) and Southport (T–02), part of the NOS vertical control network, are long-term control stations that have been in operation for many years. The tide stations were installed close to the current station deployments to get a more reliable comparison between the two physical parameters. The concentration of six gages around MOTSU (Wharfs 1, 2, and 3) is necessary to understand better the water movement in the vicinity of the complex channel configuration.

2.2. Instrumentation, Data Processing, and Output

Analog-to-digital recorder (ADR) tide gages were used for the Cape Fear River Circulatory Survey. The gage employs mechanical means to convert angular positions of a rotating shaft into coded binary digital output, the shaft rotation being a function of the rise and fall of the water level. Figure 6 shows a typical station installation, and table 3 gives the ADR gage specifications.

The ADR gage records 10 samples per hour at 6-minute intervals, the data being output onto foil-backed paper tape. The data are processed by means of a mechanical translator and computer procedures, each step being closely monitored by NOS personnel. An abbreviated processing synopsis includes the following steps: (1) visually inspecting the tape for mechanical deficiencies; (2) putting the 6-minute samples onto computer-compatible magnetic tape; (3)

TABLE 2.—Tide stations occupied during the Cape Fear River Circulatory Survey

Circulatory Survey Station Number	Station	Latitude (N)	Longitude (W)	NOS Station No.	Dates of Observation [2]	Type [3] of Gage
T-01	Bald Head [1]	33°52.8'	78°00.1'	865-8901	25 May 1976 - July 1976	ADR
T-02	Southport [1]	33°55.0'	78°01.1'	865-9084	9 May 1976 - Present	ADR
T-03	Reaves Point Channel	33°58.6'	77°56.7'	865-8681	8 March 1976 - 16 July 1976	ADR
T-04	Lower Midnight Channel	34°00.0'	77°56.4'	865-8630	3 March 1976 - 16 July 1976	ADR
T-05	MOTSU Wharf No. 2	34°00.2'	77°57.3'	865-8622	3 March 1976 - 19 July 1976	ADR
T-06	Upper Midnight Channel	34°01.2'	77°56.1'	865-8587	3 March 1976 - 11 June 1976	ADR
T-07	Orton Point [1]	34°03.4'	77°56.4'	865-8501	8 March 1976 - 16 July 1976	ADR
T-08	Marker 43A Campbell [1]	34°07.6'	77°56.2'	865-8348	19 May 1976 - 19 June 1976	ADR
T-09	Exxon Pier	34°10.6'	77°57.3'	865-8235	7 May 1976 - 18 June 1976	ADR
T-10	Zekes Island	33°57.0'	77°57.1'	865-8741	3 March 1976 - 16 July 1976	ADR
T-11	Wilmington [1]	34°13.6'	77°57.2'	865-8120	1887 - Present	ADR
T-12	Ideal Cement Pier	34°15.3'	77°57.0'	865-8062	8 May 1976 - 18 June 1976	ADR
T-13	Snows Cut	34°03.4'	77°54.1'	865-8503	7 May 1976 - 19 June 1976	ADR
T-14	MOTSU Wharf No. 3	34°01.4'	77°56.8'	865-8579	8 January 1976 - 16 July 1976	ADR
T-15	Navassa	34°15.6'	77°59.3'	865-8052	8 May 1976 - 18 June 1976	ADR
T-16	N.C. Dept. Trans. Dock	34°13.9'	77°59.2'	865-8112	11 May 1976 - 18 June 1976	ADR
T-19	MOTSU Wharf No. 1	33°59.4'	77°57.0'	865-8654	3 March 1976 - 19 July 1976	ADR
T-21	Oak Island Bridge	33°55.3'	78°04.3'	865-9161	9 May 1976 - 19 June 1976	ADR
T-22	Myrtle Sound	34°04.0'	77°53.3'	865-8488	7 May 1976 - 19 June 1976	ADR

[1] Station has been occupied prior to this survey; see section 6.2.

[2] Only the original installation date for station is given. Only the most recent gage type is given. Breaks in the data series are not indicated.

[3] Analog-to-digital recorder (ADR) gage is described in section 2.2 and in table 3.

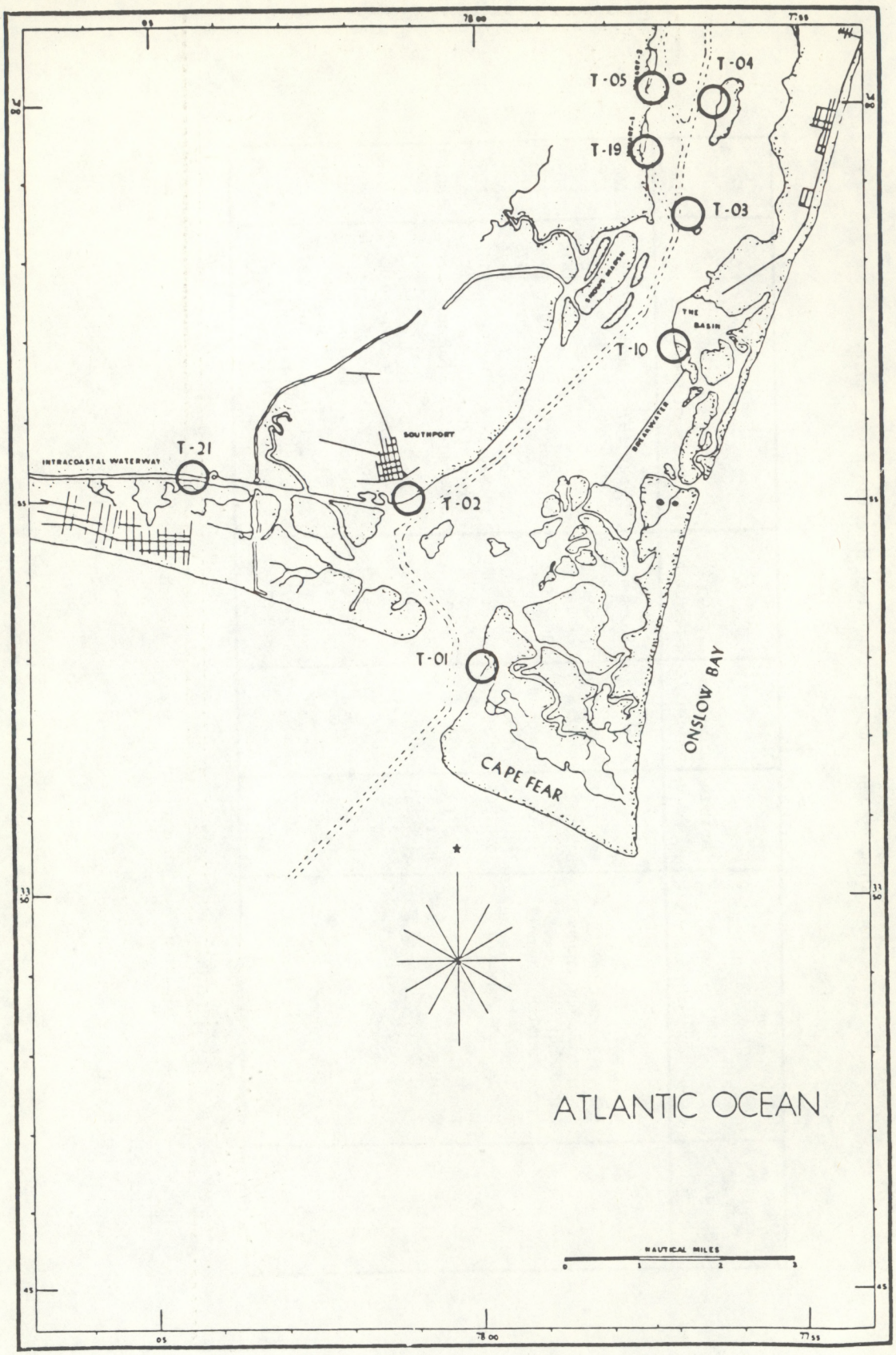

FIGURE 5.—Tide station locations.

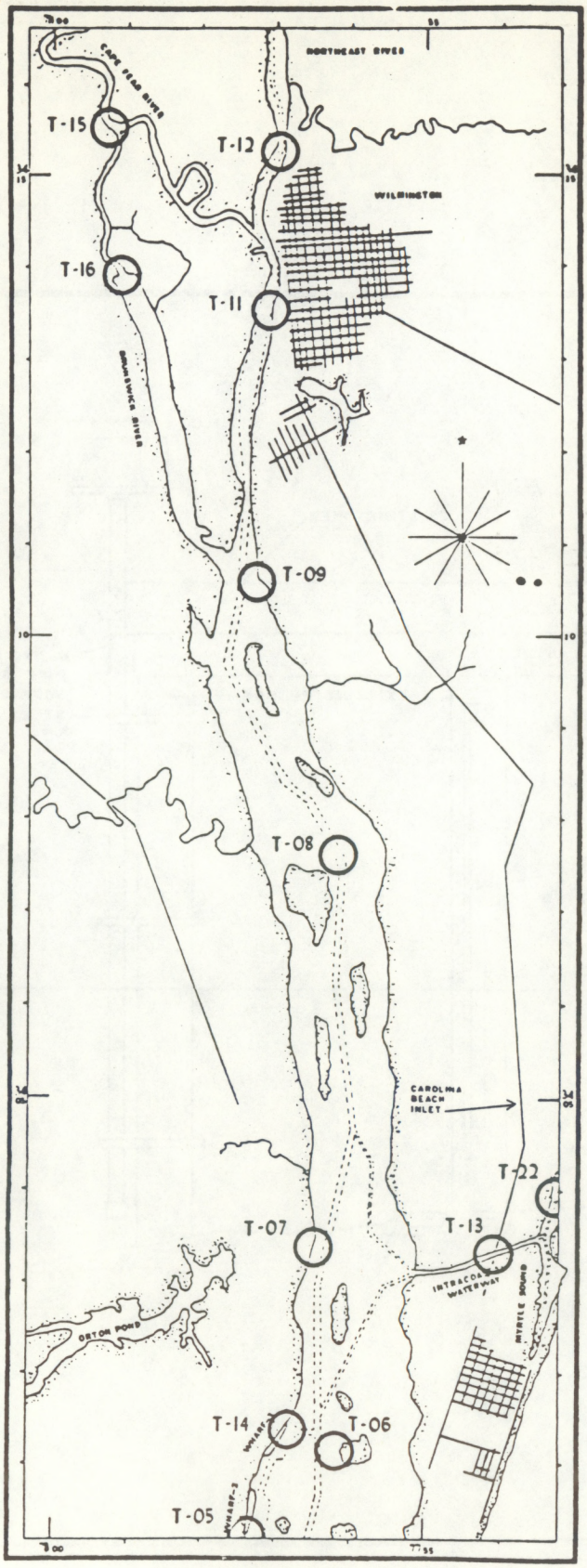

FIGURE 5.—Continued.

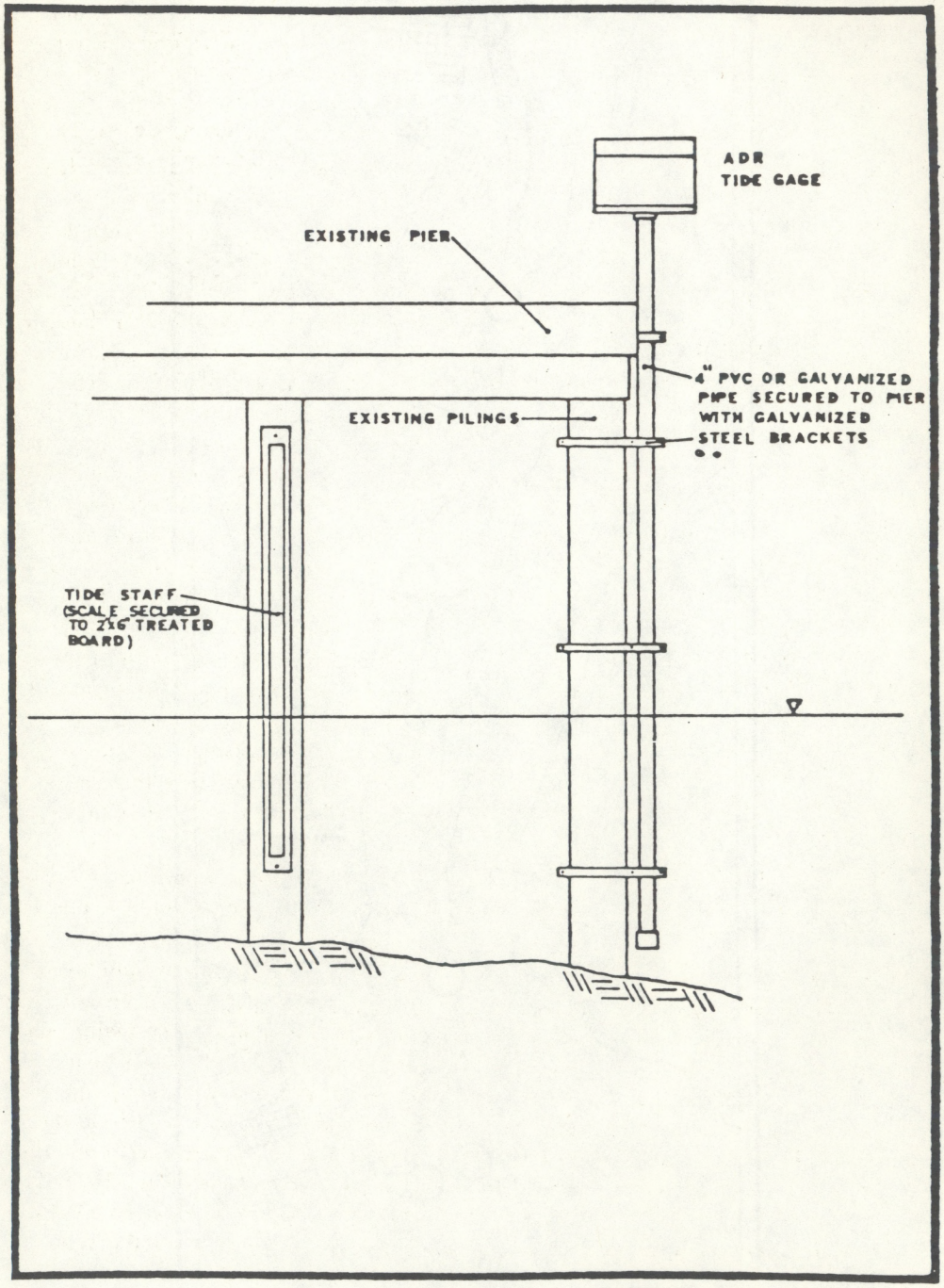

FIGURE 6.—Typical ADR tide gage installation.

TABLE 3.—Tide gage specifications

Analog-to-digital recorder (ADR)
Manufacturer: Fischer-Porter
Range: 0–99.99 feet
Precision: ±½ binary count
Recorder: Foil-backed paper tape (punch)
Record Format: Binary-decimal code
Sampling Rate: Six-minute intervals
Duration: Chart—3 months
Chart drive, battery—3 months
Processing: Mechanical translator
Mode of operation: Float movement is translated into binary code and recorded on paper tape

deriving hourly values from these 6-minute samples and storing them on cards, tape, and tabulated forms; and (4) tabulating high and low waters, various tidal datums (mean high water, mean low water, mean sea level, etc.), Greenwich intervals, and other relevant parameters.

The accuracy of the tabulated tide data is ±0.1 ft and ±0.1 hour. The processed monthly tabulations from each station are verified as to staff-marigram relationship. Equivalent 19-year mean values and tidal datums are computed for each station through simultaneous comparison with the appropriate tide control station (Wilmington, T–11). Tidal bench mark elevations are established by referencing the bench marks to the computed tidal datums.

For information regarding available data products, costs, specific available data, and any other pertinent information, address requests as fellows:

Associate Director,
Office of Oceanography
NOAA, National Ocean Survey
6001 Executive Blvd.
Rockville, MD 20852

When referring to the Cape Fear River tide stations, one should use the NOS station numbers, because they are the official station identification numbers.

2.3. Methods of Analysis

The following methods were used to analyze the tide data from each of the stations in table 2: (1) harmonic analysis, (2) spectral analysis including filtering techniques, and (3) computed parameters adjusted to accepted long-term control station parameters. Each of these techniques will be discussed in this section, and section 2.4 will present the results from the different methods of analysis.

Two methods of harmonic analysis were used for the Cape Fear River tide data, and a third method, the tidal response method, is used by NOS but not for this study. The method used for record lengths in excess of one half year is a least-squares harmonic analysis using a computer program based on Harris, Pore, and Cummings (1963). The other method used is for record lengths of 29 days, which is a Fourier harmonic analysis program (an updated version of Dennis and Long (1971), based on Schureman (1958)). The results of the Fourier method are then adjusted to the least-squares method (Parker, 1977).

In the Cape Fear River, Wilmington (T–11) was the only long-term station; therefore, the other stations were harmonically analyzed by using the 29-day Fourier method. The only constants that can be calculated for 29 days are M_2, S_2, N_2, K_1, O_1, some higher harmonics (M_4, M_6, etc.), and a few other small magnitude constants. Other constituents are either too close in frequency or their periods are too long to be separated out in 29 days. For example, K_2 and S_2 have speeds (angular frequency) of 30.0821372°/solar hour and 30.0000000°/solar hour respectively. Because their frequencies are so close, it takes 182.621 days (the synodic period) of data to separate the two constituents. The constituents *Mf*, *MSf*, *Mm*, *Sa*, and *Ssa* have periods that are so great that they can not repeat themselves adequately in 29 days. Formulas derived and described in Schureman (1958), based on equilibrium theory, are incorporated into the 29-day analysis computer program to try to correct for the contributions of nearby frequencies. Schureman (1958) presents a table and explanation of formulas used to infer values of constituents from nearby constituents that could not be separated out directly in the 29-day analysis. For example, the amplitude of K_2 is about 0.272 times the amplitude of S_2, and the epoch (phase lag) is approximated by $S_2° + 0.081 (S_2° - M_2°)$. The "°" refers to the epoch of the constituent.

Equilibrium theory is based on ideal theoretical conditions that at best may be approached in the open ocean. The inference equations and correction formulas, which are based on equilibrium theory, are not going to be as accurate in an estuary as in the open ocean. If the values of the major constituents derived directly are large compared to the values of the inferred constituents, then this problem is probably negligible. In the Cape Fear River, the value of the M_2 constituent is so large, nearly five times the value of the next largest constituent (N_2, Wilmington) and 24 times the value of the inferred constituent, P_1, that the effects of the estuary on the values of the inferred constituents will be assumed negligible.

As stated earlier, a least-squares analysis is used

for tide records in excess of one half year to harmonically analyze the data. The least-squares method is employed, and the harmonic constants are derived by the use of a multiple-correlation screening process that can be terminated when the regression equation contains a specified number of terms or when the next constituent will not explain a predetermined fraction of the variance. The output from the computer program is a listing of 37 harmonic constants routinely used by NOS.

Parker (1977) devised a method to adjust the results from a 29-day Fourier harmonic analysis to the results from a 365-day least-squares harmonic analysis. For each Cape Fear River tide station that was analyzed for 29 days, the time period for the analyses was the same within a few days. A 29-day analysis was performed on the control station data for the same time period covered by the 29-day analyses for the short-term stations. The resulting harmonic constants from the 29-day analysis of the control station data were compared to the constants from the year analysis, and the ratio of the 1-year amplitude to the 29-day amplitude for each constituent was then applied as a correction factor to each respective constituent amplitude of the short-term stations. The difference between the 1-year epoch and the 29-day epoch for each constituent also was used as a correction factor for each respective constituent epoch of the short-term stations. Tests have shown that this correction method is reasonably accurate. If two stations are close together and are occupied for the same time period, then the astronomic conditions during this time period should affect each harmonic constituent similarly. In the Cape Fear River, all of the tide stations are within 25 miles of each other; therefore, it is assumed that the basin effect is similar for each station.

So far this discussion has assumed that the yearly values are perfectly accurate. In reality, there is some variability from year to year in the harmonic constants, but this variability is quite small and can be ignored assuming that there has not been some significant hydrographic or meteorological change during the year. Table 4 shows the correction factors for the eight constituents that will be used for this report.

Program CURNT (Parker, 1975) is a multipurpose time-series analysis program that makes use of the FESTSA (1972) software package. The program options employed for the Cape Fear River tide data include an hourly plot of the demeaned original tide data superimposed over an hourly plot of the filtered-data series, and power spectrum plots (by Tukey's method) of the original, filtered, and residual time series. A Doodson 39-hour low pass filter was used to remove effectively the tide from the original time series to get a better understanding of the nontidal series. The filter removes 99.79 percent of all diurnal frequencies and 99.48 percent of all semidiurnal frequencies (Groves, 1955).

Adjusting tabulated tidal parameters to accepted long-term control station parameters, mentioned earlier in section 2.2, is done by simultaneously comparing times and heights of high and low waters of a subordinate station to the corresponding values from the project control station. Correction factors are derived and applied to the long-term control station parameters to obtain corrected values for the subordinate station. This process effectively relates each subordinate tide station to a common control station.

2.4. Results of Analysis

The eight harmonic constituents; M_2, S_2, N_2,O_1, P_1, M_4, and M_6; are presented in table 6 for the tide stations in figure 5. The constituents; M_2, S_2, N_2, K_1, O_1, and P_1; are the six largest constituents, and the M_4 and M_6 constituents are given because of their importance and interest as shallow water constituents. Table 5 presents the 37 constituents from the 1-year analysis of Wilmington to show the relative importance and magnitude of each compared to the constituents shown in table 6. The constituents in table 6 have been adjusted using the correction factors in table 4 based on the results of table 5. An explanation for each constituent including its astronomic cause and mathematical derivation can be found in Schureman (1958).

All constituent amplitudes, H, are given in feet; and all epochs, indicated by κ' are given in degrees and are relative to the 75°W time meridian. It takes the Sun 5 hours to pass over the 75°W meridian after passing over the Greenwich meridian. The κ' epoch, also referred to as g, is related to κ (the epoch relative to the station's longitude) and G (the epoch relative to the Greenwich meridian) by the following formulas (Schureman, 1958):

$$\kappa'(g) = \kappa + pL - \frac{as}{15}$$

$$= G - \frac{as}{15}$$

where p = the subscript of the constituent
L = the longitude of the tide station (in degrees reckoned west from Greenwich)

TABLE 4.—Correction factors for the 29-day period. 19 May 1976 to 16 June 1976. using Wilmington as the reference station

M_2		S_2		N_2	
$\frac{H_{yr}}{H_{29}}$	$(\kappa'_{yr}-\kappa'_{29})$	$\frac{H_{yr}}{H_{29}}$	$(\kappa'_{yr}-\kappa'_{29})$	$\frac{H_{yr}}{H_{29}}$	$(\kappa'_{yr}-\kappa'_{29})$
0.999	1.460	1.074	7.62	0.873	2.84

K_1		O_1		P_1*	
$\frac{H_{yr}}{H_{29}}$	$(\kappa'_{yr}-\kappa'_{29})$	$\frac{H_{yr}}{H_{29}}$	$(\kappa'_{yr}-\kappa'_{29})$	$\frac{H_{yr}}{H_{29}}$	$(\kappa'_{yr}-\kappa'_{29})$
0.818	2.810	1.026	-12.60	0.827	10.00

M_4		M_6	
$\frac{H_{yr}}{H_{29}}$	$(\kappa'_{yr}-\kappa'_{29})$	$\frac{H_{yr}}{H_{29}}$	$(\kappa'_{yr}-\kappa'_{29})$
0.975	6.29	0.902	-5.90

$\frac{H_{yr}}{H_{29}}$ = amplitude from year analysis (1976) divided by amplitude from 29-day analysis (19 May 1976-16 June 1976).

$(\kappa'_{yr}-\kappa'_{29})$ = epoch from year analysis minus epoch from 29-day analysis (in degrees).

*29-day amplitudes and epochs are inferred.

TABLE 5.—Thirty-seven harmonic constants for Wilmington, N.C., 1976

Constituent	Amp. H	Epoch κ′	Constituent	Amp. H	Epoch κ′	Constituent	Amp. H	Epoch κ′
M_2	1.965	281.90	$(2N)_2$	0.021	265.70	Q_1	0.050	155.20
S_2	0.243	311.90	$(OO)_1$	0.017	111.60	T_2	0.024	299.60
N_2	0.393	273.80	λ_2	0.050	259.20	R_2	0.020	175.10
K_1	0.248	154.00	S_1	0.073	125.00	$(2Q)_1$	0.007	233.30
M_4	0.190	98.80	M_1	0.038	202.30	P_1	0.083	161.60
O_1	0.178	168.30	J_1	0.008	211.20	$(2SM)_2$	0.002	151.20
M_6	0.087	213.80	Mm	0.051	17.60	M_3	0.030	279.80
$(Mk)_3$	0.041	273.20	Ssa	0.080	178.50	L_2	0.190	263.80
S_4	0.016	193.40	Sa	0.245	124.70	$(2Mk)_3$	0.041	247.30
$(MN)_4$	0.081	89.80	MSf	0.091	329.20	K_2	0.069	301.60
ν_2	0.086	261.10	Mf	0.054	355.30	M_8	0.015	40.70
S_6	0.004	59.10	ρ_1	0.005	283.50	$(MS)_4$	0.057	112.90
μ_2	0.072	21.70						

H = constituent amplitude in feet.
κ′ = epoch (in degrees) relative to 75°W time meridian.

a = the angular speed of the constituent (in degrees/hour)
S = the longitude of the time meridian (in degrees) (The 15 is 15°/hour.)

In addition to giving the eight major harmonic constituents for each tide station, table 6 gives the station number, the starting date of the analyzed data series, and the number of days of data analyzed for each tide station. Table 6 shows that the dominant contribution to the tidal wave is the M_2 constituent, the main lunar semidiurnal constituent. The next largest constituent is the N_2, the semidiurnal variation caused by the monthly variations in the Moon's distance from Earth. Following the N_2 constituent in magnitude are the S_2, the main solar semidiurnal constituent, and the K_1, which is the diurnal soli-lunar constituent describing variables caused by changes in declination of the Sun and Moon throughout their orbital cycles. The relative magnitude of the M_2 constituent is so great, especially when compared to the diurnal constituents, that in describing the tidal wave the question to ask is to what extent do the other constituents affect the M_2.

In comparing the 37 constituents for Wilmington (T–11), one notices the relatively large amplitudes for the *Sa* and *Ssa* constituents, sometimes called meteorological constituents. Each has a slow rate of angular change, designed to have one cycle and two cycles respectively each year. Because the periods of the constituents are so long, the amplitudes and epochs are usually determined from a number of years of observations. The values in table 5 are based on 1 year of observations; therefore, the *Sa* and *Ssa* results may be unreliable. The epoch of *Sa* divided by 30 denotes the maximum point of the annual variation in sea level in months after the vernal equinox, and the epoch of *Ssa* divided by 60 denotes a semiannual peak in months after the vernal equinox, followed 6 months later by another peak. The individual dates corresponding to the theoretical annual and semiannual sea level variations were checked, and no significant fluctuations could be detected. The months in which these variations theoretically take place are July for

TABLE 6.—Eight harmonic constants for all tide stations

Station Number	Station	Days Analysis	Starting Date	M_2		S_2		N_2		K_1		O_1		P_1		M_4		M_6	
				H	κ´	H	κ´	H	κ´	H	κ´	H	κ´	H	κ´	H	κ´	H	κ´
T-01	Baldhead 865-8901	29	02 June 1976	2.132	217.92	0.350	241.68	0.438	206.60	0.282	123.09	0.214	113.76	0.094	130.69	0.023	101.71	0.029	010.32
T-02	Southport 865-9084	29	18 May 1976	2.016	226.49	0.344	244.27	0.432	217.09	0.265	124.90	0.190	125.42	0.089	132.50	0.004	284.45	0.044	018.54
T-03	Reaves Point Channel 865-8681	29	18 May 1976	1.882	251.19	0.245	276.72	0.391	257.05	0.247	138.72	0.172	143.44	0.083	146.32	0.052	081.93	0.064	065.46
T-04	Lower Midnight Channel 865-8630	29	18 May 1976	1.906	252.00	0.272	270.70	0.385	244.81	0.248	138.85	0.184	143.73	0.083	146.45	0.074	064.82	0.067	073.07
T-05	MOTSU Wharf No. 2 865-8622	29	18 May 1976	1.887	253.43	0.285	271.17	0.401	244.18	0.253	139.75	0.179	145.37	0.084	147.35	0.071	063.96	0.064	082.88
T-06	Upper Midnight Channel 865-8587	29	18 May 1976	1.900	256.03	0.266	280.34	0.416	247.02	0.252	140.81	0.186	147.75	0.084	148.41	0.081	075.52	0.058	089.49
T-07	Orton Point 865-8501	29	18 May 1976	1.914	262.27	0.257	283.14	0.389	254.70	0.250	144.47	0.175	155.07	0.084	152.07	0.089	089.57	0.068	107.35
T-08	Marker 43A Campbell 865-8348	29	21 May 1976	1.931	273.04	0.284	306.09	0.383	261.00	0.275	155.53	0.217	155.92	0.092	163.13	0.112	084.99	0.078	156.48
T-09	Exxon Pier 865-8235	29	17 May 1976	1.951	281.04	0.221	303.16	0.393	273.22	0.245	153.86	0.159	174.33	0.082	161.46	0.178	113.50	0.075	185.78
T-10	Zekes Island 865-8741	29	18 May 1976	1.887	243.56	0.281	264.70	0.413	237.46	0.255	135.87	0.184	138.97	0.085	143.47	0.045	071.53	0.065	056.22
T-11	Wilmington 865-8120	366	01 Jan 1976	1.965	281.90	0.243	311.90	0.393	273.80	0.248	154.00	0.178	168.30	0.083	161.60	0.190	098.80	0.087	213.80
T-12	Ideal Cement Pier 865-8062	29	19 May 1976	1.882	288.90	0.216	315.54	0.357	280.56	0.247	159.91	0.181	178.01	0.083	167.51	0.182	107.41	0.102	232.81
T-13	Snows Cut 865-8508	29	21 May 1976	1.733	250.16	0.294	277.59	0.346	238.87	0.282	142.79	0.241	140.79	0.094	150.39	0.107	042.05	0.024	108.65
T-14	MOTSU Wharf No. 3 865-8579	29	18 May 1976	1.914	255.56	0.266	276.49	0.394	248.27	0.257	141.38	0.182	149.64	0.086	148.98	0.086	068.68	0.063	086.56
T-15	Navassa 865-8052	29	19 May 1976	1.840	293.07	0.220	324.27	0.351	282.63	0.243	162.79	0.182	181.86	0.081	170.39	0.189	112.73	0.107	242.67
T-16	NC Dept. Trans. Dock 865-8112	29	19 May 1976	1.955	286.33	0.241	314.82	0.375	276.85	0.244	156.14	0.176	169.54	0.082	163.74	0.200	110.83	0.105	222.92
T-19	MOTSU Wharf No. 1 865-8654	29	14 May 1976	1.864	251.98	0.235	270.43	0.386	244.35	0.247	141.78	0.185	139.88	0.083	149.38	0.068	047.19	0.058	071.34
T-21	Oak Island Bridge 865-9161	29	21 May 1976	2.043	235.14	0.350	261.98	0.457	227.16	0.317	138.19	0.272	135.71	0.106	145.79	0.020	316.49	0.054	042.36
T-22	Myrtle Sound 865-8488	29	21 May 1976	1.637	239.66	0.289	267.68	0.318	227.99	0.273	135.46	0.240	133.64	0.091	143.06	0.087	018.25	0.002	063.59

H = amplitude of the constituent in feet.
κ´ = epoch (in degrees) of constituent, relative to the 75°W time meridian (+5 hours from Greenwich).

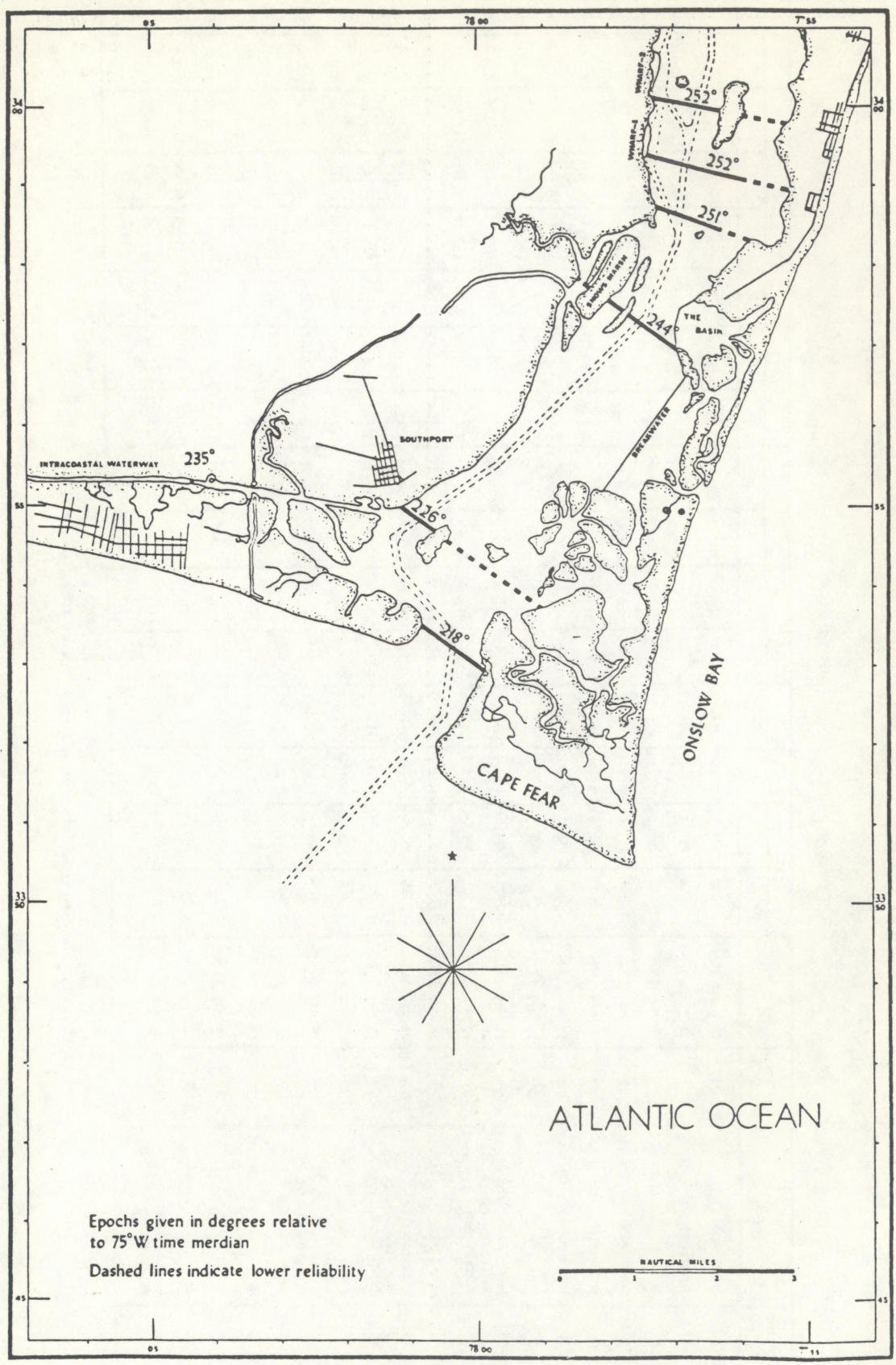

FIGURE 7.—Cotidal lines for M_2 tide.

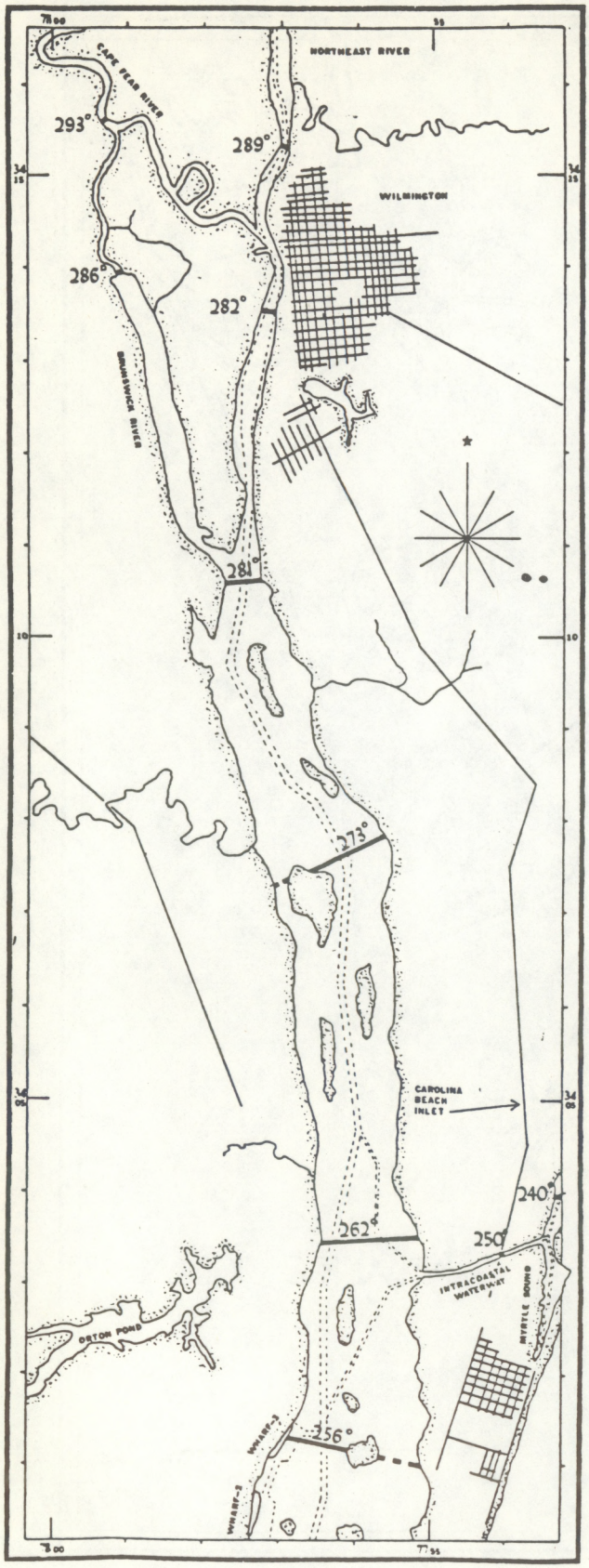

FIGURE 7.—Continued.

Sa and June and December for *Ssa*. The mean sea level for Wilmington (1976) was at a maximum in June, slightly lower in July, and just above the yearly average in December. Although the constituent values are probably unreliable, there is evidence that they may affect the sea level over a yearly cycle.

The relationships investigated using the larger harmonic constitutents for the study area include cotidal and corange lines from the M_2 and K_1 constituents, various amplitude ratios, diurnal to semidiurnal amplitude ratios, epoch relationships, and the influence of the M_4 and M_6 constituents on the tidal wave. Several necessary comments concerning these relationships are as follows:

1. The results of all tide stations are included for the purpose of completeness.

2. It is assumed that the adjusted values given in table 6 are correct for each station.

3. The intervals between cotidal or corange lines are irregular, because the change in epoch and range is not uniform throughout the system.

4. A dashed line indicates that there is some doubt as to the validity of the data.

5. Values, as a result of the heavy gage concentration around the MOTSU area, are averaged for the Wharf 1 and Wharf 2 lines.

The chart in figure 7 is a cotidal chart for M_2 (angular speed = 28.9841042°/hour; period = 12.4206 hours). The lines on the chart represent the value of the epoch in degrees, referenced to the 75°W meridian. By dividing the epoch associated with a particular line by 360° and multiplying the answer by 12.4206 hours, the resulting time will refer to the time difference between high water for the M_2 constituent at that location and lunar transit over the 75°W time meridian. The difference in M_2 epochs between Baldhead (T–01) and the control tide station at Wilmington (T–11) is about 64°, which means that it takes about 2.2 hours for the M_2 high water to progress from the mouth of the Cape Fear River up to Wilmington, a distance of about 23.6 nmi. Over this reach of the river, the M_2 wave is traveling at the average rate of 10.7 nmi per hour (kn). The lower epoch values at Snows Cut (T–13) and Myrtle Sound (T–22) are the result of the superposition of the tidal wave traveling up the river and a second tidal wave passing through Carolina Beach Inlet into Myrtle Sound and through the Intracoastal Waterway. The tidal wave has a shorter distance to travel by way of Carolina Beach Inlet than by way of the mouth of the Cape Fear River.

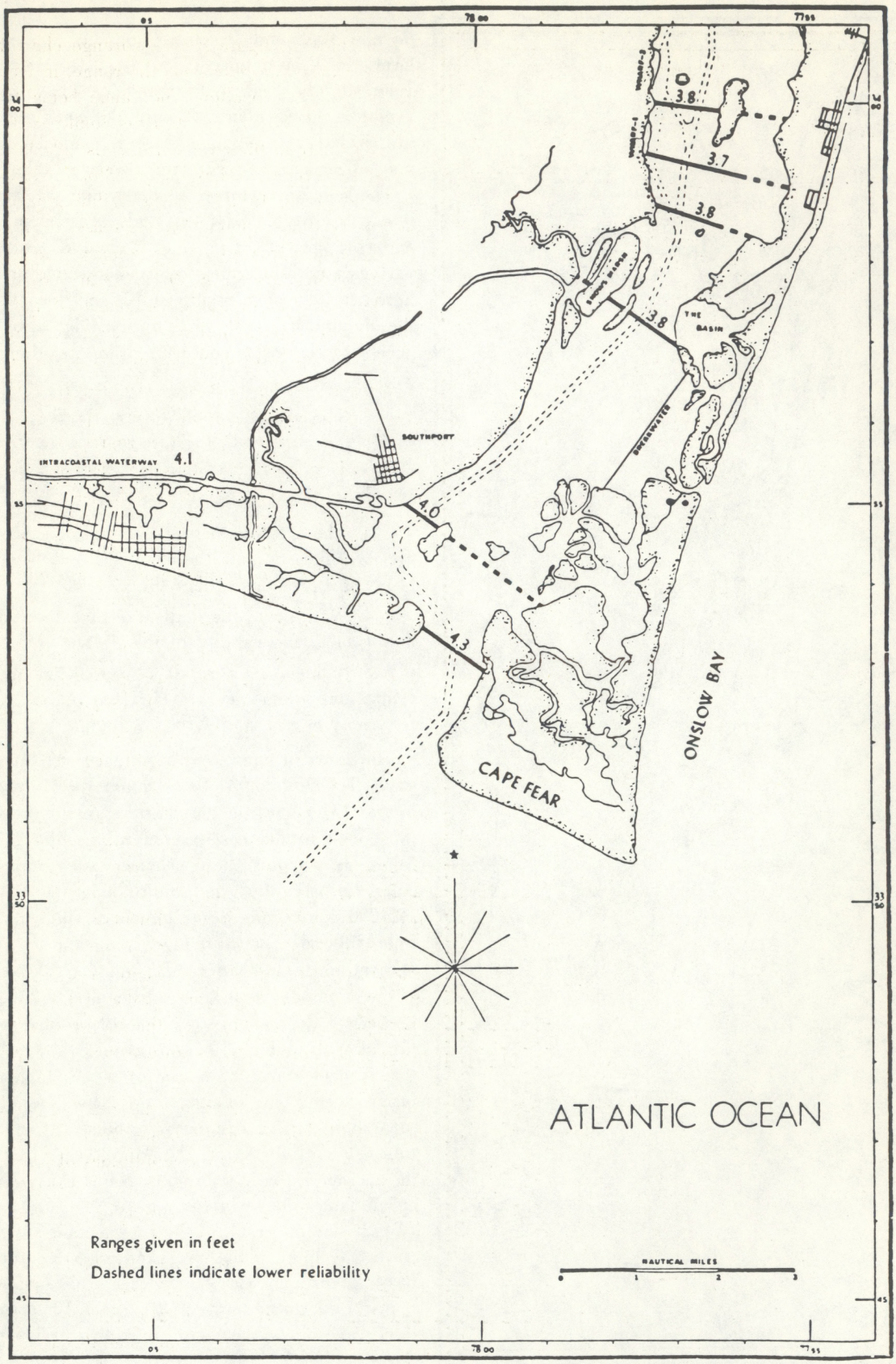

FIGURE 8.—Corange lines for M_2 tide.

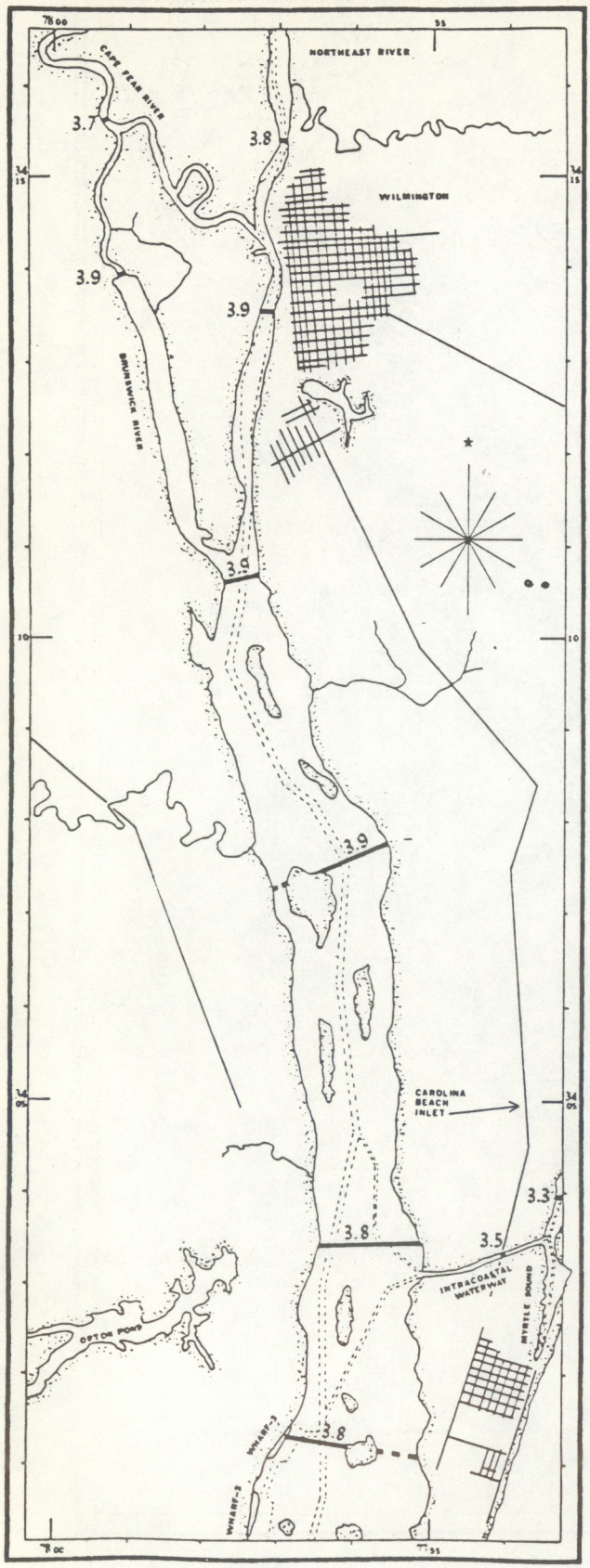

FIGURE 8.—Continued.

The chart in figure 8 is a corange chart for M_2. Each corange line represents the range, in feet, of the M_2 tide at that location (the range being twice the amplitude of the M_2 constituents found in table 6). The M_2 range at the river entrance is 4.26 ft, decreasing to 3.73 ft at MOTSU Wharf No. 1 (T–19), and then increasing to 3.93 ft at Wilmington (T–11). Section 3 will explain this decrease in range followed by an increase in range going up the river. The significant decrease in the M_2 range at Snows Cut and Myrtle Sound is probably the result of interference from the combined tidal waves mentioned above and an increase in wave damping in this constricted area.

The chart in figure 9 is a cotidal chart for K_1 (angular speed = 15.0410686°/hour; period = 23.9345 hours). The lines on the chart represent the value of the epoch in degrees, referenced to the 75°W time meridian. By dividing the epoch associated with a particular line by 360° and multiplying the answer by 23.9345 hours, the resulting time will refer to the time difference between the maximum K_1 astronomic force at this location and the lunar transit over the 75°W time meridian. The difference in K_1 epochs from Baldhead to Wilmington is about 30.9°; therefore, it takes the K_1 high water 2.1 hours to travel from the mouth of the Cape Fear River to Wilmington, an average rate of 11.2 kn. Again, it is necessary to point out that although the K_1 constituent is the largest diurnal constituent in the lower Cape Fear, its amplitude is only about $\frac{1}{8}$ of the M_2 constituent.

The chart in figure 10 is a corange line chart for K_1, each corange line representing the range, in feet, of the K_1 tide at that location (the range being twice the amplitude of the K_1 constituents in table 6). There is very little variability in the range of the K_1 constituent in the study area. There is a difference of 0.14 ft between the highest value, 0.63 ft for Oak Island Bridge (T–21), and the lowest value, 0.49 ft for six different stations spread out over the study area.

The relationship between the diurnal constituents and semidiurnal constituents was first investigated by computing the ratio of the amplitudes of K_1, the largest diurnal constituent, to M_2, the largest semidiurnal constituent. With the exception of the Intracoastal Waterway and Myrtle Sound, each ratio is around 0.13 which is expected because of the lack of significant variability in the constituent ranges. The ratios for Oak Island Bridge (T–21), Snows Cut (T–13), and Myrtle Sound (T–22) are slightly larger because of higher K_1 amplitudes and smaller M_2 amplitudes at these locations.

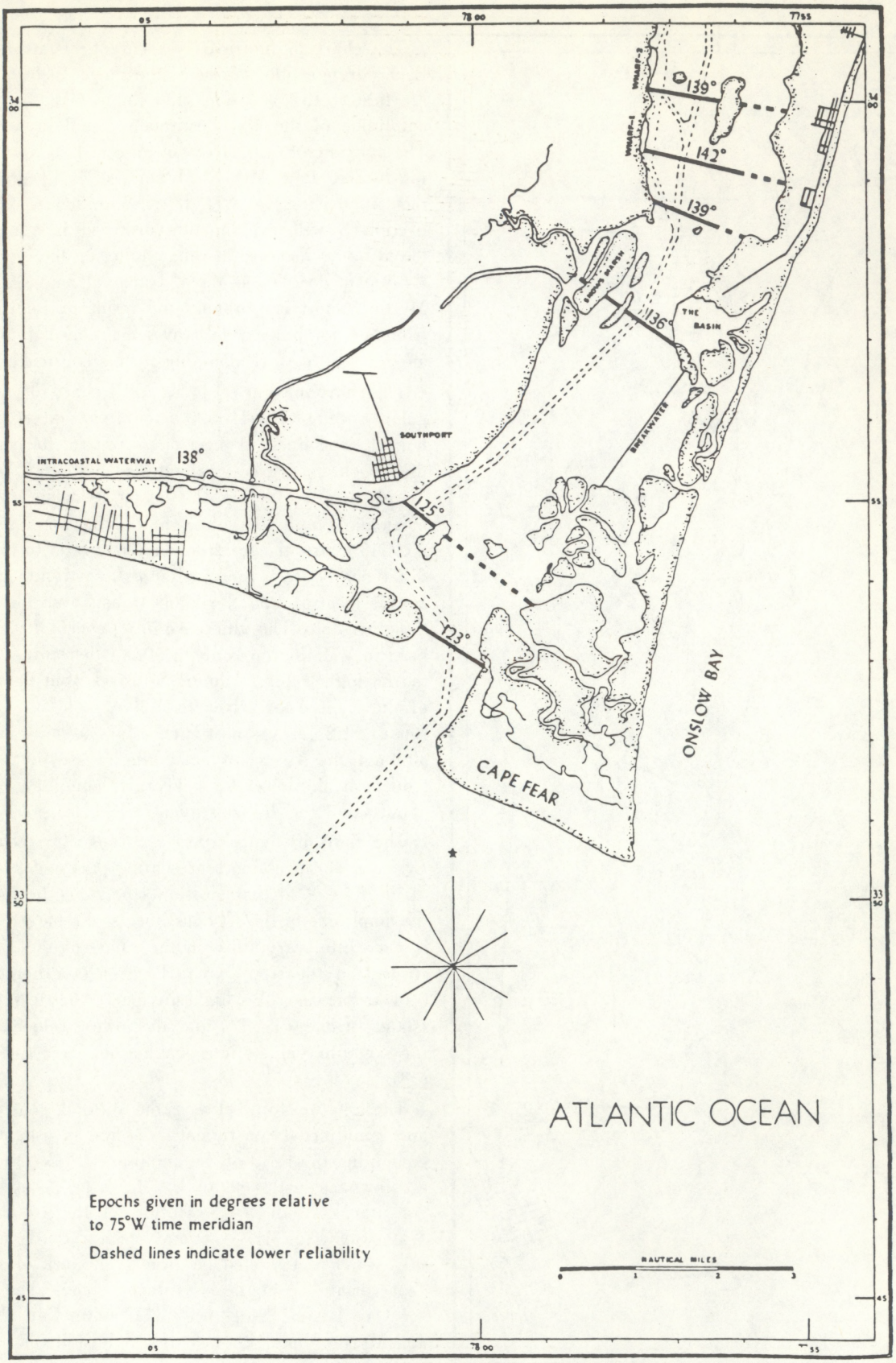

FIGURE 9.—Cotidal lines for K_1 tide.

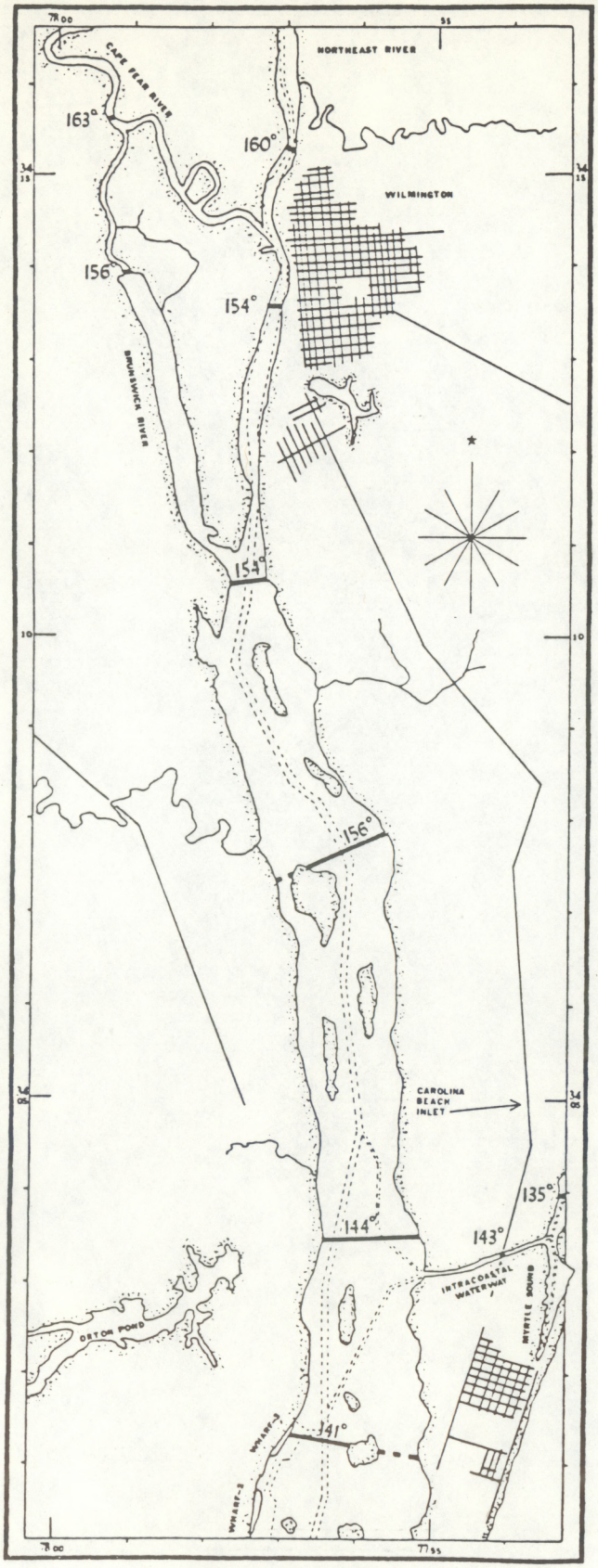

FIGURE 9.—Continued.

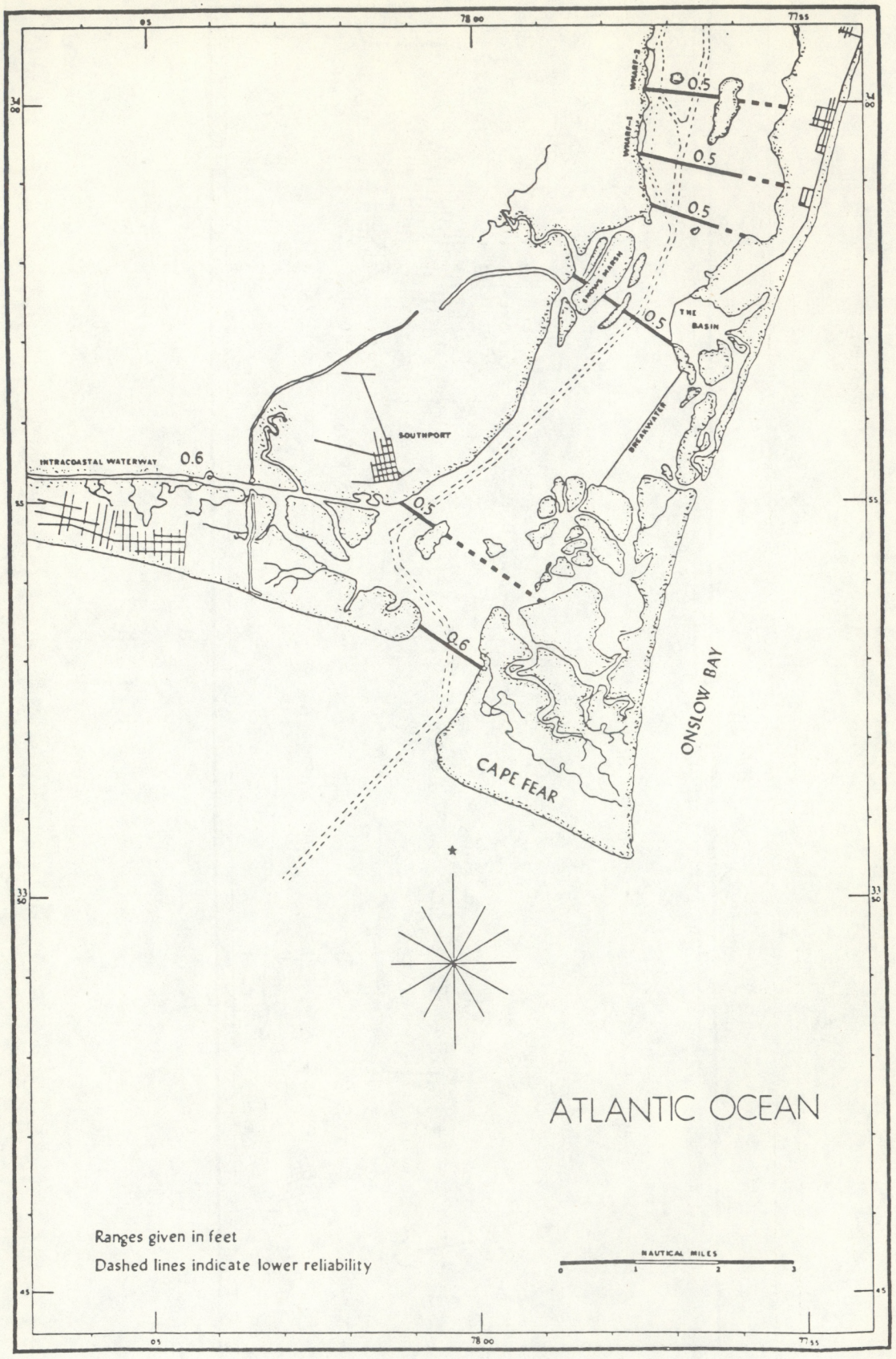

FIGURE 10.—Corange lines for K_1 tide.

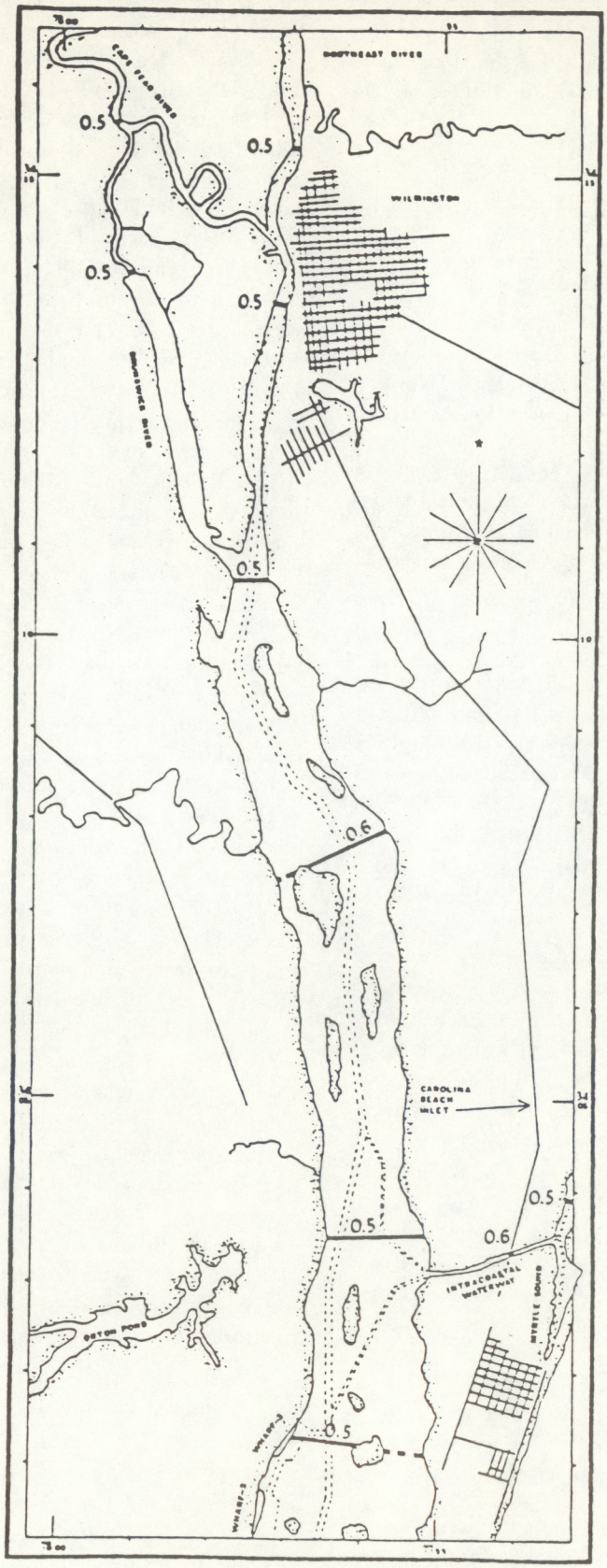

FIGURE 10.—Continued.

NOS, in defining the "type of tide," uses the ratio of the $(K_1 + O_1)$ range to the $(M_2 + S_2)$ range. The chart in figure 11 shows this ratio for the study area. Defant (1961) defines the four main tidal types as follows:

1. Semidiurnal: $\frac{K_1 + O_1}{M_2 + S_2} < 1/4$; two tidal cycles per day with both high waters and low waters usually of about equal height.

2. Mixed, mainly semidiurnal: $1/4 < \frac{K_1 + O_1}{M_2 + S_2} < 1\frac{1}{2}$; usually two tidal cycles per day with inequalities in height and time of successive high waters and/or low waters. These inequalities reach their peak when the declination of the Moon has passed its maximum.

3. Mixed, mainly diurnal: $1\frac{1}{2} < \frac{K_1 + O_1}{M_2 + S_2} < 3$; usually two cycles per day with large inequalities when the Moon is over the equator, and one cycle per day when the Moon is near maximum declination.

4. Diurnal: $\frac{K_1 + O_1}{M_2 + S_2} > 3$; usually one cycle per day.

The Cape Fear River is classified as semidiurnal because of its ratio values, shown in figure 11. The only stations that do not fit into this type by definition are Snows Cut (T–13) and Myrtle Sound (T–22) whose (K_1+O_1) to (M_2+S_2) ratios are 0.258 and 0.266 respectively, which are so small that they also can be classified as semidiurnal. The other ratios range from a low of 0.186 for the Exxon Pier (T–09) to a high of 0.246 for Oak Island Bridge (T–21).

If the tide had been classified as mixed, or even partially mixed, then it would have been necessary to study the epochs of the M_2, K_1, and O_1 constituents to determine how the successive high waters and low waters are related. The results of the relationship, $M_2° - K_1° - O_1°$, would determine if the inequality exists in the high waters, low waters, or both, and the sequence in which the high and low waters occur.

The cotidal and corange lines for N_2 (angular speed = 28.4397295°/hour; period = 12.6583 hours), the second largest constituent for the Cape Fear River, and S_2 (angular speed = 30.00°/hour; period = 12 hours), the third largest constituent, follow the same pattern as the epoch and range distribution for M_2. The difference in epochs for N_2 from Baldhead (T–01) to Wilmington (T–11) is about 67.2° or 2.4 hours, which indicates that the N_2 wave is traveling at an average rate of 9.8 kn. The N_2 range varies from a maximum of 0.91 ft at Oak Island Bridge (T–21) to a minimum of 0.64 ft at Myrtle Sound (T–22). It takes 70.2° or 2.3 hours for the S_2 wave to travel from Baldhead (T–01) to Wilmington (T–11), which results in an average rate of travel of 10.3 kn. The S_2 range varies from 0.70 ft at Baldhead (T–01) and Oak Island Bridge (T–21) to 0.44 ft at Exxon Pier (T–09) and Navassa (T–15).

By studying the relationships among the semidiurnal constituents (M_2, S_2, and N_2), one can get a better understanding of how the Cape Fear River basin affects each of these constituents differently. The chart in figure 12 shows the values for the ratio of the amplitudes of S_2 to M_2. The ratio at the river entrance is 0.16 and decreases gradually down to 0.12 north of Wilmington, the highest value being 0.18 in Myrtle Sound. The ratio of N_2 to M_2 is reasonably steady, varying from 0.21 just inside the river entrance down to 0.19 north of Wilmington.

The chart in figure 13 shows the ratio of O_1 to K_1 amplitudes in the study area. The O_1 constituent is due to the Moon's declination (angular speed = 13.9430356°/hour; period = 25.8193 hours). The values do not appear to follow any trend as can be seen from the chart. The highest values occur in the Intracoastal Waterway and Myrtle Sound. The variability in the ratio values is a result of the O_1 and K_1 amplitudes being so small. A consequence of the small constituent amplitudes is a low signal to noise ratio, which adversely affects the analysis.

The "age" is a lag (expressed in hours) between the time of an astronomical condition tending to produce a maximum effect and the actual maximum as it occurs in nature (Special Publication No. 260, 1952). The lag is known as the age of the inequality and is expressed in terms of the tidal constants. The ages for the Cape Fear River were calculated using κ', meaning that the time differences apply to the new (or full) Moon passing over the 75°W meridian.

The phase age, or "age of the tide," is the time required for the M_2 and S_2 constituents to arrive at a phase agreement. The range of the tide tends to increase in approaching the times of new or full Moon, when M_2 and S_2 are in phase agreement, and to decrease in approaching the quadratures of the Moon. The following formula, based on the hourly speeds of the M_2 and S_2 constituents, is used to calculate the phase age:

$$\text{phase age (in hours)} = 0.984\ (S_2° - M_2°)$$

The chart in figure 14 shows the phase age values in hours for the Cape Fear River. The values range from a low of 17.46 hours at MOTSU Wharf No. 2 (T–05) to a high of 32.53 hours at Marker 43A

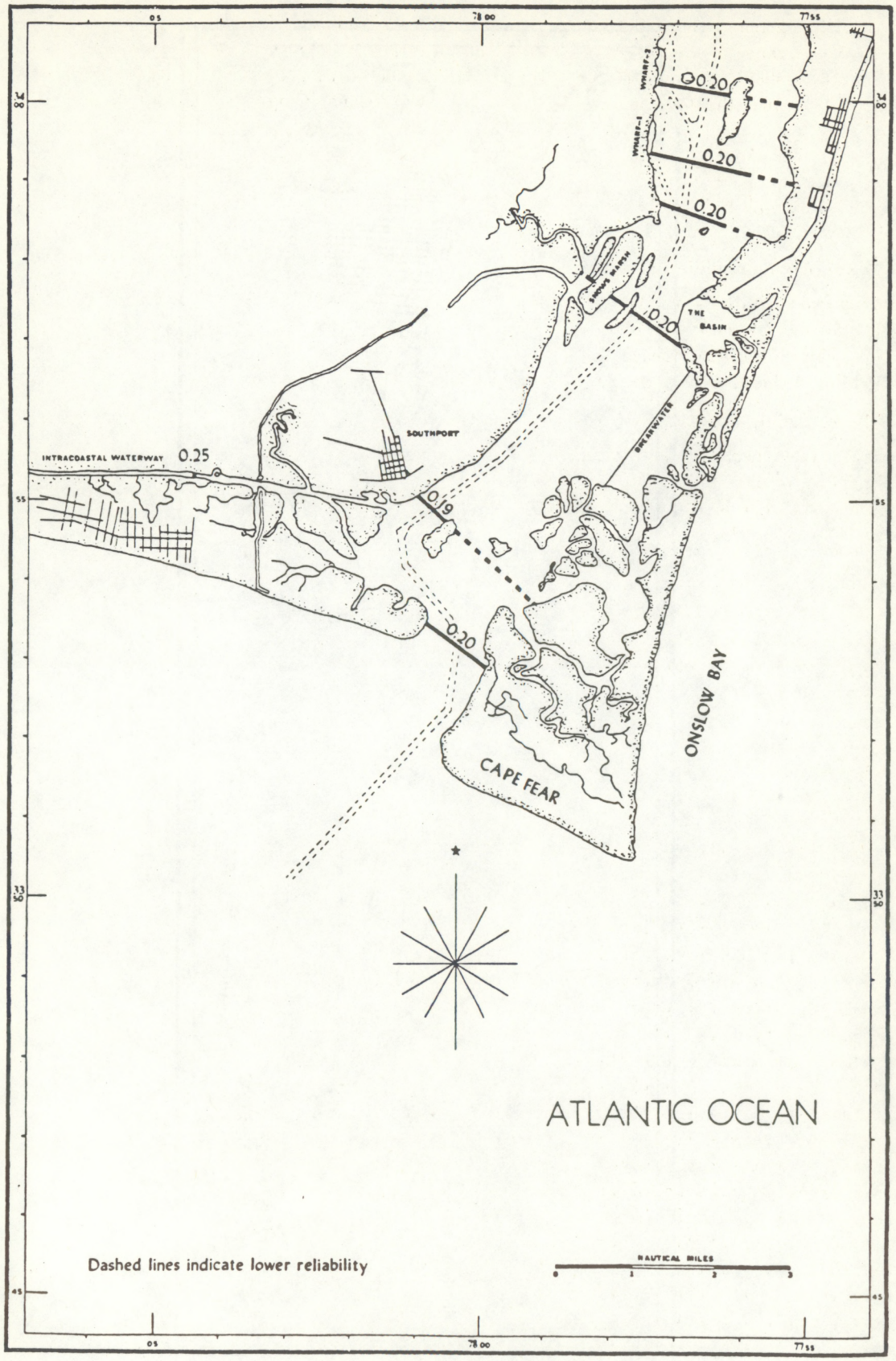

FIGURE 11.—"Type of tide," (K_1+O_1) to (M_2+S_2) ratio lines.

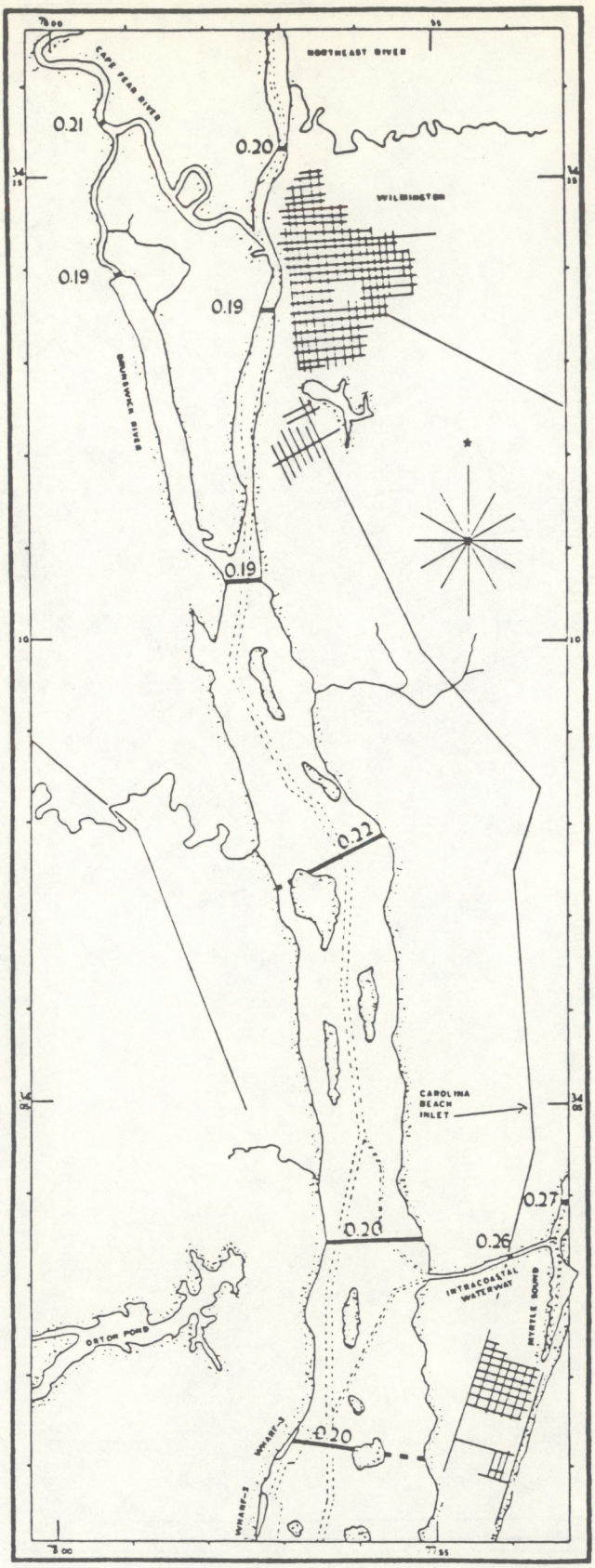

FIGURE 11.—Continued.

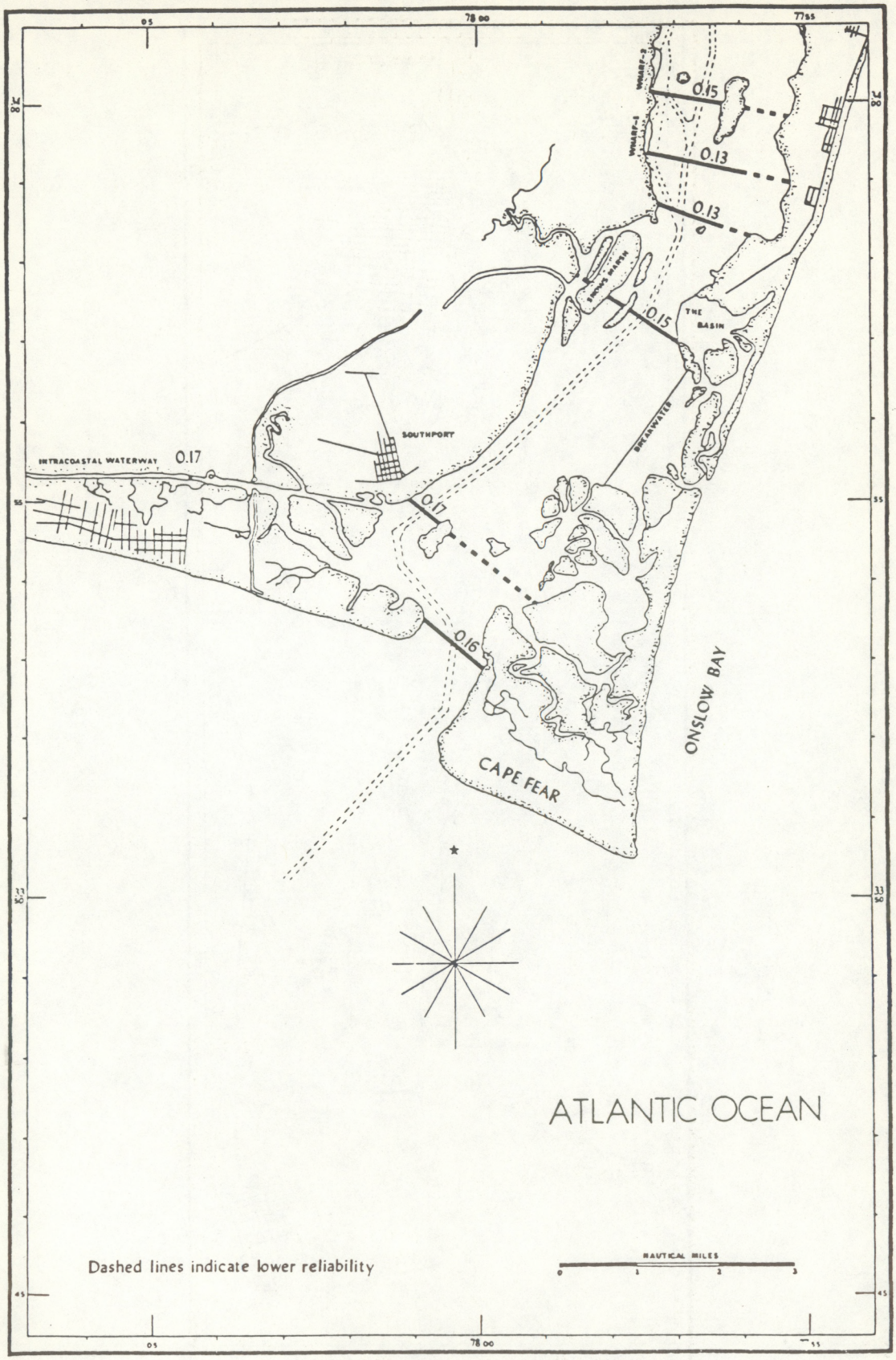

FIGURE 12.—Ratio lines S_2 to M_2 for the tide.

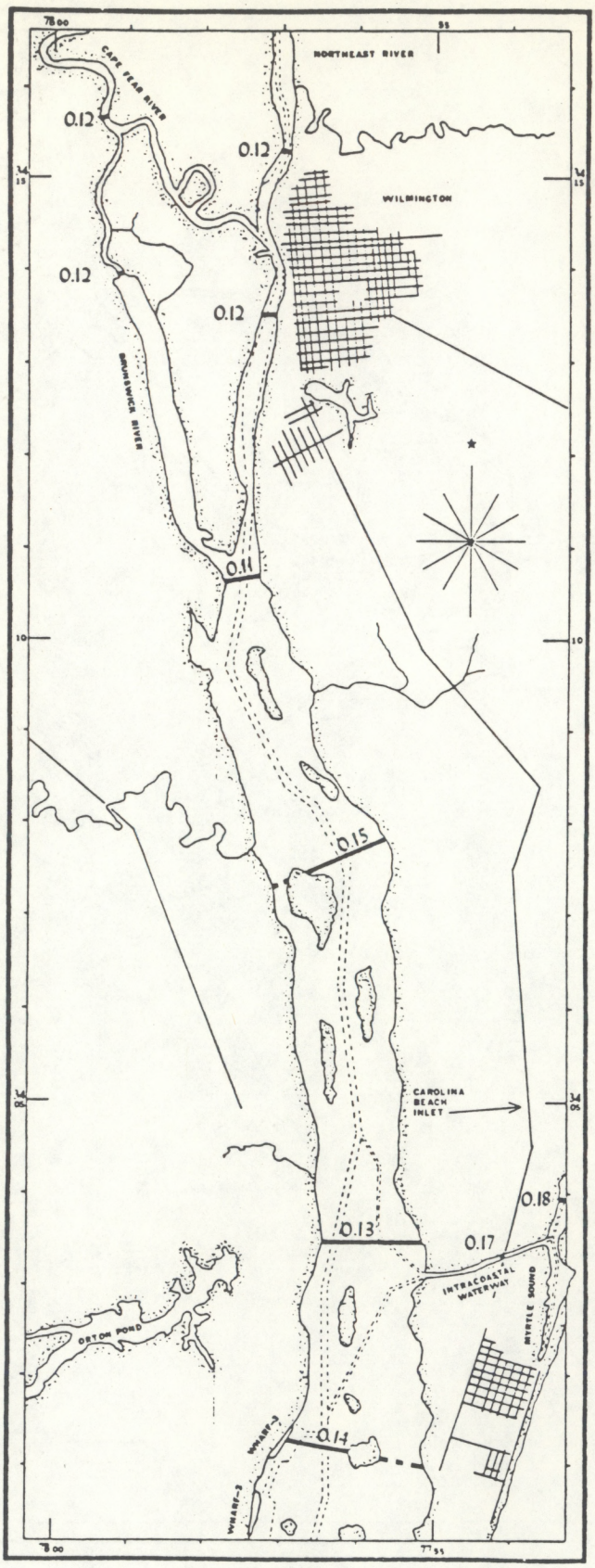

FIGURE 12.—Continued

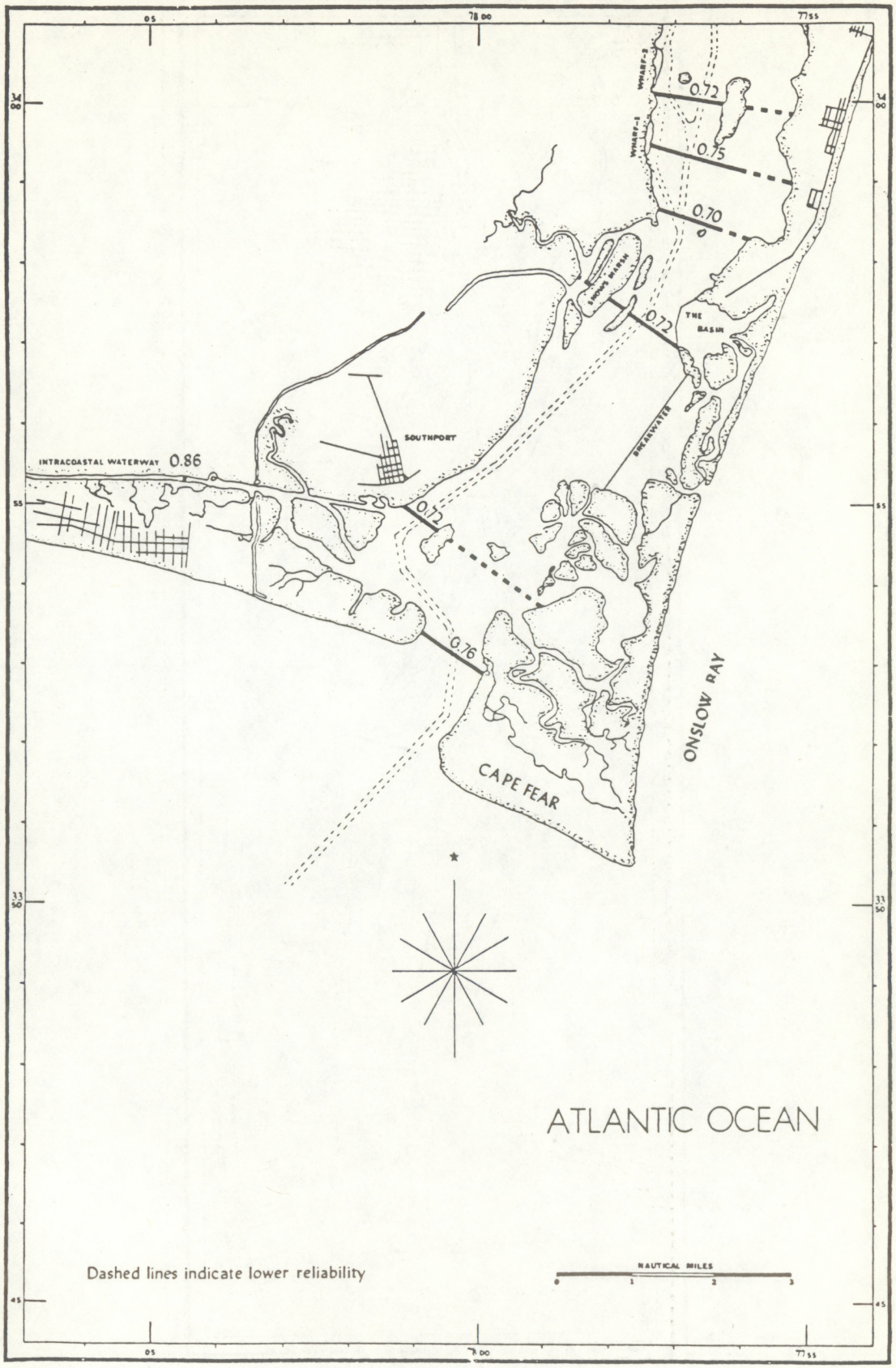

FIGURE 13.—Ratio lines O_1 to K_1 for the tide.

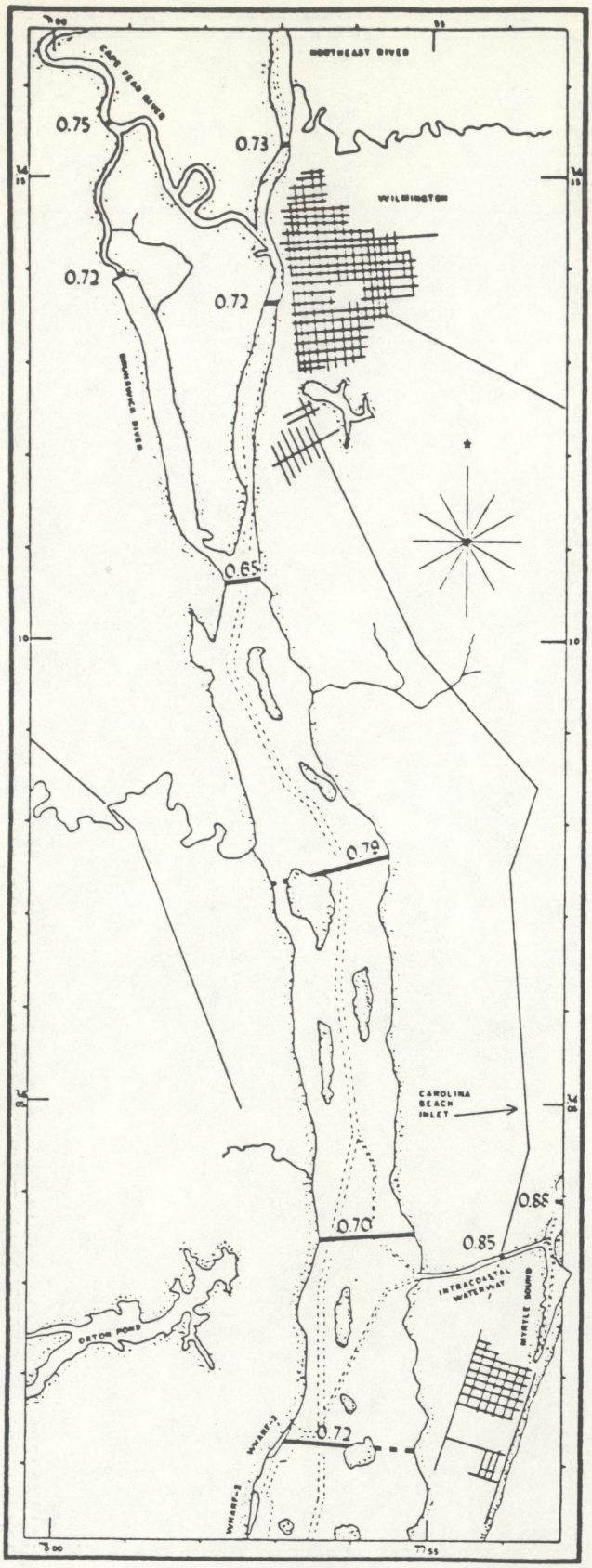

FIGURE 13.—Continued.

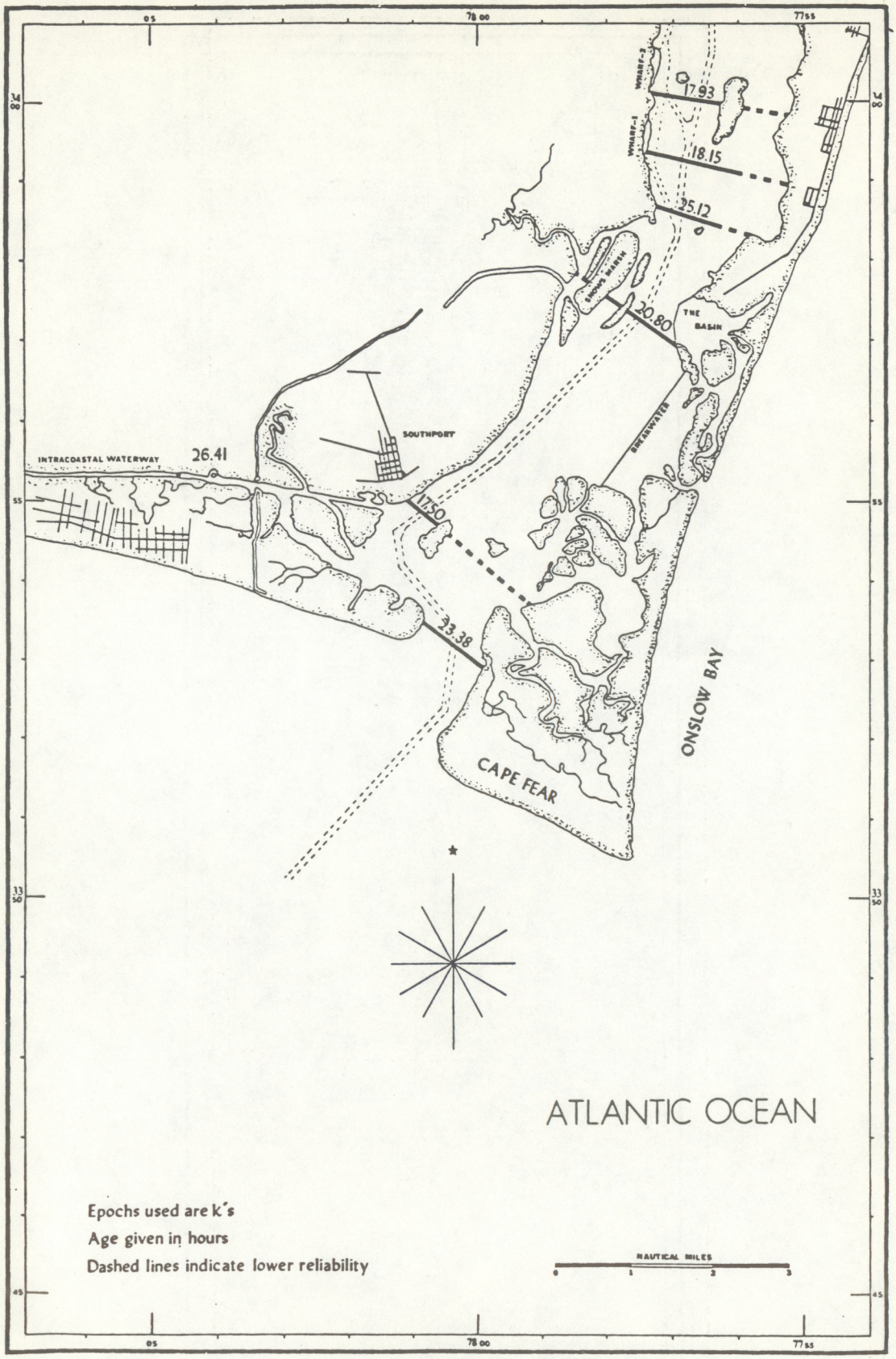

FIGURE 14.—"Phase age of the tide."

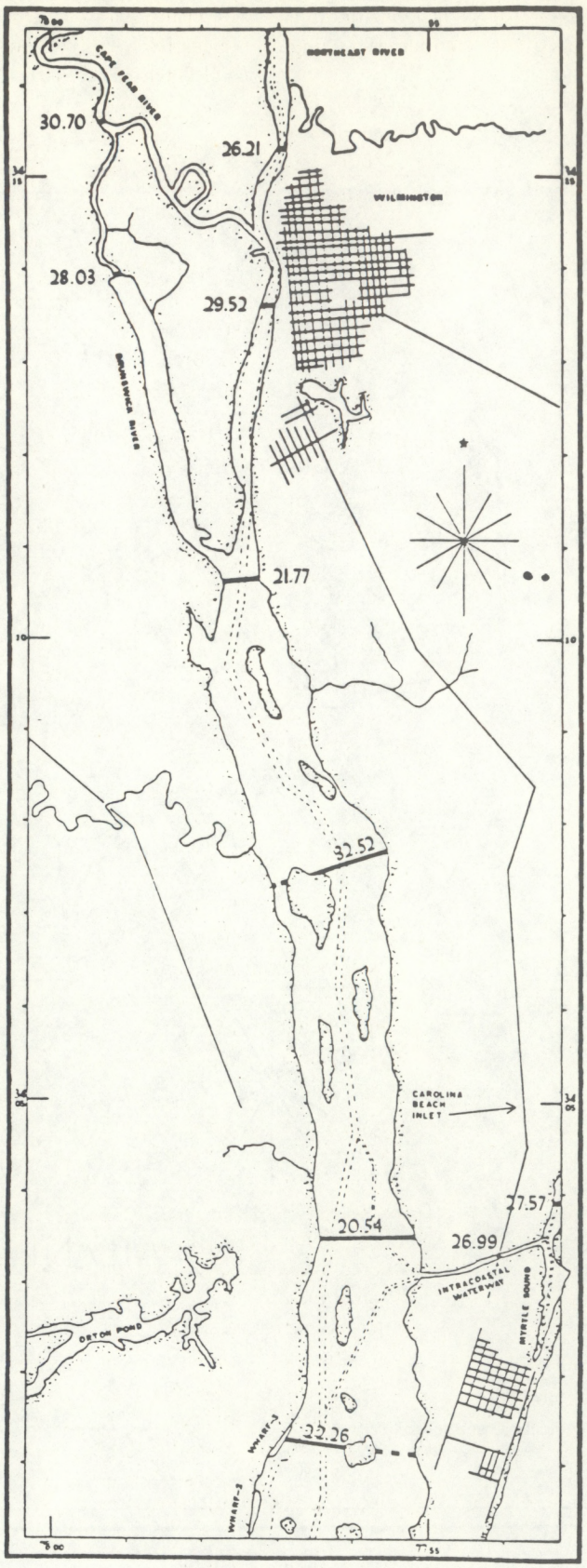

FIGURE 14.—Continued.

Campbell (T–08). Although there is considerable variability in the values, they tend to increase going up the river.

The parallax age is the interval required for the M_2 and N_2 constituents to arrive at phase agreement. The range of the tide increases as the Moon approaches its perigee and decreases as it approaches its apogee. The origin of the N_2 epoch coincides with that of M_2 when the Moon is in perigee. The equation governing the parallax age is as follows:

$$\text{parallax age (in hours)} = 1.837\ (M_2^\circ - N_2^\circ)$$

The chart in figure 15 shows the parallax age values in hours for the Cape Fear River. The values range from a low of −10.76 hours at Reaves Pt. Channel (T–03) to a high of 22.12 hours at Marker 43A Campbell (T–08). There does not appear to be any trend in the values.

The diurnal age is the interval required for the K_1 and O_1 constituents to be in phase agreement, resulting in the diurnal wave attaining its maximum amplitude. The diurnal wave is due to the declination of the tide-producing body. The diurnal inequality is the difference in heights of the two high waters or the two low waters. The relationship governing the diurnal age is as follows:

$$\text{diurnal age (in hours)} = 0.911\ (K_1^\circ - O_1^\circ)$$

The diurnal age values in the Cape Fear River range from a low of −18.65 hours at the Exxon Pier (T–09) to a high of 8.50 hours at Baldhead (T–01). There is a great amount of variability in the values with no apparent trends, again, because the K_1 and O_1 constituents are so small. The diurnal age probably has very little significance in the Cape Fear River, because the river is so strongly semidiurnal.

The shallow water constituents result from the tidal wave crest moving more rapidly than the trough, causing the wave to lose its simple harmonic form (Schureman, 1958). The M_4 and M_6 constituents, having four and six periods respectively in the lunar day, have speeds that are multiples (higher harmonics) of the M_2 constituent. The shallow water constituents reflect the amount of distortion of the cosine type curve because of the physical features of the basin (Zetler, 1959). As would be expected, the M_4 and M_6 amplitudes increase progressively in size from the Cape Fear River entrance going north up the river. The M_4 range varies from 0.008 ft at Southport (T–02) to 0.400 ft at the North Carolina Department of Transportation Dock (T–16), and the M_6 range varies from 0.004 ft at Myrtle Sound (T–22) to 0.214 ft at Navassa (T–15).

The chart in figure 16 shows the ratio of the amplitudes of M_4 to M_2 for the tide stations in the Cape Fear River. When this ratio exceeds 0.1, the distortion of the cosine curve (wave) by M_4 becomes significant (Special Publication No. 260, 1952). As can be seen from the chart, this value is approached and exceeded only at those stations in the northern section of the study area. This implies that the M_4 constituent will distort the tidal wave only in this area and even then not to a significant degree.

Distortion from M_6 becomes significant when the M_6 to M_2 ratio exceeds 0.04 (Hicks, 1964). This value is exceeded only in the northern section of the study area as can be seen in figure 17 which shows the ratio of the amplitudes of M_6 to M_2. By comparing figure 16 to figure 17, one can see that the M_6 constituent appears to influence the tidal wave from a point lower down the river than the M_4 constituent.

Table 7 shows the results of the adjusted nonharmonic tidal parameters for the Cape Fear River based on the 1976 circulatory survey. These values were obtained by adjusting the tabulated tidal parameters to the accepted long-term control station parameters (Wilmington, T–11) as mentioned in section 2.3. The high water interval (HWI) is the time difference, in hours, between the transit of the Moon over the meridian at Greenwich and the following high water at the station location. The low water interval (LWI) is the corresponding time difference for the Moon passing over the Greenwich meridian and the following low water at the station location. The mean range of tide (Mn) is the difference in feet between mean high water and mean low water for each tide station. The difference in HWIs between Southport (T–02) and Wilmington (T–11) is 1.76 hours; therefore, the high water is traveling at an average rate of 12.0 kn over this 21.1 nmi reach. The corresponding difference in LWIs is 2.52 hours for an average rate of travel of 8.4 kn. The large difference in rates of travel is due to the tidal wave crest moving more rapidly than the trough in the relatively shallow river. The Mn varies from a maximum of 4.40 ft for Oak Island Bridge (T–21) to a minimum of 3.49 ft for Myrtle Sound (T–22). As with the M_2 range, the Mn decreases in value from the river mouth to MOTSU Wharf No. 1 (T–19) and then increases in value to Wilmington (T–11). This phenomenon will be discussed in section 3.

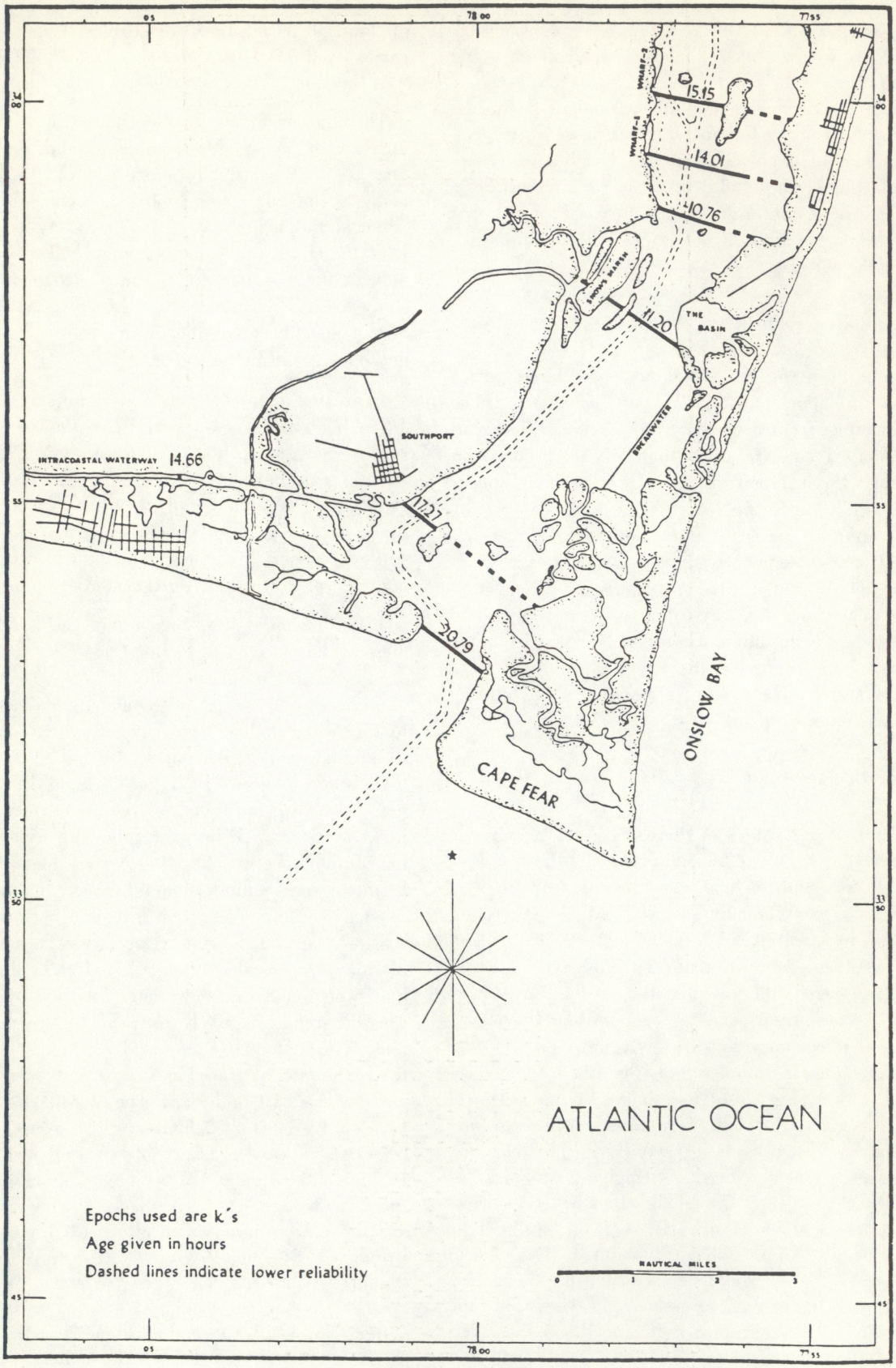

FIGURE 15.—"Parallax age of the tide."

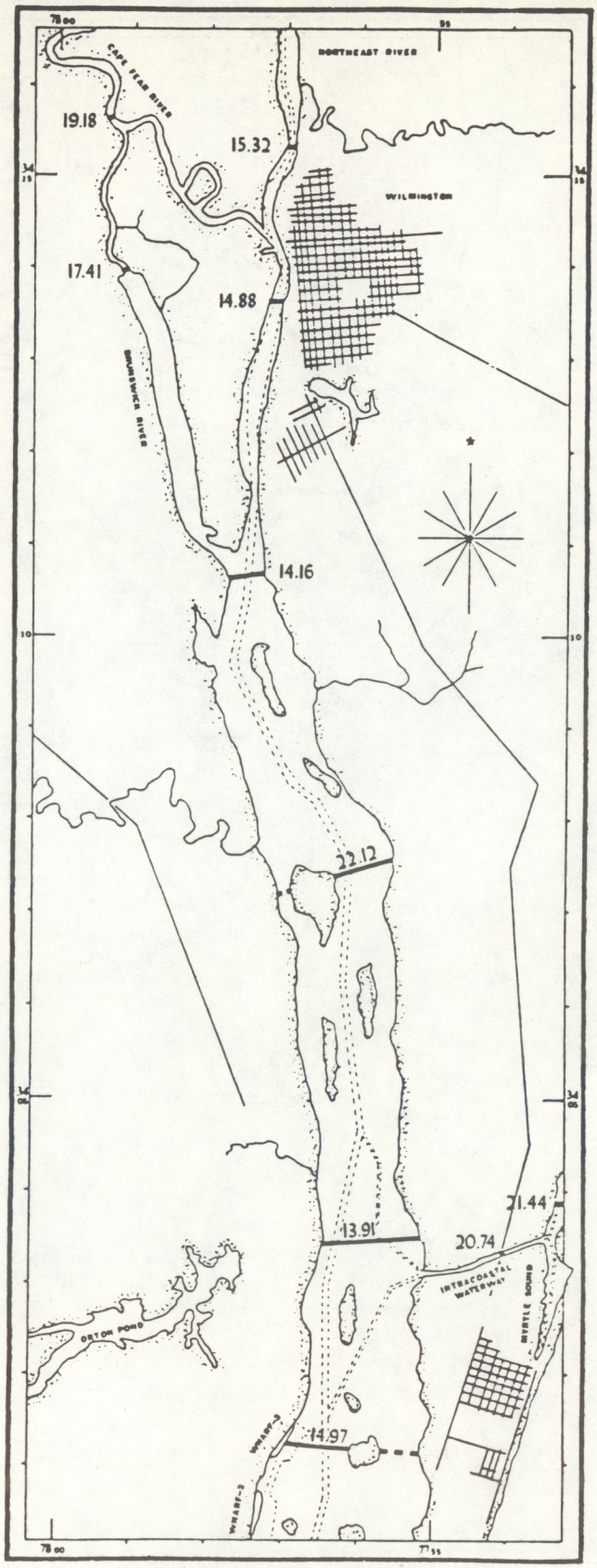

FIGURE 15.—Continued.

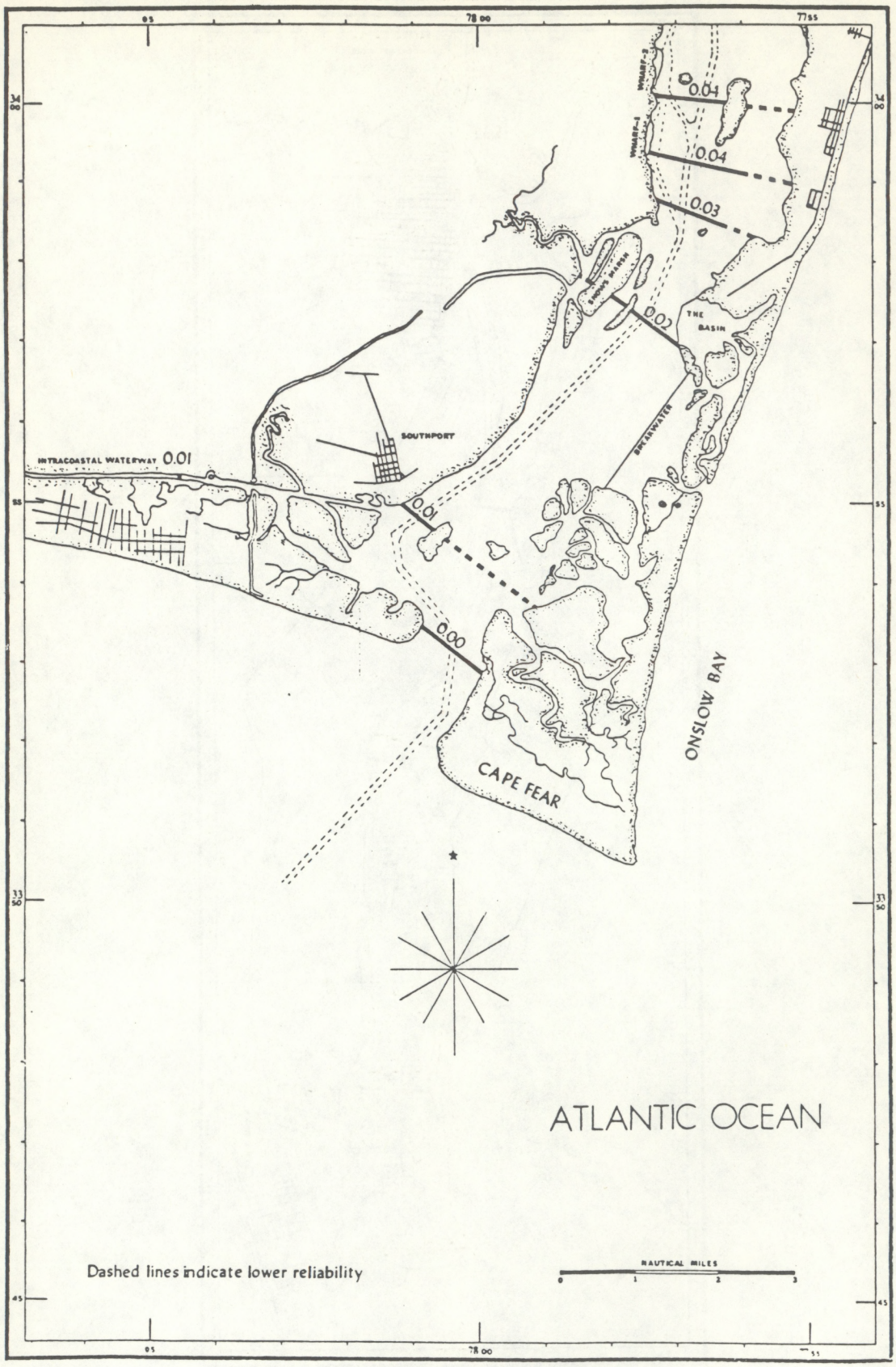

FIGURE 16.—Ratio lines M_1 to M_2 for the tide.

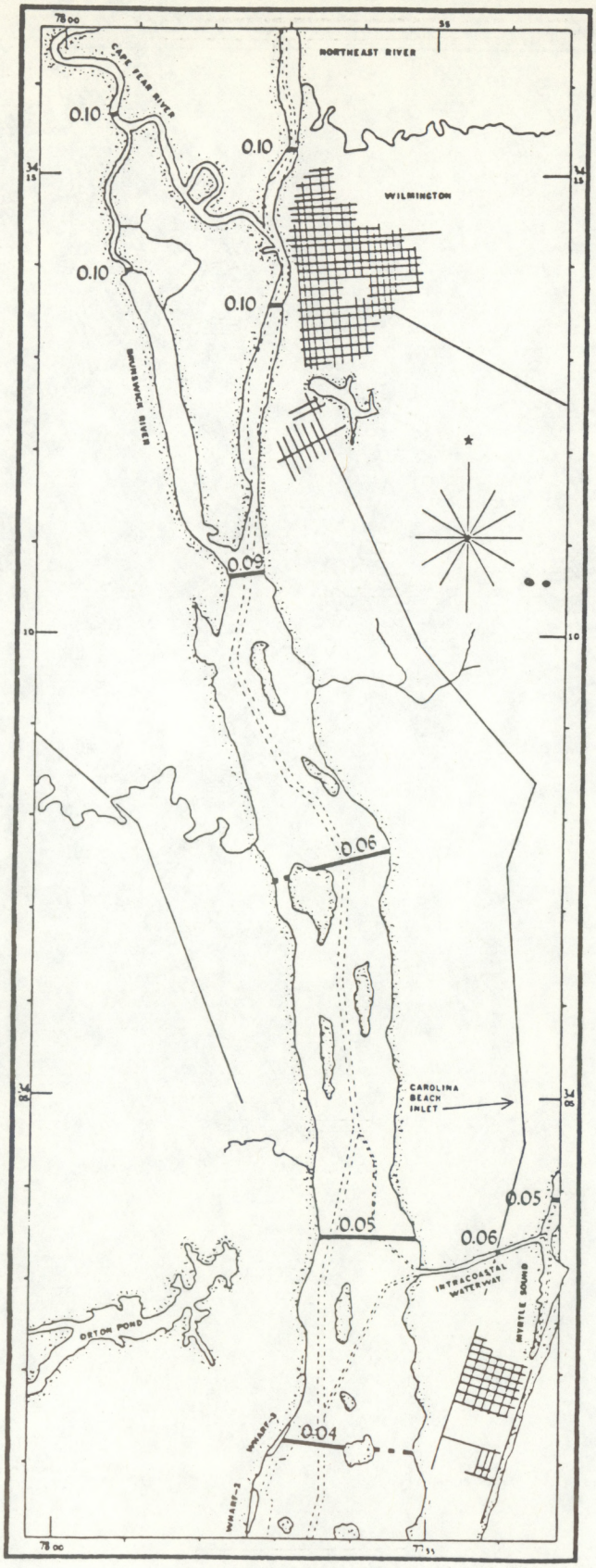

FIGURE 16.—Continued.

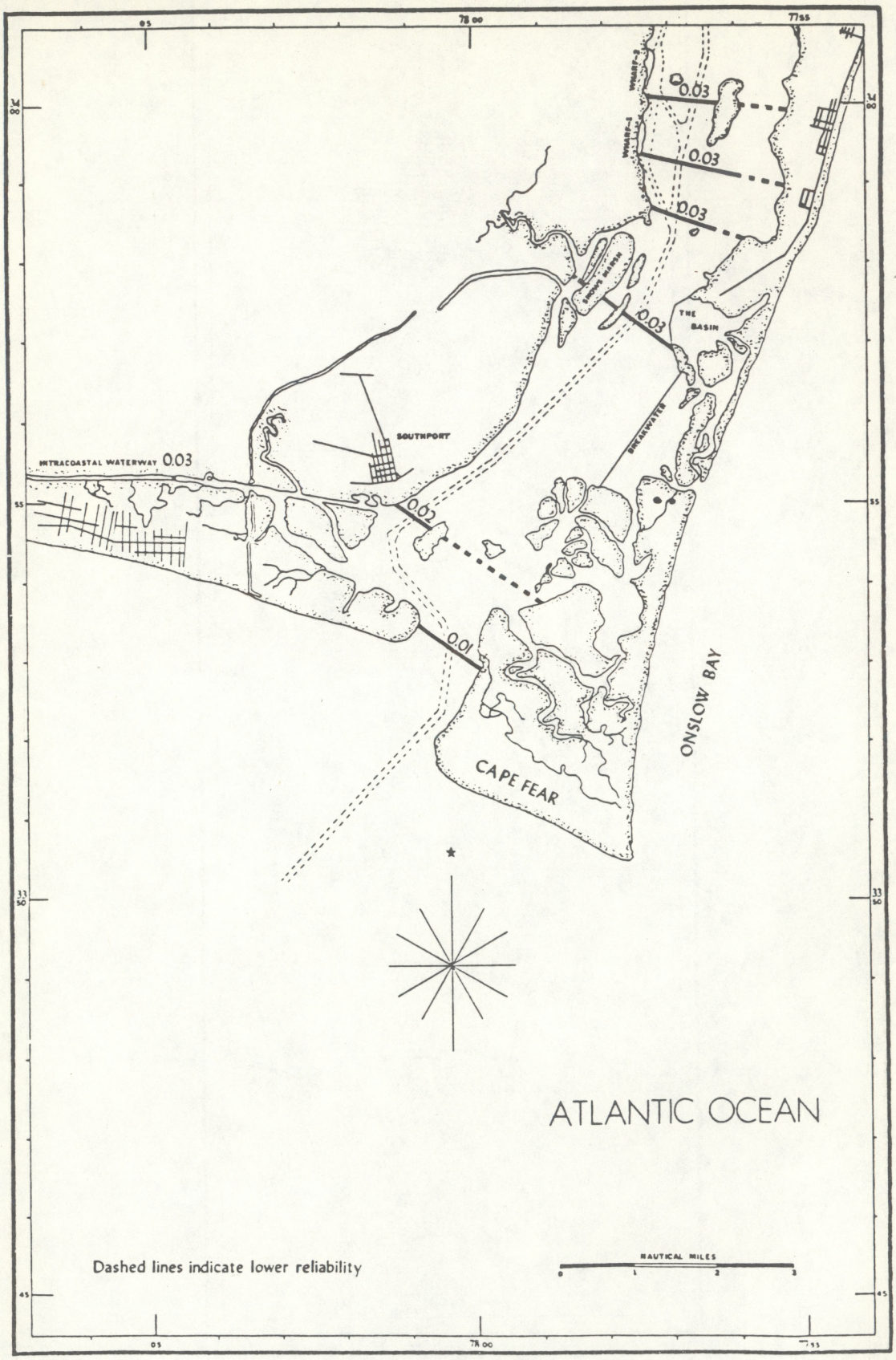

FIGURE 17.—Ratio lines M_4 to M_2 for the tide.

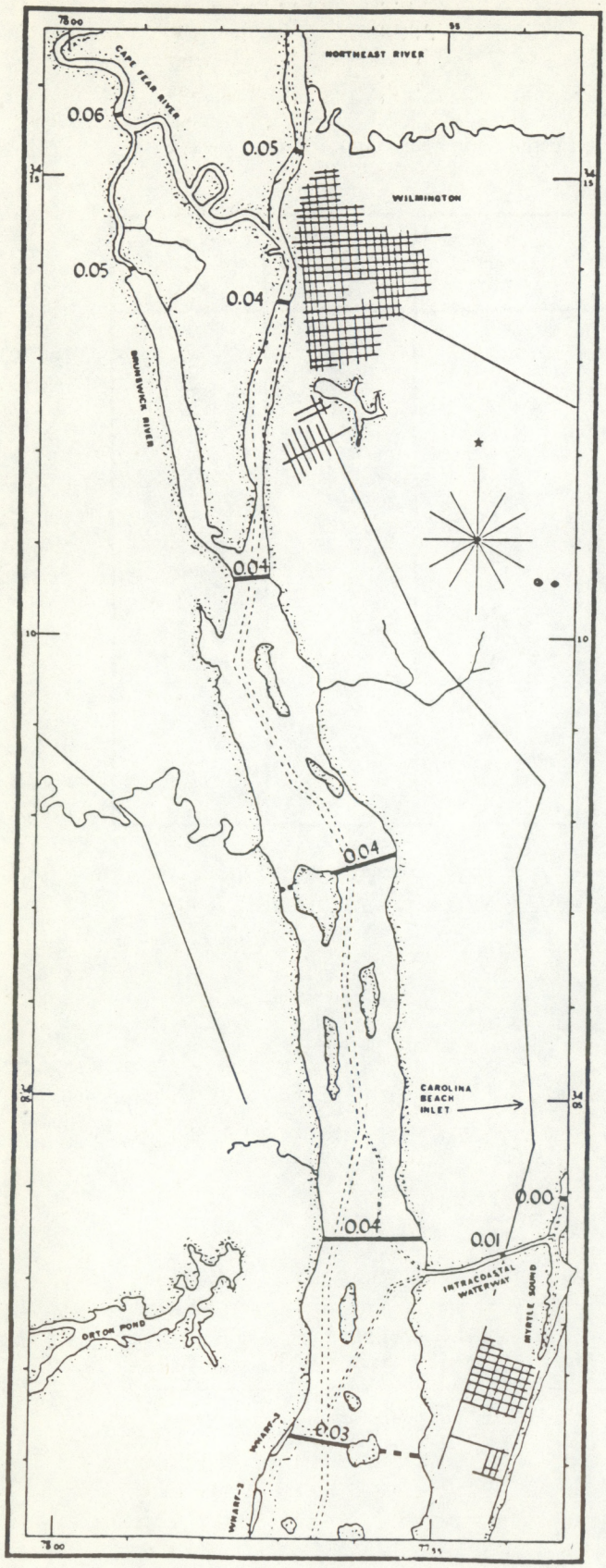

FIGURE 17.—Continued.

The tidal time series for each station was plotted by using computer program CURNT as discussed earlier. The plot of the Doodson-filtered series was superimposed over the plot of the original data series for each station. The Doodson filter effectively removes the tide from the original series, resulting in a nontidal time series. Corresponding points were determined for each station each time the nontidal series crossed the mean of the original series. By taking two stations at the survey limits, Southport (T–02) and Wilmington (T–11), several nontidal wave parameters were calculated and the results recorded in table 8. The time interval is the time period between the points at which the nontidal time series crossed the mean of the original time series. The rate of travel of the nontidal wave for each time interval was determined by taking the nautical distance between the two stations listed above (21.1 nmi) and dividing this value by the time difference between the two stations of the nontidal curve crossing of the mean of the original time series. For example, during the time period from 14 May 1976 to 23 May 1976, the nontidal curve (filtered series) crossed the mean of the original time series at Wilmington (T–11) 23 hours after crossing the mean at Southport; therefore, for that time period the rate of travel of the nontidal wave is 21.2 nmi/23 hours = 0.9 kn. Visual inspection of the nontidal series plots determined the direction of travel and status (rising or falling) of the nontidal wave.

The wind data presented in figure 18 strongly indicate that the nontidal wave is driven by prevailing winds. The wind data, furnished by CP&L, were recorded by their Environmental Monitoring System located about 2.5 mi west of Snows Marsh. By correlating the wind data in figure 18 to the time intervals in table 8, the predominant wind direction from 14 May to 23 May is from the south; 23 May to 29 May is from the north; 29 May to 3 June is from the south; and 3 June to 8 June is from the north. The only day that does not correlate well is 28 May.

Barometric pressure data (in inches of mercury) are presented in figure 19 for the same time period as the wind data in figure 18. CP&L also furnished the barometric pressure data. There is a fairly good correlation between the wind data in figure 18 and the barometric pressure data in figure 19. The wind shift on 23 May corresponds to a falling barometric pressure which reaches a low on 24 May. The wind shift on 28 to 29 May corresponds to a rising barometric pressure which reaches a high on 28 May. The wind shift on 3 June does not correlate as well

TABLE 7.—Tidal parameters for the Cape Fear River, 1976

Station Number	Station Name	High Water[1] Interval (HWI)	Low Water[2] Interval (LWI)	Mean Range[3] of Tide (Mn)
T-01	Baldhead	N.A.	N.A.	4.34
T-02	Southport	0.61	6.76	4.21
T-03	Reaves Pt. Channel	1.37	7.81	3.97
T-04	Lower Midnight Channel	1.32	7.85	3.97
T-05	MOTSU Wharf No. 2	1.48	8.01	3.97
T-06	Upper Midnight Channel	1.46	8.06	3.98
T-07	Orton Point	1.80	8.32	4.04
T-08	Marker 43A Campbell	2.21	8.81	4.10
T-09	Exxon Pier	2.36	9.20	4.15
T-10	Zekes Island	1.18	7.59	3.96
T-11	Wilmington	2.37	9.28	4.15
T-12	Ideal Cement Pier	2.76	9.52	3.97
T-13	Snows Cut	1.08	7.72	3.65
T-14	MOTSU Wharf No. 3	1.44	8.03	4.02
T-15	Navassa	2.93	9.72	3.92
T-16	N.C. Dept. Trans. Dock	2.60	9.55	4.15
T-19	MOTSU Wharf No. 1	1.33	7.86	3.93
T-21	Oak Island Bridge	1.05	7.19	4.40
T-22	Myrtle Sound	0.71	7.31	3.49

[1]High water interval, in hours, relative to the Greenwich Meridian.

[2]Low water interval, in hours, relative to the Greenwich Meridian.

[3]Mean range of tide, in feet.

TABLE 8.—Nontidal wave parameters

Time Interval (Days)	Rate of Travel[2] (Kts)	Direction of Flow (North or South)	Nontidal Status (Rising or Falling)
14 May 1976–23 May 1976[1]	0.9	S→N	Rising
23 May 1976–29 May 1976	3.5	N→S	Falling
29 May 1976–03 June 1976	1.5	S→N	Rising
03 June 1976–08 June 1976	1.0	S→N	Falling

[1] Time interval may precede 14 May 1976.

[2] Rate of travel of the nontidal wave, in knots.

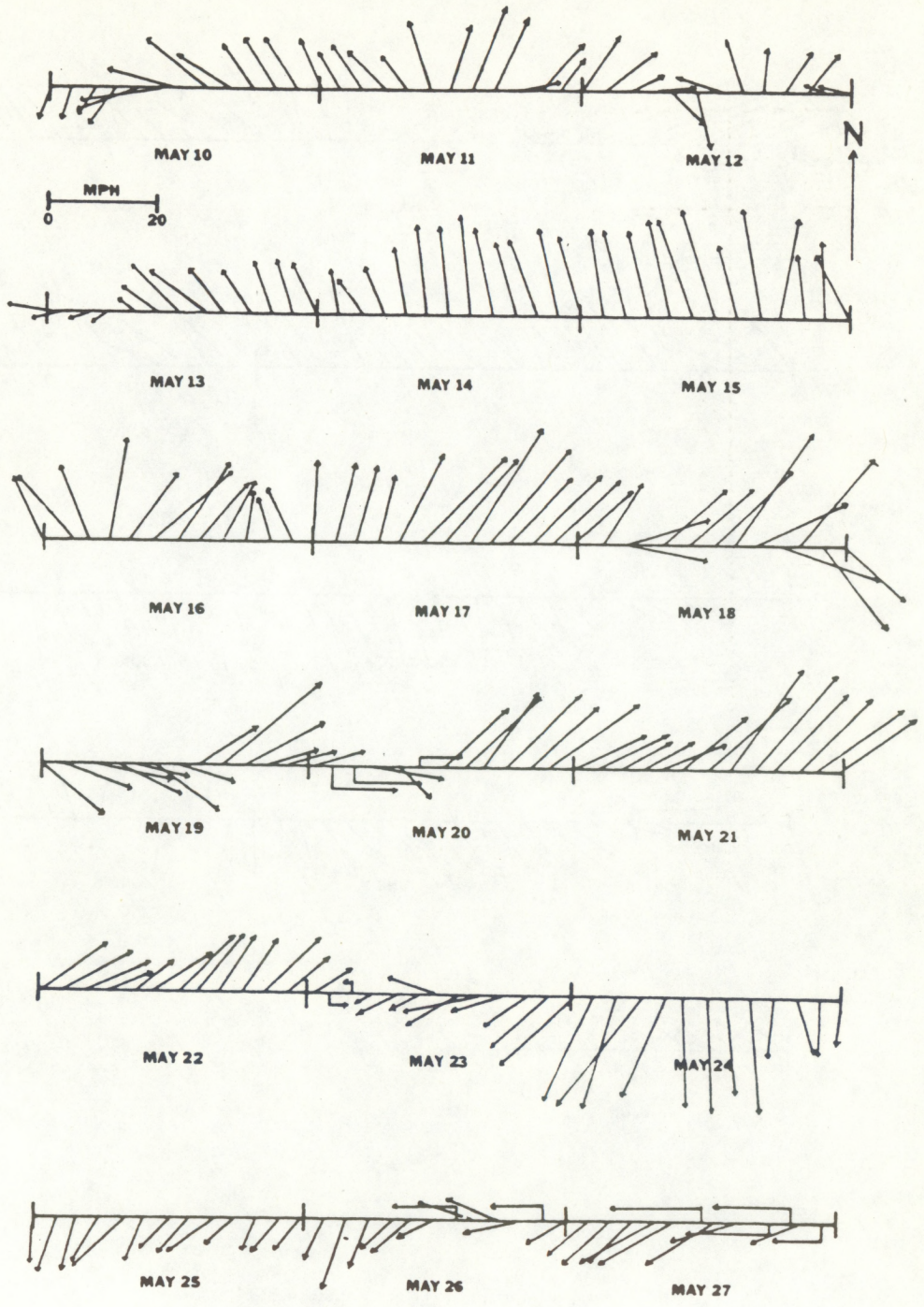

FIGURE 18a.—Vector wind diagram, 1976, 2.5 miles west of Snows Marsh, N.C. (Courtesy of Carolina Power and Light Company).

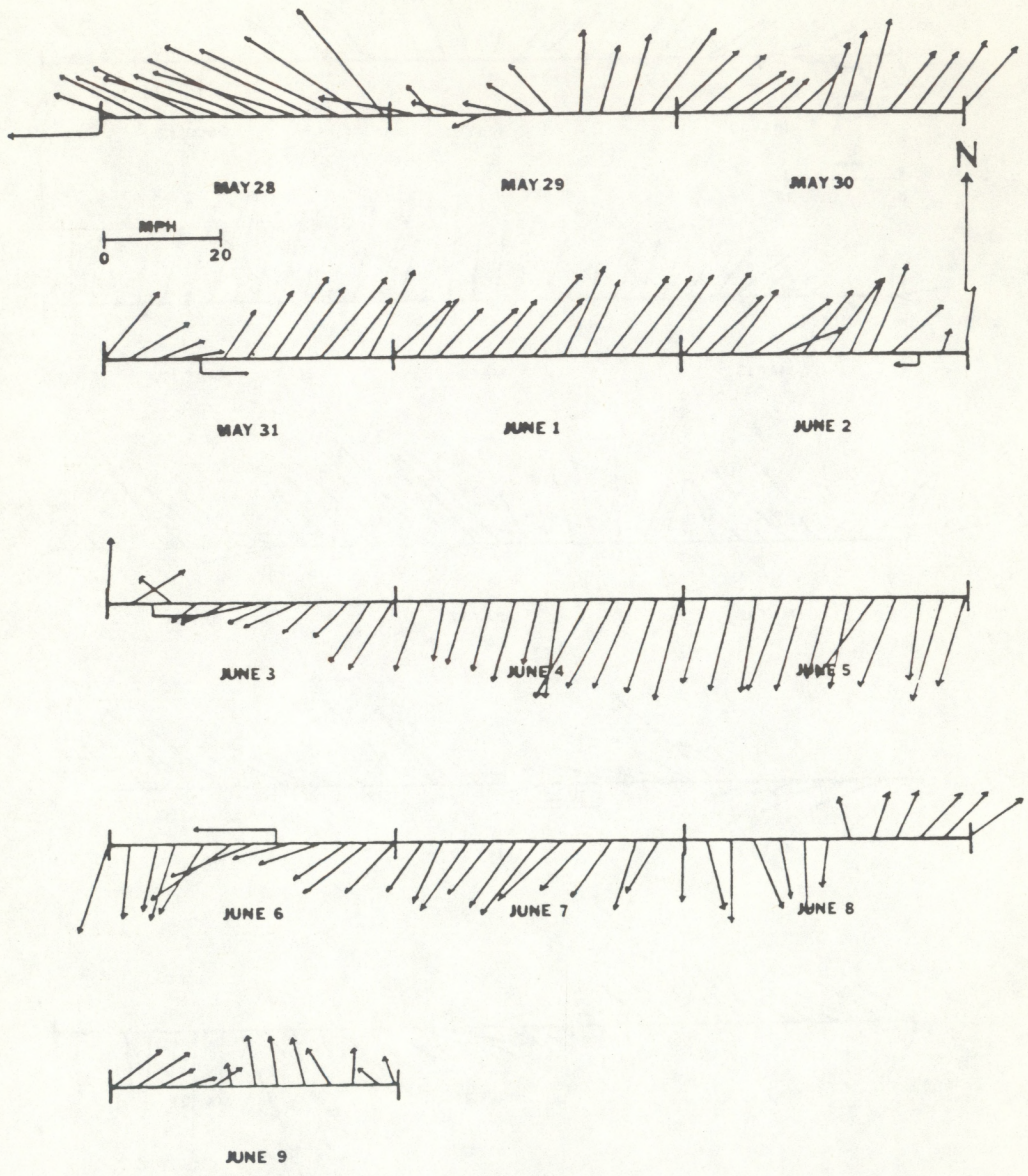

FIGURE 18b.—Vector wind diagram, 1976, 2.5 miles west of Snows Marsh, N.C. (Courtesy of Carolina Power and Light Company).

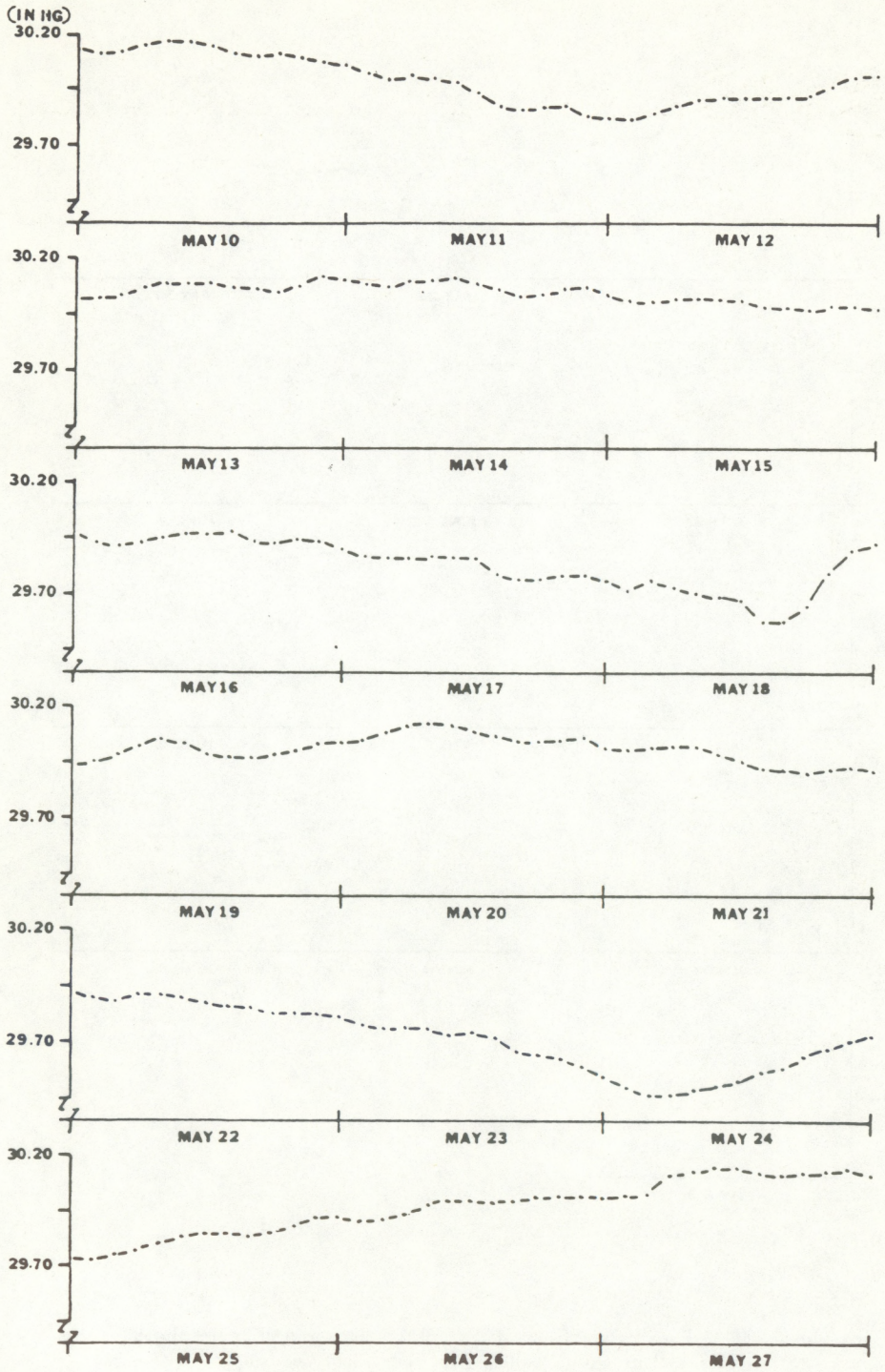

FIGURE 19a.—Barometric pressure data, 1976, 2.5 miles west of Snows Marsh, N.C. (Courtesy of Carolina Power and Light Company)

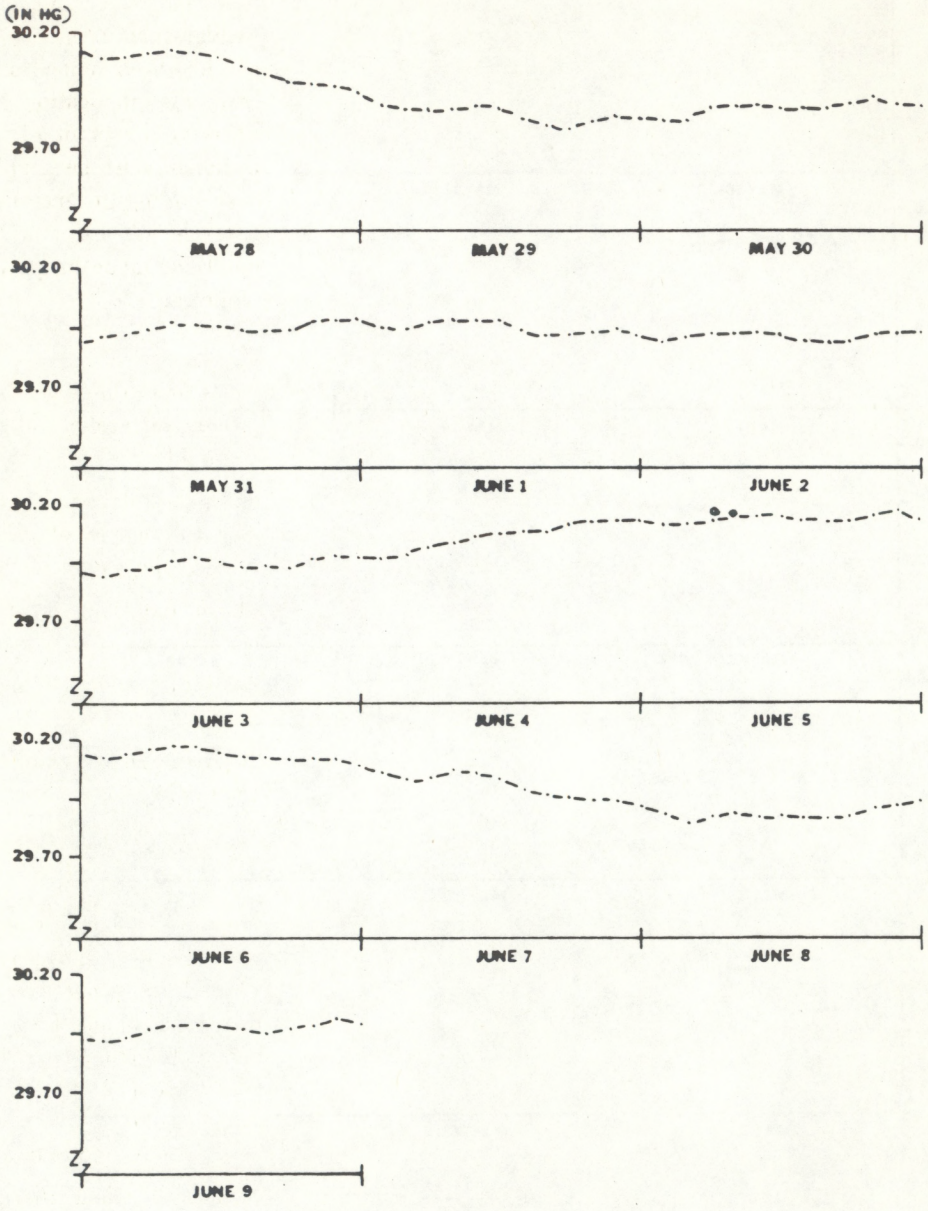

FIGURE 19b.—Barometric pressure data, 1976, 2.5 miles west of Snows Marsh, N.C. (Courtesy of Carolina Power and Light Company)

with the barometric pressure trend as the shifts on 23 May and 28 to 29 May, but it does appear to occur at a relatively low point. The wind shift on 8 June occurs during a barometric pressure low.

To get a better idea of the relative magnitudes of the original time series and the filtered time series (nontidal), the total energy in the frequency domain of the power spectrum of the original series analyzed for Wilmington (T–11) is 1.188, and the total energy in the frequency domain for the filtered series is 0.034 (original value is 35 times the nontidal value). For this report, no attempt has been made to correlate the magnitude of the wind speed and the barometric pressure to the nontidal wave parameters.

There is a difference in duration of floods (slack before flood to slack before ebb) and ebbs (slack before ebb to slack before flood) in a river, whose freshwater outflow generally accentuates the ebb flow (lengthening its duration) and diminishes the flood flow (shortening its duration). Superimposed on this effect is the gravitational effect, due to density differences, that will cause a compensating up river flow along the bottom, which, if the river flow is not too fast, can cause greater flood durations along the bottom. Shallow water effects can also influence the respective durations, but to a far lesser degree than the freshwater river flow. Defant (1961) remarks that the shallow water effects may result in the water level showing a quicker rise and a slower fall which means that the flood will be shorter than the ebb. The duration of floods and ebbs for the tides has been determined from high and low water intervals, the time that it takes for the entire water column to reach its maximum high or low value. Tidal height is a scalar function, and tidal intervals are a function of the tidal height (water level) at a particular location. The average flood and ebb durations for the Cape Fear River were calculated for all tide stations excluding Oak Island Bridge (T–21), Snows Cut (T–13), and Myrtle Sound (T–22), because these stations were not in the main river basin. The results are an ebb duration average of 6.58 hours and a flood duration average of 5.84 hours. Further discussion on the tides in the Cape Fear River will be given in section 7.

3. SIMPLE ONE-DIMENSIONAL TIDAL HYDRODYNAMICS MODEL

3.1. Theory and Application

The following is a description of a one-dimensional analytical model used to describe mathematically the tidal hydrodynamics of a long narrow estuary. Tidal currents, which are more affected by local geography and frictional effects, are not discussed here. This one-dimensional approach is based on the addition of the exponentially damped incident and reflected tidal waves with no cross channel currents or Coriolis force. This approach, which has been used by Redfield (1950) and others, has been refined and modified by Parker (1979) for this application to include the effect of energy loss at the point of reflection. This model is quite useful, because geographic dimensions are eliminated by specifying distance in terms of fractions of a tidal wavelength (M_2 for the Cape Fear River). The assumptions made in the development of this model are as follows:

1. The system is driven only by the periodic rise and fall of the water surface at the river entrance caused by the ocean tide.

2. The period of the tidal wave entering the river is so great that the wavelength of the tidal wave in the river is longer than the length of the river.

3. The length of the river is greater than the width of the river.

4. The width of the river is much greater than the depth of the river.

5. The depth of the river is much greater than the amplitude of the tidal wave.

6. The depth of the river is constant.

As stated earlier, the river is narrow enough that the Coriolis forces have no effect, and cross channel currents can be neglected. In order for the governing equations to reduce to a simple form, the depth of the river must be much greater than the amplitude (0.5 range). In the Cape Fear River, this condition is marginally met in that the river is generally slightly less than 20 times the tidal amplitude.

The distance measured along the length of the river will be given by "x", where $x = 0$ is located at the point of reflection (or point of partial reflection), and the positive x direction is from the river entrance to the point of reflection. The model assumes a simple progressive tidal wave moving up the river, being reflected at a constriction in the river, and then traveling back down the river. The waves have the same amplitude at the point of reflection, and the energy of the reflected wave remains in the same specified frequency as that of the incident wave.

For the purpose of brevity, the mathematical derivation of the governing equations will not be fully developed here (for further information, see Parker, 1979). The representation of the tidal wave may be derived from the equations of motion with the addition of a linearized friction term. The elevation of the incident wave is governed by the following equation:

$$\eta_1 = a_0 e^{-\mu x} \cos(\sigma t - kx) \tag{1}$$

where a_0 is the amplitude of the wave at $x = 0$; t is time measured from the time of high water at $x = 0$; μ is the frictional damping coefficient that is assumed constant for a particular estuary; k is called the wave number ($k = \frac{2\pi}{L}$; L is the wavelength); and σ is the frequency of the wave. In a similar formulation, the reflected wave is governed by the following equation:

$$\eta_2 = \mathrm{pa}_0 e^{\mu x} \cos(\sigma t + kx) \tag{2}$$

where the only differences from (1) are the signs and p, which is the fraction of the incident wave amplitude that is reflected at $x = 0$. The value of p will vary from 0 to 1, and if the energy loss at the reflection point is expressed as a percentage decrease in the amplitude of the reflected wave, the percentage decrease would be $pp = (1-p) \times 100$. At the point of reflection, $x = 0$, η_1 equals η_2, if $p = 1.0$. The incident wave amplitude decreases as it moves toward the reflection point; the reflected wave amplitude decreases as it moves away from the reflection point.

The damping coefficient is being made proportional to the phase change of the wave along the river, as opposed to the actual geographical distance. This is done to avoid the problems of varying frictional effects owing to irregularities along the estuary. The effect of the geographical irregularities is to alter the velocity of the waveform, and consequently, to distort the geographical distribution of the phase change, kx. The phase change during a lapse of time, σt, is measured relative to the time of the high water at the reflection point, and the phase change due to a change of position, kx, is also relative to the reflection point. The expression, $e^{\pm \mu x}$, represents the attenuation of the waves, based on proportions of the wavelength from the reflection point.

By combining the equations for η_1 and η_2, taking the first derivative of the result with respect to time, and setting this result equal to zero, the following equation is derived for σt_H:

$$\sigma t_{\mathrm{H}} = \tan^{-1}\left(-\tan kx \frac{pe^{\mu x} - e^{-\mu x}}{pe^{\mu x} + e^{-\mu x}}\right) \tag{3}$$

where t_H is the time of high water, and σt_H is the phase of high water. Both t_H and σt_H are relative to the time or phase of high water at the point of reflection.

When equation (3) is substituted into the equation for the superposition of η_1 and η_2 and reduced, the equation for the high water elevation becomes

$$\eta_H = a_0 \sqrt{2p \cos 2kx + p^2 e^{2\mu x} + e^{-2\mu x}}. \tag{4}$$

At the closed end of the river ($x = 0$, river constriction), the high water elevation is

$$\eta_0 = (1 + p) a_0, \tag{5}$$

and the ratio of the high water elevation at any point along the river to the high water elevation at the closed end is

$$\frac{\eta_H}{\eta_0} = \frac{1}{1 + p} \sqrt{2p \cos 2kx + p^2 e^{2\mu x} + e^{-2\mu x}}. \tag{6}$$

The incident and reflected waves have the same amplitude at the point of reflection (if $p = 1.0$), and as one moves down the estuary away from the closed end, the amplitude of the reflected wave relative to the amplitude of the incident wave decreases. Incident and reflected waves of equal amplitudes would cancel each other out at $kx = -90°$ and result in a node (a point of zero range), if there was no damping. For the case of large frictional damping, the reflected wave will decrease rapidly relative to the incident wave.

By including energy loss at the point of reflection, this model has greater utility. This energy loss is incorporated into the model using the p term in the reflected wave, which tells what portion of the incident wave amplitude at $x = 0$ is reflected. For example, if someone specified a "10 percent of amplitude lost at the reflection point," this would mean that 90 percent of the wave at that point is going to be reflected back down the river. The length of the estuary relative to the wavelength of the tidal wave in the estuary, the

amount of frictional damping, and the amount of energy loss at the point of reflection will determine how the high water at the estuary entrance will be modified at the point of reflection. The dimensions of the estuary determine how the wave will be amplified by the estuary.

3.2. Model Results for the Cape Fear River

The results of equations (6) and (3), $\frac{\eta_H}{\eta_0}$ and σt_H, are plotted in figure 20 for the Cape Fear River. For the M_2 tidal wave, one point is plotted for each station in table 9. The numbers corresponding to the stations in table 9 are the numbers plotted on the graph in figure 20. Wilmington was chosen as the point of partial reflection, because it is around this area that the river constricts and divides. The M_2 range at each station divided by the M_2 range at Wilmington is plotted along the vertical axis. The difference between the M_2 epochs (κ') at each station and the M_2 epoch at Wilmington is plotted along the horizontal axis, σt_H. The percentage of amplitude decrease (pp) at the point of partial reflection was varied until a best fit for μ was established.

TABLE 9.—M_2 tide ranges and epochs used for the one-dimensional tidal hydrodynamics model

Number on Plot	Constituent[1] Range (feet)	Epoch[2] (κ')	Station
1	3.93	281.9	Wilmington (T–11)
2	3.90	281.0	Exxon Pier (T–09)
3	3.86	273.0	Marker 43A Campbell (T–08)
4	3.83	262.3	Orton Point (T–07)
5	3.83	255.6	MOTSU Wharf No. 3 (T–14)
6	3.80	256.0	Upper Midnight Chan. (T–06)
7	3.77	253.4	MOTSU Wharf No. 2 (T–05)
8	3.81	252.0	Lower Midnight Chan. (T–04)
9	3.73	252.0	MOTSU Wharf No. 1 (T–19)
10	3.76	251.2	Reaves Pt. Channel (T–03)
11	3.77	243.6	Zekes Island (T–10)
12	4.03	226.5	Southport (T–02)
13	4.26	217.9	Baldhead (T–01)

[1] Constituent range is twice the M_2 amplitude.
[2] Epoch, in degrees, relative to the 75°W time meridian.

Results of the model indicate that there is a 20-percent loss of amplitude in the reflected wave at Wilmington. The wave that continues up the river must have the same amplitude, by continuity, as the wave at the point of partial reflection; it will, however, be steadily reduced by frictional damping. The river becomes more shallow and narrow north of Wilmington, and the M_2 amplitude decreases from 1.965 ft at Wilmington (T–11) down to 1.840 ft north of Wilmington at Navassa (T–15). The kx value at the entrance, $-72°$, indicates that there is not a node in the system, because only about 0.20 of the M_2 wave can fit in the estuary. With the high damping coefficient of $\mu = 4.0$, both the incident and the reflected waves are reduced quickly (55 percent in only 0.2 of a M_2 wavelength). Near the mouth, the reflected wave is very small compared to the incident wave, and near the reflection point both waves are nearly the same and added together are about 92 percent of the incident wave at the mouth. The reflected wave tends to subtract slightly from the incident wave progressing down the river from the point of reflection, because it gets more out of phase with the incident wave as it moves away from the reflection point. The reflected wave subtracts from the incident wave until the reflected wave becomes too small and then the tide range begins to increase again. The resultant tidal wave at $kx = -47°$ shows how the M_2 amplitude decreases at that point and increases slightly for those values larger and smaller than $kx = -47°$.

Section 2 states that an explanation would be given for the decrease in M_2 amplitudes around MOTSU Wharf No. 1 (T–19), $kx = -47°$. Figure 20 shows that this decrease is a result of the superposition of the incident and reflected highly damped progressive tidal waves in this area. Further implications of this simple model will be discussed in section 7.

4. CURRENT DATA, DESCRIPTION AND ANALYSIS

4.1. Locations of Current Stations and Installation Information

The TICUS current system, deployed and monitored from the NOAA Ship FERREL, was used to gather all current data. Each station was located by a simultaneous three-point sextant fix to prominent land marks to verify its geographic location.

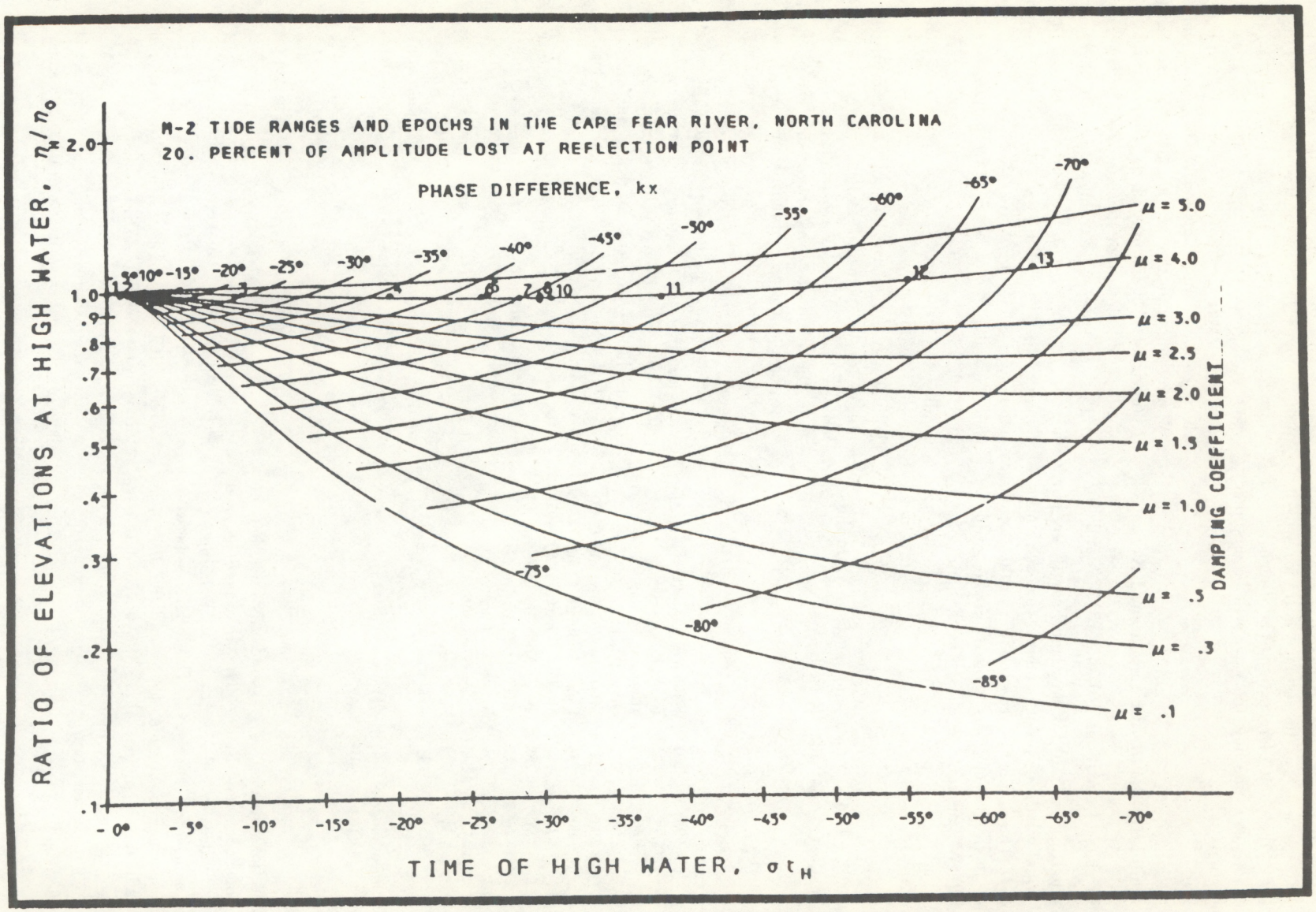

FIGURE 20.—Ratio of elevation at high water, η_H/η_0, to time of high water, σt_H (Parker, 1979).

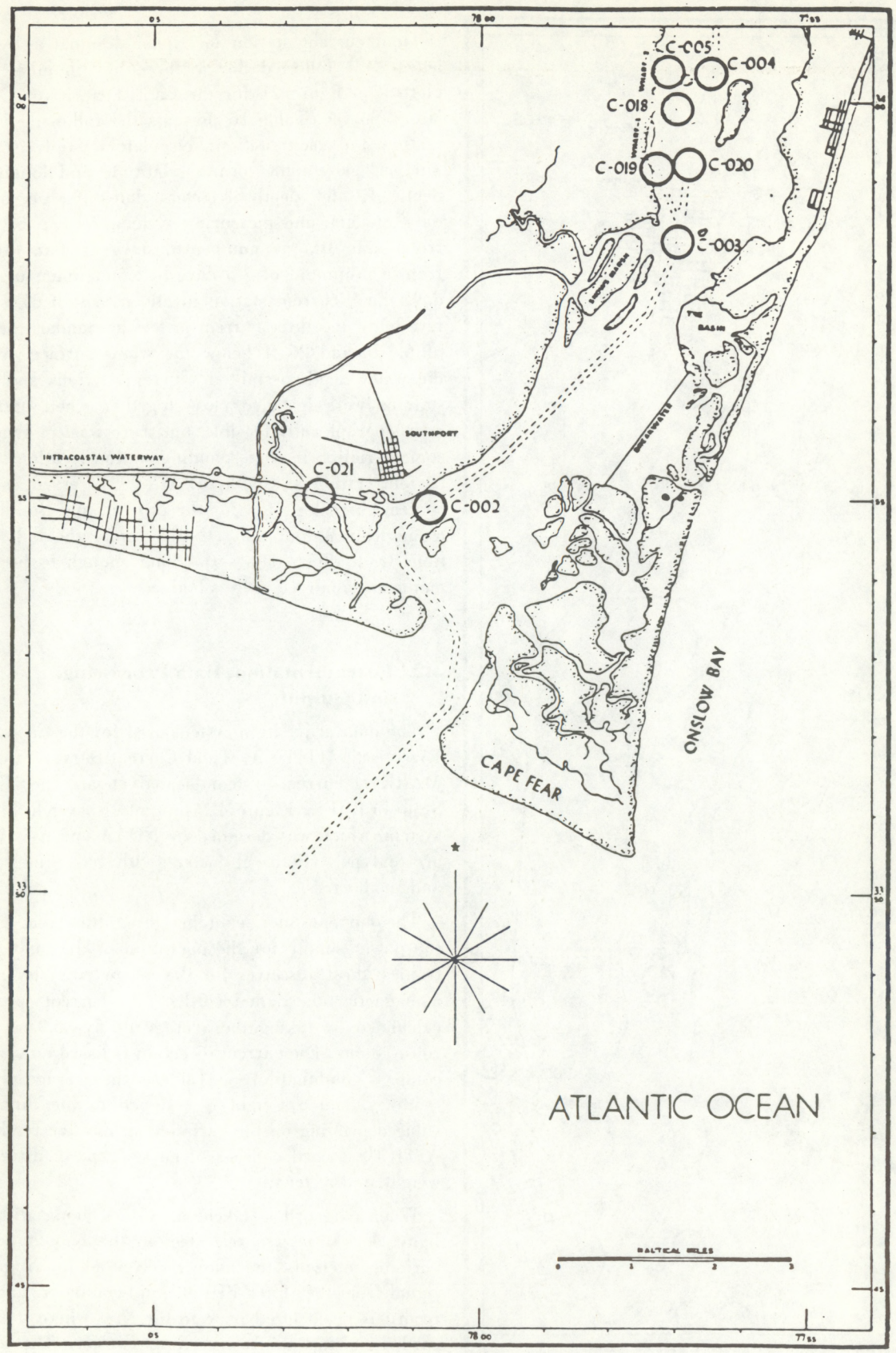

FIGURE 21.—Tidal current station locations.

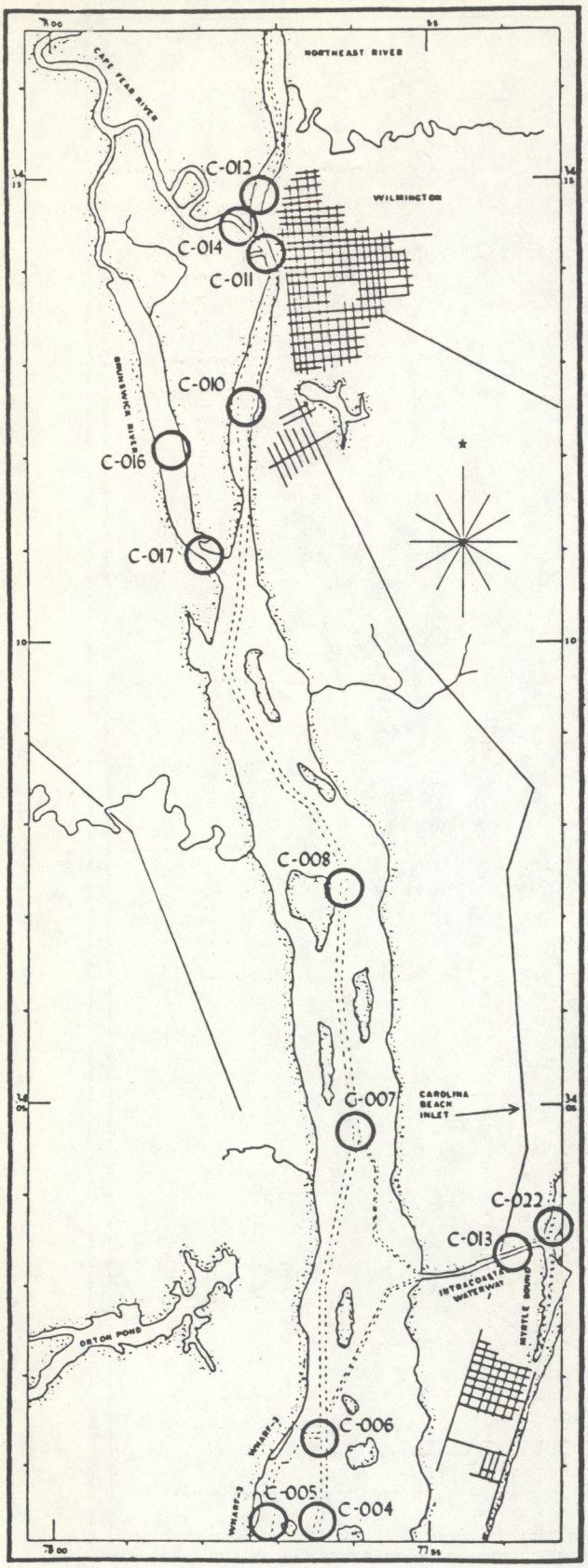

FIGURE 21.—Continued.

Tidal current station locations, designated by the letter "C" followed by a three-digit number, are plotted on figure 21 for the Cape Fear River Circulatory Survey. Table 10 presents the following information for each station: circulatory study station number, geographic location, latitude and longitude, depth of water, depth of meters, dates of observation, days of data, and measuring system. As can be seen from table 10, the number of days of data ranged from a minimum of 3.5 days to a maximum of 36.8 days. Each current station ideally consisted of a surface buoy and three current meters at standard depths of 6, 16, and 26 ft below the water surface, where the water depth permitted. Current stations and tide stations were installed close together when possible and geographically feasible, but there was, in general, some variation in corresponding station locations. The current station at Southport (C–002) served as the control current station for the project, and Southport along with Wilmington (C–011) were the only stations from which data series long enough to be harmonically analyzed were obtained.

4.2. Instrumentation, Data Processing, and Output

The data acquisition system used for the Cape Fear River is the TICUS I (Tidal Current Survey System) MARK II current system located aboard the NOAA Ship FERREL. Figure 22 presents a sketch of the system, which was designed by NOAA and uses Richardson-type cylindrical meters with Savonius rotors and small vanes.

The current buoy contains three tubs that house the power supply for the operation of the buoy electronics, the transceiver for the telemetry system, and a magnetic tape data recorder. The current speed is calculated by taking the average of five 5.8 seconds rotor counts. The current direction is based on a vane-compass combination: its value is the average of five readings, and a weight is assigned to the direction value depending on the variation in the five readings. A TICUS record consists of current speed, direction, weight, and meter tilt.

When a record is taken, its values along with the buoy clock time are recorded on the buoy tape. At periodic intervals, the buoy receives an interrogation signal from the ship's PDP–8 mini-computer, and the record is telemetered back to the ship where it is recorded on the ship's recording console. The ship's personnel will also manually interrogate the buoys

TABLE 10.—Tidal current stations occupied during the Cape Fear River Circulatory Survey

Circulatory Survey Station Number	Station	Latitude (N)	Longitude (W)	Depth[2] of Water (FT)	Depth[3] of Meter (FT)	Dates of Observation	Days of Data	Type of System
C-002[1]	Southport	33°54.9'	78°00.7'	44	-6	14 May 1976 - 01 June 1976	18.5	TICUS
						08 June 1976 - 18 June 1976	10.0	TICUS
					-16	13 May 1976 - 19 June 1976	36.8	TICUS
					-26	13 May 1976 - 19 June 1976	36.8	TICUS
C-003[1]	Horseshoe Shoal	33°58.2'	77°56.9'	39	-6	10 May 1976 - 21 May 1976	10.7	TICUS
					-16	10 May 1976 - 21 May 1976	10.7	TICUS
					-26	10 May 1976 - 21 May 1976	10.7	TICUS
C-004[1]	Reaves Pt.,0.8 miles NE of	34°00.4'	77°56.5'	41	-6	10 May 1976 - 21 May 1976	10.8	TICUS
					-16	10 May 1976 - 21 May 1976	10.8	TICUS
					-26	10 May 1976 - 21 May 1976	10.8	TICUS
C-005[1]	Reaves Pt.,0.4 miles N of	34°00.4'	77°57.2'	31	-6	15 May 1976 - 24 May 1976	9.5	TICUS
					-16	15 May 1976 - 24 May 1976	9.5	TICUS
					-26	15 May 1976 - 24 May 1976	9.5	TICUS
C-006[1]	Upper Midnight Channel	34°01.3'	77°56.4'	44	-6	25 May 1976 - 29 May 1976	3.5	TICUS
					-16	25 May 1976 - 29 May 1976	3.5	TICUS
					-26	25 May 1976 - 29 May 1976	3.5	TICUS
C-007[1]	Doctor Pt., 0.6 miles NNW of	34°04.7'	77°56.0'	40	-6	25 May 1976 - 01 June 1976	7.1	TICUS
					-16	25 May 1976 - 01 June 1976	7.1	TICUS
					-26	25 May 1976 - 01 June 1976	7.1	TICUS
C-008[1]	Campbell Island	34°07.2'	77°56.2'	43	-6	24 May 1976 - 02 June 1976	8.5	TICUS
					-16	24 May 1976 - 02 June 1976	8.5	TICUS
					-26	24 May 1976 - 30 May 1976	6.3	TICUS
C-010[1]	Dram Tree Pt., 0.8 miles N of	34°12.6'	77°57.5'	40	-26	02 June 1976 - 10 June 1976	7.6	TICUS
C-011[1]	Wilmington	34°14.2'	77°57.2'	41	-6	24 May 1976 - 08 June 1976	15.0	TICUS
					-20	24 May 1976 - 08 June 1976	15.0	TICUS
C-012	Turning Basin	34°14.8'	77°57.2'	33	-6	08 June 1976 - 17 June 1976	9.0	TICUS
					-20	08 June 1976 - 17 June 1976	9.0	TICUS
C-013[1]	Snows Cut	34°03.4'	77°54.0'	17	-6	11 June 1976 - 19 June 1976	7.9	TICUS
C-014	Point Peter	34°14.5'	77°57.5'	26	-6	10 June 1976 - 17 June 1976	6.6	TICUS
C-016	Brunswick River, 1.8 miles N of mouth	34°12.3'	77°58.5'	10	-6	02 June 1976 - 10 June 1976	7.9	TICUS

TABLE 10.— Continued.

Circulatory Survey Station Number	Station	Latitude (N)	Longitude (W)	Depth of Water (FT)	Depth of Meter (FT)	Dates of Observation	Days of Data	Type of System
C-017	Brunswick River, 0.4 miles N of mouth	34°10.9'	78°58.0'	26	-6	02 June 1976 - 10 June 1976	7.6	TICUS
					-16	02 June 1976 - 10 June 1976	7.6	TICUS
C-018	Reaves Pt., 0.3 miles E of	33°59.9'	77°57.0'	35	-6	11 May 1976 - 21 May 1976	9.7	TICUS
					-16	11 May 1976 - 21 May 1976	9.7	TICUS
					-26	11 May 1976 - 21 May 1976	9.7	TICUS
C-019	Sunny Point	33°59.2'	77°57.3'	36	-6	11 May 1976 - 21 May 1976	9.6	TICUS
					-16	11 May 1976 - 21 May 1976	9.6	TICUS
					-26	11 May 1976 - 21 May 1976	9.6	TICUS
C-020	Reaves Pt. Channel	33°59.1'	77°55.8'	40	-6	10 May 1976 - 21 May 1976	10.8	TICUS
					-16	10 May 1976 - 21 May 1976	10.8	TICUS
					-26	10 May 1976 - 21 May 1976	10.8	TICUS
C-021	Intracoastal Waterway, 1.1 miles W of Southport	33°55.1'	78°02.5'	12	-6	11 June 1976 - 19 June 1976	7.8	TICUS
C-022	Myrtle Sound	34°04.7'	77°53.4'	19	-6	11 June 1976 - 19 June 1976	8.0	TICUS

[1]Station has been occupied prior to this survey, see section 6.

[2]In reference to mean low water.

[3]Feet below surface.

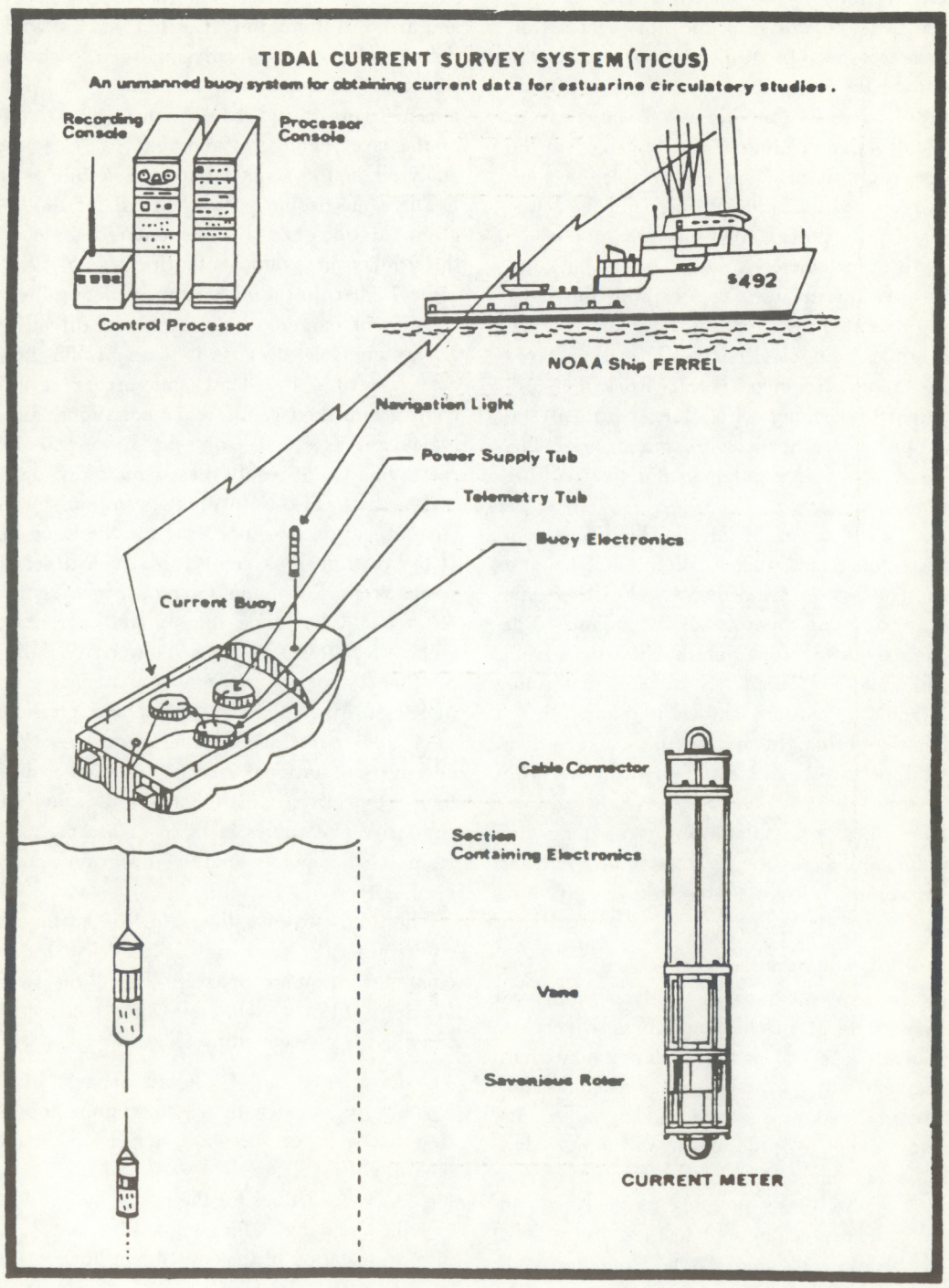

FIGURE 22.—Tidal Current Survey System (TICUS).

several times a day to ensure that the meters are operating properly and that the buoy times are not drifting from the ship's console clock time.

The TICUS system can be operated in several different modes. In Mode 1, the records are telemetered back and recorded onboard ship and not recorded on the buoy data recorder. In Mode 2, the records are recorded onboard the buoy but not on the ship; Mode 2 is generally used when the ship is too far away to receive the buoy's signal. Mode 3, as described in the previous paragraph, is the most desirable, because the record is recorded on both the ship and the buoy.

For processing purposes, NOS prefers to use the buoy tapes with the telemetered data tapes as backups. Shipboard processing includes transcribing the buoy tape data onto computer compatible tape and correcting for bad times and clock drift. The telemetered and processed tapes are then sent to Rockville, Md. (NOS Headquarters) along with other pertinent station information, where headers are put on each file, some missing data are interpolated, and final editing is completed.

The current speed accuracy of the TICUS system is 2 cm per second for a meter tilt up to 10°, and the direction accuracy is ±2.5 degrees. For the Cape Fear River, a sampling interval of 12 minutes was used. It is necessary to point out that the data from three stations could not be processed, and that some of the data from the stations shown in figure 21 required extensive editing. Most bad data and system malfunctions appear to be the result of problems with the buoy electronics.

NOS current data are available on cards, magnetic tape, microfilm, and computer listings. Tidal current data requests should be sent to the address given in section 2.2.

4.3. Methods of Analysis

The three different methods of analysis employed for the current data from the Cape Fear River are harmonic analysis, spectral analysis, and rotary analysis. Tidal current ellipses of the main harmonic constituents were graphically displayed from the results of the harmonic analysis of the major and minor components of the current records from Southport and Wilmington. Each of these methods of analysis and some of the problems encountered in their use will be discussed in this section, and results from the analyses will be discussed in section 4.4.

Unfortunately, there were only two stations that had data series long enough to be harmonically analyzed. The 29-day harmonic analysis computer program described in section 2.3 was used to analyze the records from Southport (C–002) at the depths of −16 and −26 ft below the water surface. A special version of the 29-day program with additional inference and correction formulas was used to analyze the 15-day current records from Southport (C–002) at −6 ft and from Wilmington (C–011) at −6 and −20 ft. Before being harmonically analyzed, each data record was first broken down into major and minor components (the major component being the alignment of the river channel), and then each component was analyzed in the same manner as a tide series.

The same problems that existed for the 29-day program for tides are still encountered for currents. For the 15-day program, only the M_2, S_2, K_1, O_1, and some higher harmonics can be determined. The N_2 constituent can not be determined directly from the 15-day analysis, because it takes 27.555 days to separate N_2 from M_2. The same errors resulting from equilibrium theory, inference equations, and meteorological forces are still present. It was possible to correct 29-day tide results based on a 365-day tide control station, but unfortunately a long-term primary current station does not exist for the Cape Fear River. If the relationships among tidal constituents were the same as those among current constituents, then an effort could be made to estimate current constituent values for those stations between Wilmington and Southport, but the current constituents are generally more sensitive to geographical and physical changes than tidal constituents; therefore, even if both tide and current stations were in the exact same locations, their respective constituents would not be affected similarly. The values in table 11 are the actual results from the harmonic analysis programs and have not been corrected.

The tidal current ellipses for the harmonic constituents were calculated and graphically displayed by a computer graphics program based on Doodson and Warburg (1941). The following parameters are determined from each ellipse:

1. Orientation of the major axis of the ellipse (usually identical with the maximum flood-ebb direction, except when the flood and ebb directions are not separated by 180°).
2. Speed values for the major and minor axes.
3. Time angles for each axis.
4. Rotation of the constituent flow.

The major and minor time angles are basically epochs for the respective parts of that constituent's cycle relative to a reference time meridian (75°W for the Cape Fear River). The value for the time of maximum flood for the constituent relative to the reference time

meridian is given in degrees and hours. The small dots on the ellipse, if connected to the center, represent the direction of flow for each hour of the constituent cycle (with 0 hour being the time of the maximum astronomic force over the 75°W time meridian). Sample ellipses for the five main constituents at the three depths for Southport (C–002) and the two depths for Wilmington (C–011) are shown in figures 23a through 23c and figures 24a and 24b.

The exact direction of maximum constituent flow is a valuable result from ellipse analysis. If it had been possible to plot ellipses for each current station, then the ellipses could be transferred to a chart of the Cape Fear River, and the direction and magnitude of flow for each constituent could be accurately determined for each standard depth at each station. Ellipses provide knowledge about the rotary tidal current flow at a particular station. A common occurrence is the reversal in rotation from the surface to the bottom. It is easily seen how essential it is to have current record lengths of at least 15 days from the water surface down to the bottom to describe accurately the water movement at that station location.

Program CURNT, described in section 2.3, was employed for the current data from each station on the Cape Fear River. The results from each station have been used to investigate the relative magnitude of the energy at each frequency in the power spectrum and to compare the Doodson-filtered series (power spectra and data plot) to the original tidal current series.

Tidal current parameters can be calculated from short records (less than 15 days) or long records by using a nonharmonic comparison analysis. Current data from nearby locations will have similar harmonic characteristics. If the data series from one station is long enough to harmonically analyze, then that data series can be compared to a shorter data series, and time differences and velocity ratios can be computed to calculate tidal current parameters for the short-term station.

NOS uses a half-hourly rotary reduction to calculate tidal parameters for short-term stations from a long-term accepted reference station by use of a computer program called ROTARY (Parker, 1977) adapted from manual techniques found in Special Publication No. 215 (1950). Results from program ROTARY include the following: maximum ebb and flood times, speeds, and directions (Greenwich Mean Time): slack before ebb and flood times, speeds, and directions: maximum observed current velocity and direction: nontidal current velocity and direction: and the velocity and direction for each half-hour interval for the entire tidal cycle.

4.4. Results of Analysis

Table 11 presents values obtained from the tidal current ellipses in figures 23a through 24b, graphed from the major and minor components of the harmonic constituents. P_1 is not included, because it was inferred for all five time series, and although N_2 is included, it was inferred for the 15-day series. The following parameters are given for each constituent: (1) direction of the major axis in degrees true (flood direction), (2) amplitudes (speeds) of the major and minor axes in knots, (3) epoch for the maximum flood strength of the major axis relative to the 75°W meridian, and (4) rotation of the ellipse. To get the epoch of the minor axis, add 90° to the major axis epoch if the rotation is clockwise, and subtract 90° if the rotation is counterclockwise.

All of the ellipses are drawn to the same scale; the longer the ellipse, the greater the current speed. In studying the ellipses, the two most prominent features are the relative magnitude of the M_2 constituent compared to the other constituents, and that the current flow is almost purely reversing. For Southport (C–002), the major M_2 amplitude varies from a maximum of 2.28 kn at −6 ft to a minimum of 1.85 kn at −26 ft. The M_2 value at −6 ft is the largest constituent value for the study area. The next largest constituent value at Southport (C–002) is N_2, and its major amplitude values range from a maximum of 0.44 kn at −6 ft to a minimum of 0.38 kn at −26 ft. At Wilmington (C–011), the major M_2 amplitude ranges from a maximum of 1.48 kn at −6 ft to a minimum of 1.43 kn at −20 ft. The next largest constituent at Wilmington (C–011) is S_2 whose major amplitude varies from 0.46 kn at −6 ft to 0.36 kn at −20 ft. The extent to which the currents are reversing can be determined by comparing the amplitudes of the major and minor components for each constituent. As can be seen from the ellipses, the minor components are negligible for both Wilmington and Southport. Results from current direction histograms for all of the current stations indicate that the directions of flow generally coincide with the channel configuration as indicated by the flow at both Southport and Wilmington.

Before elaborating further on the results from the harmonic analysis of the current data from Southport (C–002) and Wilmington (C–011), it is necessary to discuss the nature of tidal currents and problems that exist in the analysis of tidal current data. For tides, one is analyzing a scalar function of height: whereas

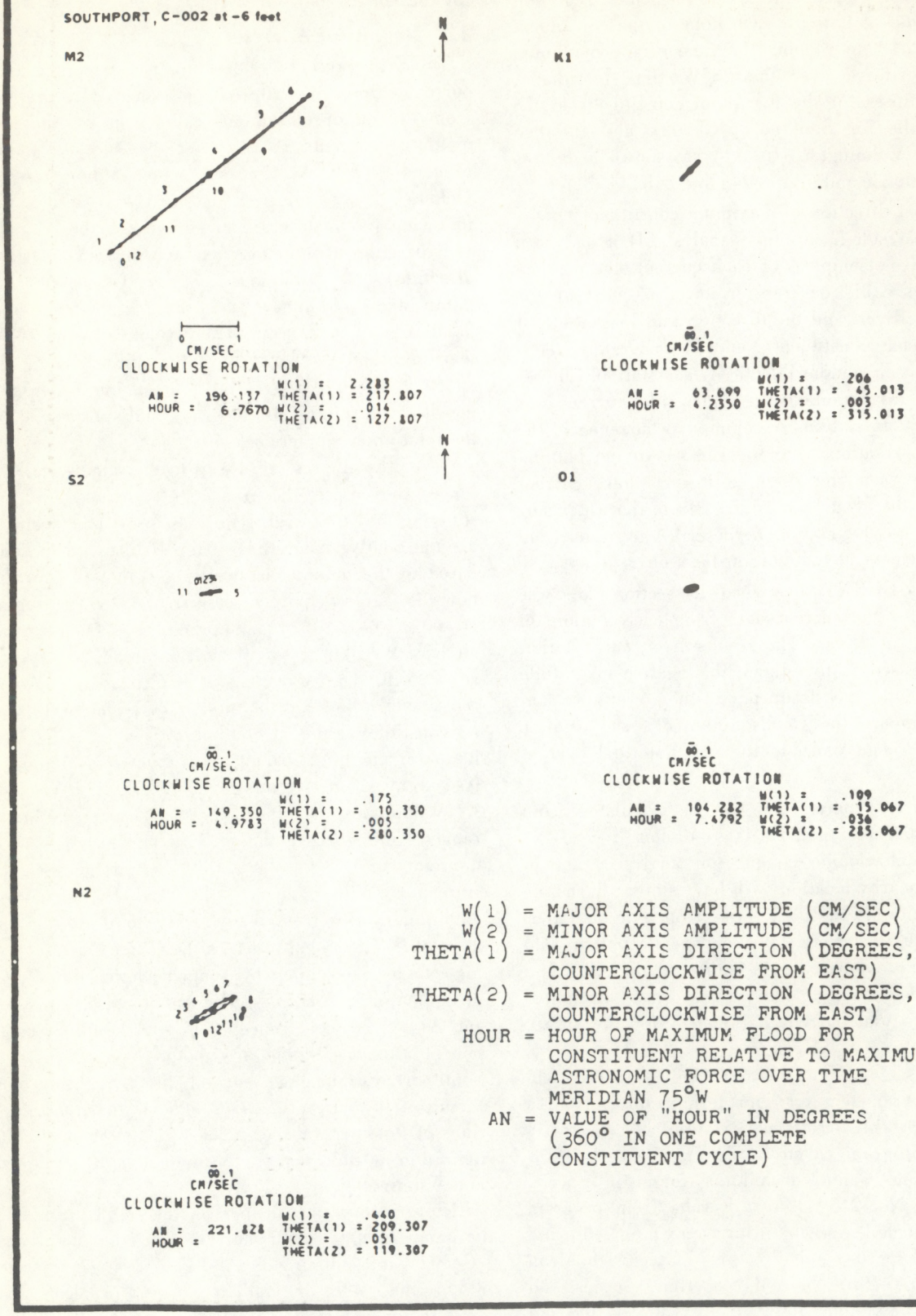

FIGURE 23a.—Tidal current ellipses for —6-foot depth at station C–002.

SOUTHPORT, C-002 at -16 feet

M2

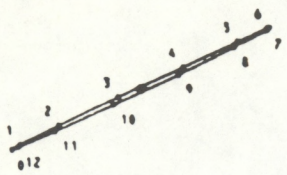

CM/SEC

CLOCKWISE ROTATION

AN = 186.855
HOUR = 6.4468

W(1) = 2.060
THETA(1) = 205.613
W(2) = .038
THETA(2) = 115.613

K1

CM/SEC

CLOCKWISE ROTATION

AN = 63.877
HOUR = 4.2469

W(1) = .165
THETA(1) = 31.749
W(2) = .023
THETA(2) = 301.749

S2

CM/SEC

CLOCKWISE ROTATION

AN = 186.266
HOUR = 6.2088

W(1) = .233
THETA(1) = 204.895
W(2) = .019
THETA(2) = 114.895

O1

CM/SEC

COUNTER-CLOCKWISE ROTATION

AN = 91.422
HOUR = 6.5568

W(1) = .078
THETA(1) = 18.519
W(2) = .006
THETA(2) = 108.519

N2

CM/SEC

CLOCKWISE ROTATION

AN = 165.545
HOUR = 5.8209

W(1) = .413
THETA(1) = 31.200
W(2) = .029
THETA(2) = 301.200

W(1) = MAJOR AXIS AMPLITUDE (CM/SEC)
W(2) = MINOR AXIS AMPLITUDE (CM/SEC)
THETA(1) = MAJOR AXIS DIRECTION (DEGREES, COUNTERCLOCKWISE FROM EAST)
THETA(2) = MINOR AXIS DIRECTION (DEGREES, COUNTERCLOCKWISE FROM EAST)
HOUR = HOUR OF MAXIMUM FLOOD FOR CONSTITUENT RELATIVE TO MAXIMUM ASTRONOMIC FORCE OVER TIME MERIDIAN 75°W
AN = VALUE OF "HOUR" IN DEGREES (360° IN ONE COMPLETE CONSTITUENT CYCLE)

FIGURE 23b.—Tidal current ellipses for —16-foot depth at station C-002.

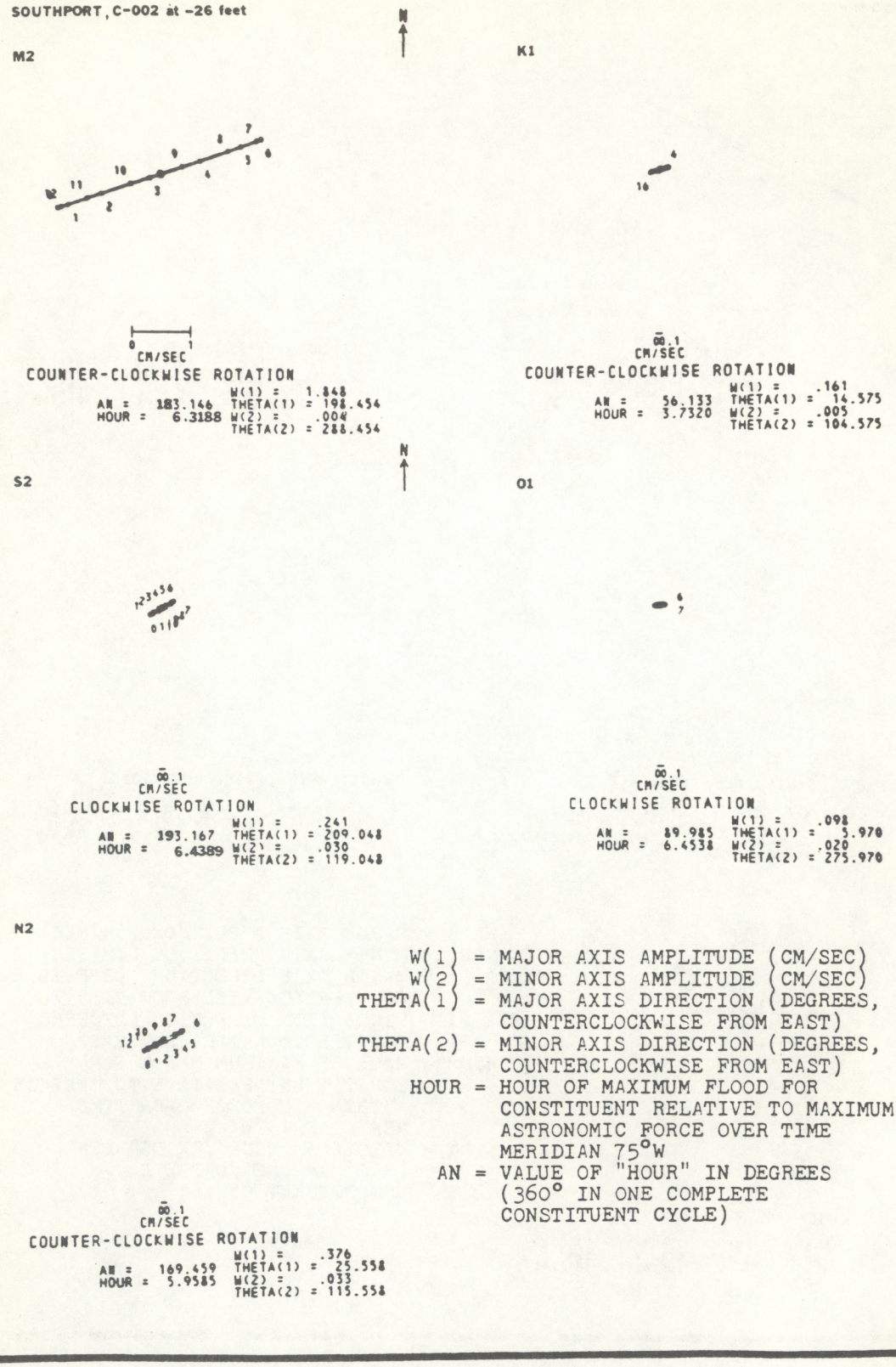

FIGURE 23c.—Tidal current ellipses for —26-foot depth at station C–002.

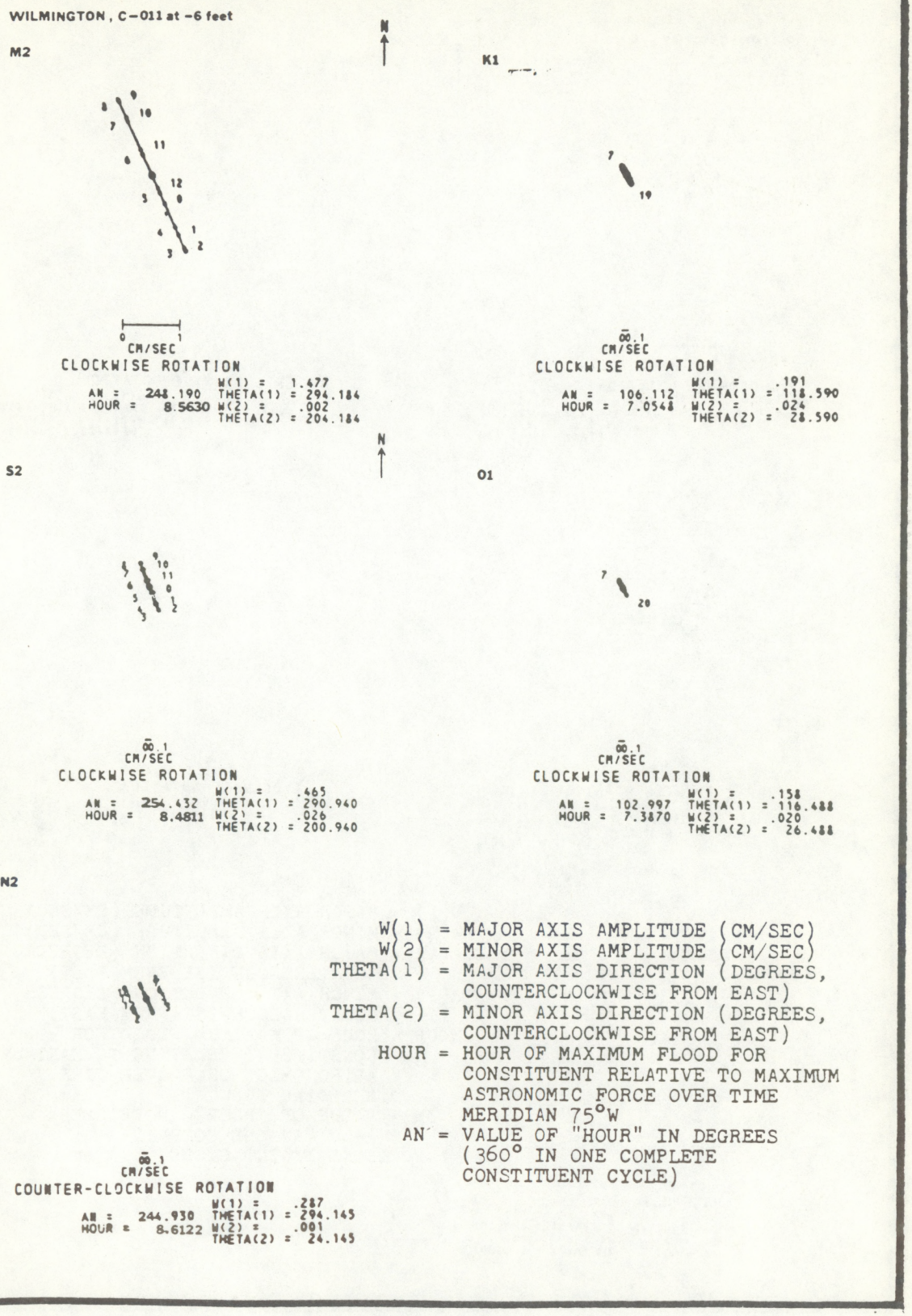

FIGURE 24a.—Tidal current ellipses for —6-foot depth at station C–011.

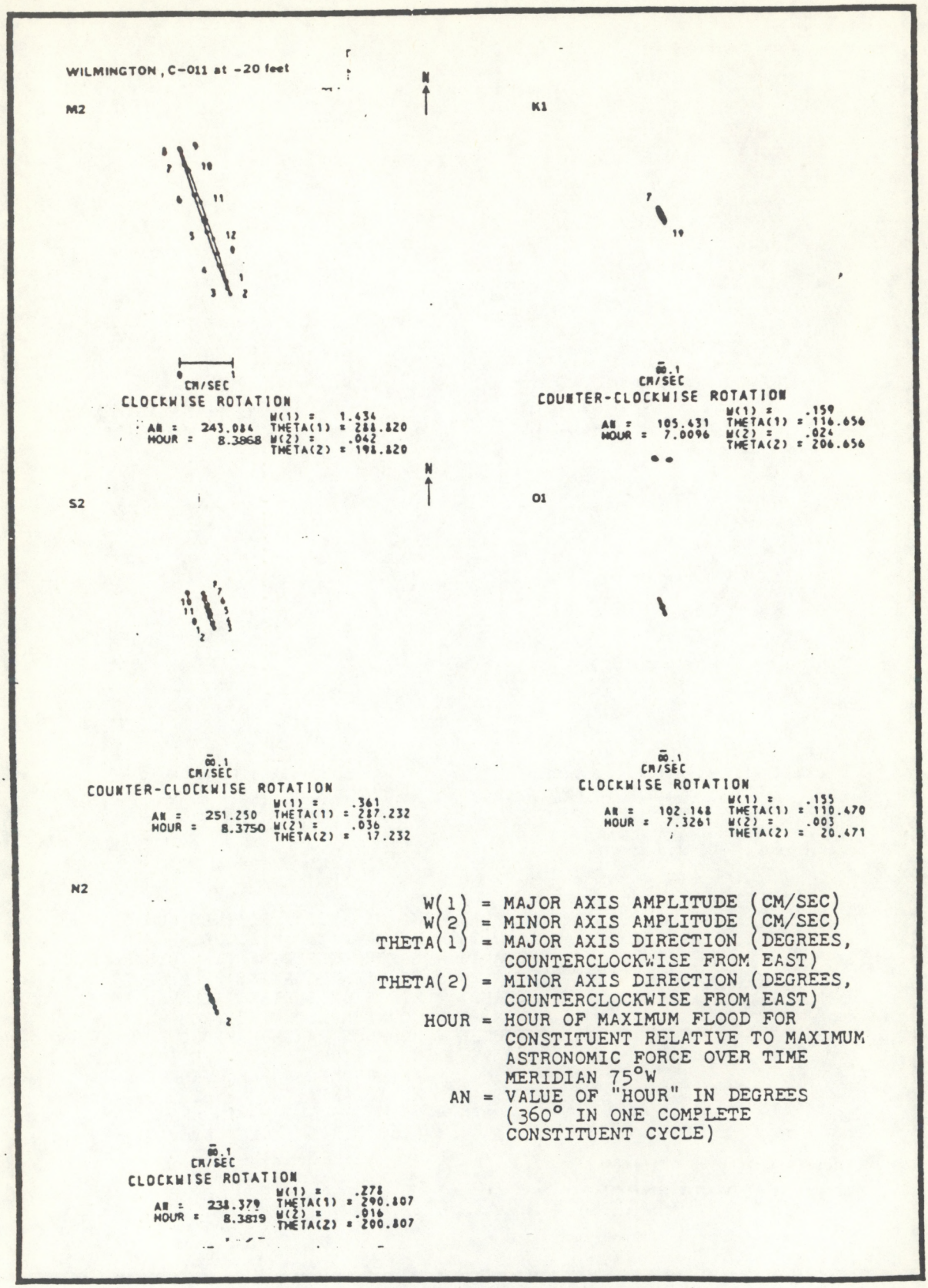

FIGURE 24b.—Tidal current ellipses for —20-foot depth at station C–011.

TABLE 11.—Five most important harmonic constants for five current station depths

Stat. No.	Depth[1] of Data (ft)	Approx. Water Depth (ft)	Length of Series (Days)	Beginning of Series	M_2					S_2				
					Major[2] Dir. (°)	Speed (kts)		Major[3] Epoch	Rot.[4]	Major Dir. (°)	Speed (kts)		Major Epoch	Rot.
						Major	Minor				Major	Minor		
C-002	-6	44	15	16 May 1976	52	2.28	0.01	196	C	80	0.18	0.00	149	C
C-002	-16	44	29	19 May 1976	64	2.06	0.04	187	C	65	0.23	0.02	186	C
C-002	-26	44	29	19 May 1976	72	1.85	0.00	183	CC	61	0.24	0.03	193	C
C-011	-6	41	15	24 May 1976	336	1.48	0.00	248	C	339	0.46	0.03	254	C
C-011	-20	41	15	24 May 1976	341	1.43	0.04	243	C	343	0.36	0.04	251	CC

Stat. No.	N_2					K_1					O_1				
	Major Dir. (°)	Speed (kts)		Major Epoch	Rot.	Major Dir. (°)	Speed (kts)		Major Epoch	Rot.	Major Dir. (°)	Speed (kts)		Major Epoch	Rot.
		Major	Minor				Major	Minor				Major	Minor		
C-002	61	0.44	0.05	222	C	45	0.21	0.00	64	C	75	0.11	0.04	104	C
C-002	59	0.41	0.03	166	C	58	0.16	0.02	64	C	71	0.08	0.01	91	CC
C-002	64	0.38	0.03	169	CC	75	0.16	0.00	56	CC	84	0.10	0.02	90	C
C-011	336	0.29	0.00	245	CC	331	0.19	0.02	106	C	334	0.16	0.02	103	C
C-011	339	0.28	0.02	238	C	333	0.16	0.02	105	CC	340	0.16	0.00	102	C

[1]Depth of gage below surface.

[2]Directions are in degrees true.

[3]Major epoch, in degrees, relative to 75°W time meridian.

[4]Rot. = rotation; C = clockwise; CC = counterclockwise.

with currents, one is dealing with a vector function of speed and direction. A tide gage measures the rise and fall of the water surface, while a current meter is measuring the horizontal movement of water at a fixed point below the water surface. The current vector will have a different value for each point in the water column. A problem that exists for the Cape Fear River is that there are no current data for depths greater than 26 ft below the surface. The analysis of the data from each station will often be based on averages of the current meter values for that station along with valid assumptions of what phenomena are taking place below the bottom meter. There is more noise and high frequency energy in tidal current data than in tide data because of wave noise, frictional effects, geographic effects, inappropriate station locations, meter malfunctions resulting in excessive editing of data, complicated channel configurations, and the influence of adjacent bodies of water. By comparing the power spectrum plots of tide data to the plots of the tidal current data, the higher frequency energy and fluctuations in the tidal current data are shown.

The values of the M_2 epochs for Southport (C–002) and Wilmington (C–011) were investigated by taking the average of the major component M_2 epochs from table 11 for each station. The epoch (in degrees) at each station was divided by 360° and multiplied by 12.4206 hours (M_2 period) to get the time difference between maximum flood strength for the M_2 constituent at each location and lunar transit over the 75°W time meridian. The difference in major component M_2 epochs between Southport and Wilmington is about 57°, which means that it takes 2.0 hours for the maximum flood speed (strength) to progress from Southport to Wilmington, a distance of 21.2 nmi, for an average rate of travel of 10.9 kn. The difference in the average of the major component epochs for the largest diurnal tidal current constituent, K_1, between Southport and Wilmington is 44° or 3.0 hours, which means that the K_1 flood strength is traveling at a rate of 7.3 kn. The M_2 constituent is so large compared to the other constituents that figures for the rates of travel of the other constituents are not included.

Table 12 presents the "ages of the tidal currents" and ratios of the speeds of the harmonic constituents for Southport and Wilmington. There is an insufficient number of stations to establish any definite trends from the data available. Each of the ratio values presented is derived from the major component of the tidal current harmonic constituents. The ratio of $(K_1 + O_1)$ to $(M_2 + S_2)$ speeds for the tidal current does not exceed 0.180 for the available data, which indicates that the tidal current is semidiurnal; two tidal cycles per day usually with both maximum floods and ebbs of about equal strength.

Values for the M_4 and M_6 tidal current constituents were obtained from the harmonic analysis of the data from Southport and Wilmington, but the results were not used to plot ellipses for the two constituents. The M_4 to M_2 and M_6 to M_2 ratios were investigated to see if they followed the same trend as the corresponding tide ratios. One would expect both ratios to increase going up the river because of the nature of the shallow water constituents. The average M_4 to M_2 ratio does increase from 0.052 at Southport to 0.102 at Wilmington, but the M_6 to M_2 ratio decreases from 0.055 at Southport to 0.040 at Wilmington. There are not enough data to make a positive statement concerning the variability of the M_4 and M_6 amplitudes.

When a time series is not long enough to run a harmonic analysis, the next best method of extracting tidal current parameters is a half-hourly rotary reduction by use of the computer program ROTARY. As stated in section 4.3, the tidal current parameters for the short-term stations in the Cape Fear River were calculated by making use of the predicted values for the long-term accepted tidal current station at Charleston Harbor, S.C. Table 13 presents the results from the half-hourly rotary reductions. The reason for having to use this nonharmonic comparison analysis is that a limitation on available ship time means that most current station durations must be short.

To better interpret the results from table 13, a few comments are necessary. The times for the flood and ebb strengths represent the number of hours for the maximum strengths to occur after the Moon's passage over the Greenwich meridian. The times progress from zero hours at the moment of passage to 12.42 hours and then once again from zero hours. For example, the time of maximum flood strength for station C–005 at −16 ft is 12.42 + 0.22 = 12.64 hours after the Moon's passage over the Greenwich meridian. The nontidal results are actually mean values for all of the current data at that particular station depth. The nontidal results are quite important, because they provide an indication of the resultant direction and strength of flow. The results need careful interpretation, because whenever the flood and ebb strength directions are not separated by 180°, the nontidal results may be somewhat erroneous. The times for the flood and ebb strengths can be compared to the high and low water intervals for the tide data in table 7 to better classify the type of wave which is present in the Cape Fear River.

The flow regime in the Cape Fear River can be

TABLE 12.—Ratios of amplitudes, and ages of tidal currents for Southport (C-002) and Wilmington (C-011)

Station Number	Depth of Data	$\frac{K_1}{M_2}$	$\frac{K_1 + O_1}{M_2 + S_2}$	$\frac{S_2}{M_2}$	$\frac{N_2}{M_2}$	$\frac{O_1}{K_1}$	Phase Age (hours)	Parallax Age (hours)	Diurnal Age (hours)
Southport (C-002)	-6	.092	.130	.079	.193	.524	-46.248	-47.762	-36.440
	-16	.078	.105	.112	.199	.500	-0.984	38.577	24.597
	-26	.086	.124	.130	.205	.625	9.840	25.718	30.974
Average		.085	.120	.107	.199	.550	-12.464	5.511	-30.670

Station Number	Depth of Data	$\frac{K_1}{M_2}$	$\frac{K_1 + O_1}{M_2 + S_2}$	$\frac{S_2}{M_2}$	$\frac{N_2}{M_2}$	$\frac{O_1}{K_1}$	Phase Age (hours)	Parallax Age (hours)	Diurnal Age (hours)
Wilmington (C-011)	-6	.128	.180	.311	.196	.842	5.904	5.511	2.733
	-20	.112	.179	.252	.196	1.00	7.872	9.185	2.733
Average		.120	.180	.281	.196	.921	6.888	7.348	2.733

*Each amplitude value (speed) is derived from the major component of the tidal current ellipses. The "ages," in hours, are in reference to the 75°W time meridian and were calculated from the major component epochs.

TABLE 13.—Results from program ROTARY for the tidal current stations in the Cape Fear River

Stat. No.	Depth of[1] Data (ft)	Dates of Observation	Flood Strength			Ebb Strength			Nontidal[4]		Largest Obs.	
			Time[2] (hours)	Speed (kts)	Dir[3] (°)	Time (hours)	Speed (kts)	Dir (°)	Speed (kts)	Dir (°)	Speed (kts)	Dir (°)
C-002	-6	14 May 1976 - 01 June 1976	10.91	1.56	059	5.37	2.65	225	0.53	221	3.00	227
	-16	13 May 1976 - 19 June 1976	11.03	1.63	062	5.37	2.38	244	0.29	247	3.00	242
	-26	13 May 1976 - 19 June 1976	11.22	1.72	082	5.34	2.13	247	0.18	205	2.97	249
C-003	-6	10 May 1976 - 21 May 1976	11.40	1.48	019	5.99	1.85	198	0.23	190	2.61	196
	-16	10 May 1976 - 21 May 1976	11.41	1.51	025	5.96	1.77	199	0.17	178	2.65	197
	-26	10 May 1976 - 21 May 1976	11.52	1.34	012	5.61	1.44	193	0.06	186	2.38	025
C-004	-6	10 May 1976 - 21 May 1976	11.61	1.35	020	6.53	1.54	197	0.17	187	2.28	020
	-16	10 May 1976 - 21 May 1976	11.53	1.43	021	6.58	1.35	196	0.06	121	2.54	020
	-26	10 May 1976 - 21 May 1976	11.38	1.19	017	6.28	1.00	167	0.21	067	2.40	020
C-005	-6	15 May 1976 - 24 May 1976	11.60	0.81	027	6.43	0.86	198	0.14	168	1.53	198
	-16	15 May 1976 - 24 May 1976	0.22	0.87	011	6.23	0.69	191	0.03	028	1.35	020
	-26	15 May 1976 - 24 May 1976	11.90	0.89	050	5.55	0.75	183	0.28	078	1.37	064
C-006	-6	25 May 1976 - 29 May 1976	11.65	0.73	010	6.48	1.17	184	0.29	177	1.51	184
	-16	25 May 1976 - 29 May 1976	11.90	1.05	000	6.23	0.87	188	0.14	252	1.43	350
	-26	25 May 1976 - 29 May 1976	12.35	1.12	359	6.27	0.87	179	0.12	329	1.43	352
C-007	-6	25 May 1976 - 01 June 1976	12.00	1.55	015	6.63	1.97	192	0.28	188	2.10	179
	-16	25 May 1976 - 01 June 1976	11.88	1.51	006	6.48	1.57	177	0.11	132	1.96	019
	-26	25 May 1976 - 01 June 1976	12.15	1.46	327	6.48	1.39	177	0.20	266	2.01	356
C-008	-6	24 May 1976 - 02 June 1976	12.39	1.48	020	6.76	1.37	193	0.12	155	1.99	020
	-16	24 May 1976 - 02 June 1976	12.09	1.40	003	6.65	1.38	182	0.03	095	1.87	184
	-26	24 May 1976 - 30 May 1976	12.40	1.20	004	6.68	0.95	185	0.13	015	1.60	035
C-010	-26	02 June 1976 - 10 June 1976	1.28	0.78	034	7.38	0.52	165	0.18	102	1.13	027
C-011	-6	24 May 1976 - 08 June 1976	1.54	1.40	337	7.23	1.40	153	0.19	147	1.94	337
	-20	24 May 1976 - 08 June 1976	0.98	1.34	341	7.73	1.39	164	0.17	166	1.91	346
C-012	-6	08 June 1976 - 17 June 1976	1.64	0.62	021	7.98	0.71	207	0.11	219	1.31	015
	-20	08 June 1976 - 17 June 1976	1.71	0.66	026	7.98	0.67	200	0.07	194	1.17	003
C-013	-6	11 June 1976 - 19 June 1976	2.63	1.15	080	9.63	0.97	264	0.12	062	1.63	081
C-014	-6	10 June 1976 - 17 June 1976	2.73	0.61	307	9.23	0.73	124	0.12	116	1.26	306
C-016	-6	02 June 1976 - 10 June 1976	12.40	0.50	354	6.98	0.83	170	0.24	167	1.01	172
C-017	-6	02 June 1976 - 10 June 1976	11.50	0.79	290	5.48	1.22	118	0.32	121	1.71	128
	-16	02 June 1976 - 10 June 1976	11.70	0.80	301	5.48	1.03	127	0.19	129	1.49	120
C-018	-6	11 May 1976 - 21 May 1976	11.90	0.31	351	4.98	0.33	181	0.04	021	0.71	341
	-16	11 May 1976 - 21 May 1976	11.90	0.70	332	4.78	0.38	159	0.15	322	1.23	330
	-26	11 May 1976 - 21 May 1976	11.56	1.00	331	5.73	0.15	160	0.36	330	1.52	332
C-019	-6	11 May 1976 - 21 May 1976	10.77	0.88	003	5.52	1.23	176	0.27	167	1.56	166
	-16	11 May 1976 - 21 May 1976	11.65	0.92	347	6.04	1.12	160	0.15	153	1.62	354
	-26	11 May 1976 - 21 May 1976	11.65	1.05	350	5.98	1.05	167	0.02	138	1.70	337
C-020	-6	10 May 1976 - 21 May 1976	11.35	1.31	009	6.40	1.61	195	0.22	202	2.48	207
	-16	10 May 1976 - 21 May 1976	10.96	1.49	013	6.43	1.71	192	0.10	181	2.87	199
	-26	10 May 1976 - 21 May 1976	11.94	1.11	017	5.98	1.07	194	0.04	020	2.13	019
C-021	-6	11 June 1976 - 19 June 1976	11.30	0.84	280	2.87	0.78	095	0.06	294	1.90	270
C-022	-6	11 June 1976 - 19 June 1976	3.38	1.20	017	9.86	1.11	195	0.12	020	1.75	202

[1]Depth of gage below surface.

[2]In reference to Greenwich mean time; the time in hours starts at zero hours and goes up to 12.42 hours and then starts again at zero. For example, the flood strength time for station C-005 at -16 ft is actually 12.42 + 0.22 = 12.66 hours after the Moon's transit over the Greenwich meridian.

[3]Directions are in degrees true.

[4]Nontidal flow is actually a mean flow

attributed to several physical factors. The gravitation effects due to salinity intrusion (discussed in section 5) will result in a mean flow in on the bottom and a mean flow out on the top. The freshwater river flow is superimposed over the gravitational flow. For those stations in the river itself, there should be a decrease in the mean downstream flow from the surface down to the bottom. The nontidal results show that the Cape Fear River has a dominant ebb flow regime owing primarily to the freshwater river runoff. There are exceptions to the principle ebb theory. Both sections of the Intracoastal Waterway, represented by current stations C–021, C–013, and C–022, have a dominant flood flow direction which indicates that the water entering these canals during a flood cycle is probably being partially dispersed to the adjacent bodies of water and leaving the river system, resulting in a decrease in ebb flow. The Intracoastal Waterway at Snows Cut (C–013) is connected to Myrtle Sound (C–022) which in turn is joined to the Atlantic Ocean by way of Carolina Beach Inlet, about 1.5 nmi north of Snows Cut. The other stations that show a flood dominance are C–018, C–005, and the bottom depths of C–020, C–004, and C–006. Each of these stations is in the area of the complex channel configuration around the Military Ocean Terminal at Sunny Point (MOTSU), which may cause some of the channels to be flood-dominated while the others are ebb-dominated. In the MOTSU region, the ebb flow may be less confined to the maintained channels than during the flood cycle, which would explain the recorded results. The flood dominance at station C–018 is at all depths with the bottom current the strongest (indicating again the additional gravitational effect).

The flood and ebb speeds (amplitudes) follow a predictable trend, decreasing from the river mouth going up the river past the stations north of Wilmington. The stations in the main channel around MOTSU (C–003, C–020, and C–004) have velocities that are greater than those stations in the secondary channels (C–019, C–018, C–005, and C–006). The volume of flow through the main channel is greater, and there are less frictional effects than in the secondary channels. Because of the multichannel configuration and the width of the river in the MOTSU area, the velocities tend to be a little lower than those for the stations south and north of MOTSU, C–002 and C–007. The two stations, C–017 and C–016, in the Brunswick River, which is relatively shallow with no maintained channels and greater friction, have lower velocities than the comparable stations in the Cape Fear River, C–010 and C–011. Notice that for station C–010, the only valid data are at the −26 ft depth. The velocities for the two stations north of Wilmington (C–011), C–012 and C–014, are considerably lower than those for Wilmington. The maximum flood strength velocity is 1.72 kn at the −26 ft depth at Southport (C–002), and the minimum flood velocity is 0.31 kn at the −6 ft depth at 0.3 mi east of Reaves Point (C–018). The low velocity at station C–018 can be attributed to the nonparallel channel orientation and the shoals that surround the channel. The ebb strength velocities vary from a maximum of 2.65 kn at the −6 ft depth at Southport (C–002) to a minimum of 0.15 kn at the −26 ft depth at station C–018.

By taking the average of the flood strength times and ebb strength times for each station, the progression of the floods and ebbs can be followed up the river. It takes 2.35 hours for the flood strength to progress from Southport (C–002) to Wilmington (C–011), and it takes 2.45 hours for the ebb strength to transverse the same distance. The rates of travel for the floods and ebbs are 9.0 and 8.7 kn respectively. As would be expected, the progression from station to station is not uniform. Both the flood and ebb times at station C–017 at the mouth of the Brunswick River occur earlier than would be expected, and the ebb times in the Intracoastal Waterway are probably being influenced by the adjacent bodies of water.

One option of program CURNT is the computation and plotting of the power spectra from the original, Doodson-filtered (other filters may be used), and residual tidal current series. Figures 25a through 25c present the plots from several stations in the Cape Fear River. Each plot is a straight line best fit representation of the actual log point plots from program CURNT. The autocorrelation functions, from which the power spectra are computed, were calculated from continuous demeaned data reduced to hourly values. A compromise had to be made in selecting the number of lags to compute for the autocorrelation functions. The greater the number of lags, the greater the resolution of the resulting spectral plot, but there is a point at which too much resolution will result in some instability in the plots. A value of 120 was chosen for the maximum number of lags for the Cape Fear River tidal current data based on one value per hour. On the plots the vertical scale is a log scale that has limits based on the magnitude of the current speeds for each individual time series.

The plots in figures 25a through 25c are of the major component of the original demeaned tidal current series reduced to hourly values. The actual energy values have been left out, because they are relative to each plot. Along the horizontal scale, the values 0 through 6, 7, or 8 indicate the number of cycles per

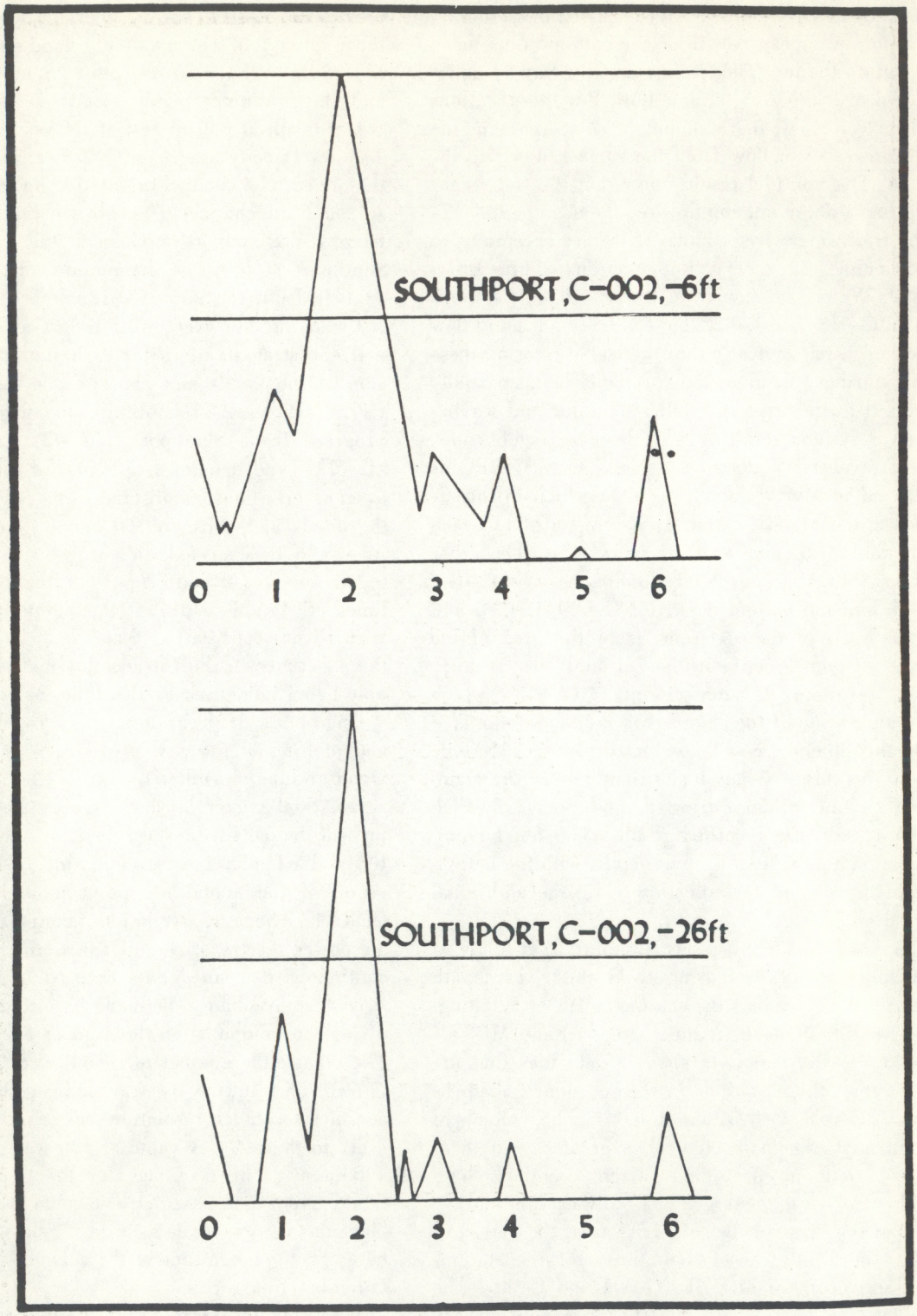

FIGURE 25a.—Power spectra of original demeaned tidal current series, station C–002 at —6 feet and —26 feet.

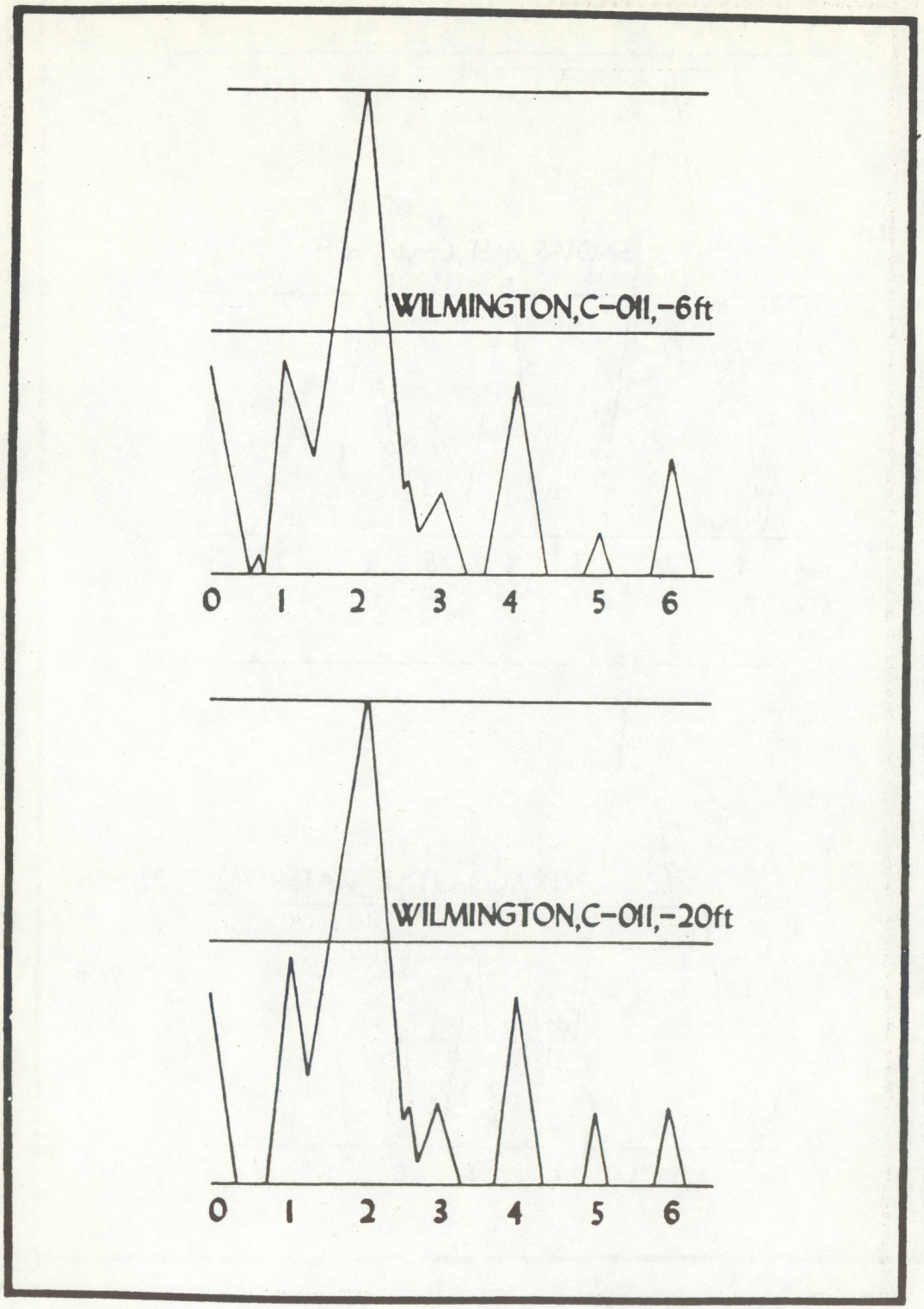

FIGURE 25b.—Power spectra of original demeaned tidal current series, station C–011 at —6 feet and —20 feet.

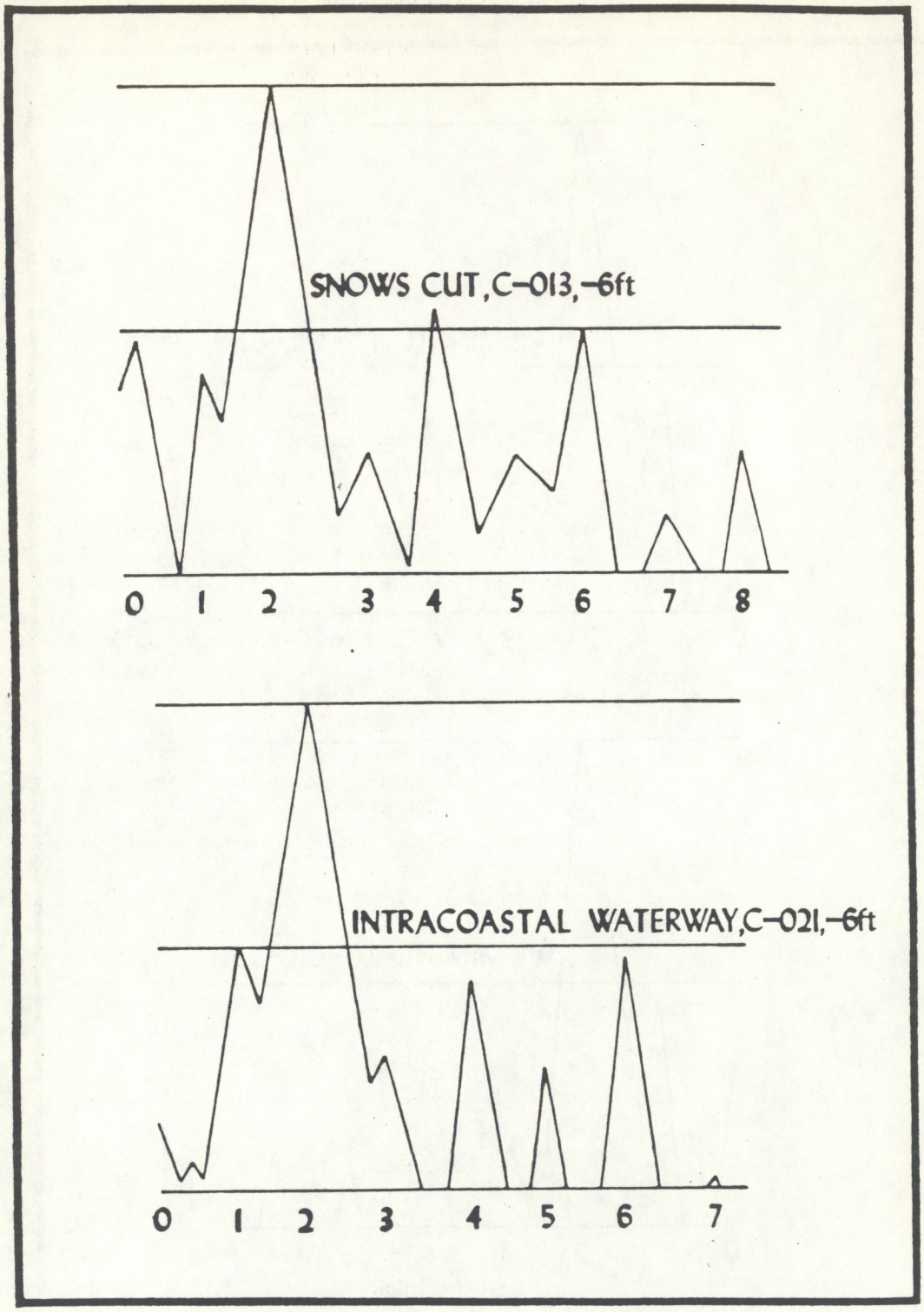

FIGURE 25c.—Power spectra of original demeaned tidal current series, stations C–013 and C–021 at —6 feet.

TABLE 14.—Volume transport during average flood and ebb cycles

Cross Section Station No.	Cross Section Location	Volume Transport Flood (ft^3)	Volume Transport Ebb (ft^3)
C–002	Southport	1.86×10^9	3.00×10^9
C–007	Doctor Pt., 0.6 miles N of	1.33×10^9	1.57×10^9
C–017	Brunswick River, 0.4 miles N of mouth	1.02×10^8	1.96×10^8
C–011	Wilmington	2.94×10^8	3.85×10^8
C–021	Intracoastal Waterway, 1.1 miles W of Southport	6.29×10^7	6.02×10^7
C–013	Snows Cut	9.86×10^7	6.44×10^7

day. The low frequency energy at and near 0 results from river runoff, meteorological effects, and geographical disturbances. The plots are for Southport (−6 and −26 ft), Wilmington (−6 and −20 ft), Snows Cut (−6 ft), and the Intracoastal Waterway at Southport (−6 ft). These stations were chosen to show how the tidal current energy varies over the study area.

As would be expected, the maximum amount of energy is concentrated around two cycles per day for each station. At the −26 ft depth for Southport (C–002), there appears to be more energy at one cycle per day relative to two cycles per day than at the −6 ft depth, and there is less energy at the higher frequencies of 3, 4, 5, and 6 cycles per day than at the −6 ft depth. At Wilmington (C–011), the plots for −6 and −20 ft are quite similar, indicating that the tidal current characteristics are similar throughout the water column. The plots for C–013 and C–021 at −6 ft are included to show the effects of a narrow shallow channel on the tidal current curve. Both plots show the greater relative magnitudes of the higher harmonics, especially at four and six cycles per day, than at Southport (C–002) and Wilmington (C–011).

The durations of the floods and ebbs were calculated for the tidal currents to see if a difference in durations exists as did for the tides. Tidal current durations are based on rotary analysis results, and the durations of the floods and ebbs were computed from slack water before and after maximum flood and maximum ebb. The average flood duration at −6 ft is 5.48 hours, and the average ebb duration at the same depth is 6.94 hours. The average flood duration at the bottom depth of either −20 or −26 ft is 6.24 hours, and the average ebb duration at the same depth is 6.17 hours. The average of the two depths is 5.86 hours for flood and 6.56 hours for ebb. If current data had been available from the river bottom then the difference in durations would probably be closer and might even reverse. Stations C–013, C–022, C–021, C–018, and C–010 were not included in these calculations.

Volume transports during the average ebb and flood cycles were calculated for the cross sections containing the stations listed in table 14. The cross sectional areas were calculated from NOS Chart 11537 (1976); the velocities and duration of ebbs and floods were taken from the rotary analysis results. The velocities were adjusted to get an average value for each cross section flood and ebb average duration. The transports are approximate, and results should be used to compare the relative differences and not the actual values as computed. During the flood cycle, one can see how the volume flow decreases going up the river. It is interesting to note that the volume flowing up the Cape Fear River past Wilmington is almost three times that which enters the Brunswick River. The resulting ebb volume flow follows the same pattern as the flood flow. The increased volume during ebb flows can be attributed to the river runoff. Results are included for both portions of the Intracoastal Waterway that intersect the Cape Fear River to show their relative contributions. Further discussion on the tidal current results is included in section 7.

5. SALINITY AND TEMPERATURE DATA, DESCRIPTION AND ANALYSIS

5.1. Locations of Salinity and Temperature Stations, and Relevant Information

Salinity and temperature data (STD), measured at standard depth intervals, were collected at stations that are designated by the letters "SP" followed by a three-digit number. The station locations are presented in figure 26. Table 15 contains the following information for each station: station latitude and longitude, date on which the STD cast was taken, time of the cast,

TABLE 15.—STD stations occupied during the Cape Fear River Circulatory Survey

Station	Latitude (N)	Longitude (W)	Date	Time[1] (GMT)	Depth (ft)	No. Data Depths[2]	Bottom Data Depth (ft)
SP-001	33°52.5'	78°00.5'	26 May 1976	1135	40	10	40
				1925	46	11	45
			18 June 1976	1338	45	11	45
				1844	49	11	45
SP-002	33°55.0'	78°00.5'	26 May 1976	1200	43	10	40
				1950	43	10	40
			27 May 1976	F 1030	40	(min) 7	(min) 25
				L 2330	40	(max) 10	(max) 40
			18 June 1976	1328	41	10	40
				1907	42	10	40
SP-003	33°58.1'	77°56.9'	26 May 1976	1225	48	11	45
				2010	39	9	35
			17 June 1976	1333	39	9	35
			18 June 1976	1927	41	10	40
SP-004	34°00.4'	77°56.5'	26 May 1976	1245	44	10	40
			01 June 1976	2325	28	7	25
			16 June 1976	1755	45	10	40
			17 June 1976	1348	42	10	40
SP-005	34°00.4'	77°57.2'	26 May 1976	2035	33	8	30
			01 June 1976	1540	33	8	30
			17 June 1976	1305	28	7	25
			18 June 1976	1948	34	8	30
SP-006	34°01.3'	77°56.4'	26 May 1976	1300	44	10	40
			01 June 1976	2335	38	9	35
			16 June 1976	1805	44	10	40
			17 June 1976	1403	41	10	40
SP-007	34°04.7'	77°56.0'	26 May 1976	1315	43	10	40
			01 June 1976	2345	38	9	35
			16 June 1976	1820	45	10	40
			17 June 1976	1420	40	10	40
SP-008	34°07.2'	77°56.2'	26 May 1976	1330	40	9	35
			01 June 1976	2400	45	11	45
			07 June 1976	F 1015	42	(min) 8	(min) 30
				L 2315	42	(max) 10	(max) 40
			16 June 1976	1834	46	11	45
			17 June 1976	1433	41	10	40
SP-009	34°09.5'	77°57.6'	26 May 1976	1345	42	10	40
			01 June 1976	1655	44	10	40
			02 June 1976	0012	38	9	35
			03 June 1976	1900	42	10	40
			05 June 1976	2030	44	10	40
			07 June 1976	2338	38	9	35
			10 June 1976	1230	44	10	40
			14 June 1976	1730	40	10	40
			16 June 1976	1447	39	9	35
				1845	42	10	40
			19 June 1976	2045	44	10	40

TABLE 15.—Continued.

Station	Latitude (N)	Longitude (W)	Date	Time (GMT)	Depth (ft)	No. Data Depths	Bottom Data Depth (ft)
SP-010	34°11.5'	77°57.5'	26 May 1976	1355	43	10	40
			02 June 1976	0040	39	9	35
			16 June 1976	1912	43	10	40
			17 June 1976	1512	41	10	40
SP-011	34°14.2'	76°57.2'	01 June 1976	1713	37	9	35
			02 June 1976	1350	36	9	35
			16 June 1976	1925	39	9	35
			17 June 1976	1525	37	9	35
SP-012	34°14.9'	76°57.4'	01 June 1976	1720	34	8	30
			02 June 1976	1400	30	8	30
			15 June 1976	F 1030	30	(min) 7	(min) 25
				L 2330	30	(max) 9	(max) 35
			16 June 1976	1930	35	8	30
			17 June 1976	1530	33	8	30
SP-013	34°03.3'	77°54.1'	01 June 1976	1552	15	5	15
				2255	10	3	9
			17 June 1976	1243	19	5	15
			18 June 1976	1805	21	6	20
SP-014	34°14.6'	77°57.6'	01 June 1976	1730	34	8	30
			02 June 1976	1408	26	7	25
			16 June 1976	1940	29	7	25
			17 June 1976	1535	36	8	30
SP-015	34°15.6'	77°59.3'	01 June 1976	1740	34	8	30
			02 June 1976	1420	33	8	30
			16 June 1976	1950	40	9	35
			17 June 1976	1550	47	11	45
SP-016	34°11.5'	77°58.5'	26 May 1976	1420	10	3	9
			02 June 1976	0030	11	3	9
			16 June 1976	1905	11	3	9
			17 June 1976	1504	7	2	6
SP-017	34°10.9'	77°54.8'	26 May 1976	1410	34	8	30
			02 June 1976	0020	21	6	20
			16 June 1976	1855	40	10	40
			17 June 1976	1455	21	6	20
SP-018	33°59.9'	77°57.0'	26 May 1976	2030	31	8	30
			01 June 1976	1535	31	8	30
			17 June 1976	1313	33	8	30
			18 June 1976	1944	34	8	30
SP-019	33°59.2'	77°57.3'	26 May 1976	2020	30	8	30
			01 June 1976	1527	27	7	25
			17 June 1976	1322	36	9	35
			18 June 1976	1935	37	9	35
SP-020	33°59.1'	77°55.8'	26 May 1976	1235	41	10	40
			01 June 1976	2315	36	9	35
			16 June 1976	1745	42	10	40
			17 June 1976	1340	39	9	35

TABLE 15.—Continued.

Station	Latitude (N)	Longitude (W)	Date	Time (GMT)	Depth (ft)	No. Data Depths	Bottom Data Depth (ft)
SP-021	34°03.6'	77°54.4'	26 May 1976	1155	15	5	15
				1940	24	6	20
			18 June 1976	1315	13	4	12
				1900	15	4	12
SP-022	33°55.1'	78°02.5'	01 June 1976	1600	13	4	12
				2300	10	3	9
			17 June 1976	1247	16	5	15
			18 June 1976	1800	23	6	20

[1]GMT = Greenwich Meridian Time;
"F" refers to the first cast of a time series;
and "L" refers to the last cast of a time series.

[2]"Min." refers to the minimum number of data depths of a time series and the minimum bottom data depth of the time series, and "max" refers to the maximum values of that same time series.

water depth at the station, number of data intervals for each cast, and depth of the bottom data interval for each cast. The STD station locations correspond reasonably well with the current station locations with the following exceptions: SP–021 and SP–022 are opposite to the corresponding current station locations. SP–010 and SP–016 are about 0.8 nmi south of the corresponding current stations; and SP–001, SP–009, and SP–015 do not have corresponding current station locations. The STD data were measured with an *in situ* salinometer by personnel from the NOAA Ship FERREL.

Three separate types of STD operations were performed. Stations SP–002, SP–008, and SP–012 were each occupied as a time series station that consists of half-hourly casts to near bottom at intervals of 3 ft during a continuous 13-hour period. These series are used to investigate tidal influences on the salinity and temperature structure over a tidal cycle. One station, SP–009, was occupied 10 times during the survey at slack before ebb to get a better understanding of how the salinity structure varies over an extended time period. Unfortunately, the station was not occupied over a time period long enough to get a true seasonal variation in the salinity and temperature fields. The third type of STD operation is the study of the longitudinal spatial variation in the salinity and temperature structure. Six longitudinal transects were taken during the survey over different sections of the river, three at about slack before ebb and three at about slack before flood. During a transect, the stations were occupied as quickly as possible to provide an accurate physical description. In addition to the operations listed above, STD data were also collected for the other stations shown in figure 26.

5.2. Instrumentation, Processing, and Methods of Analysis

A Kahlsico RS5–3 *in situ* salinometer was used to collect the STD data in the Cape Fear River. The unit is self-contained and measures conductivity and temperature from which it computes salinity. Table 16 lists the instrument specifications.

At each station, temperature and salinity readings were taken at 3-ft intervals, the first reading being taken at 3 ft below the surface followed by readings all the way down to a point just above the bottom. The *in situ* salinometer was kept in calibration by taking periodic Nansen casts that were checked by a laboratory salinometer and then compared to the *in situ* results. The data from all stations were sent to NOS headquarters in Rockville, Md., along with the Nansen casts results, and put on punched cards.

An NOS in-house contouring program (Patchen, 1975) was used to plot the salinity and temperature contours in figures 27a through 31b. Figures 27a

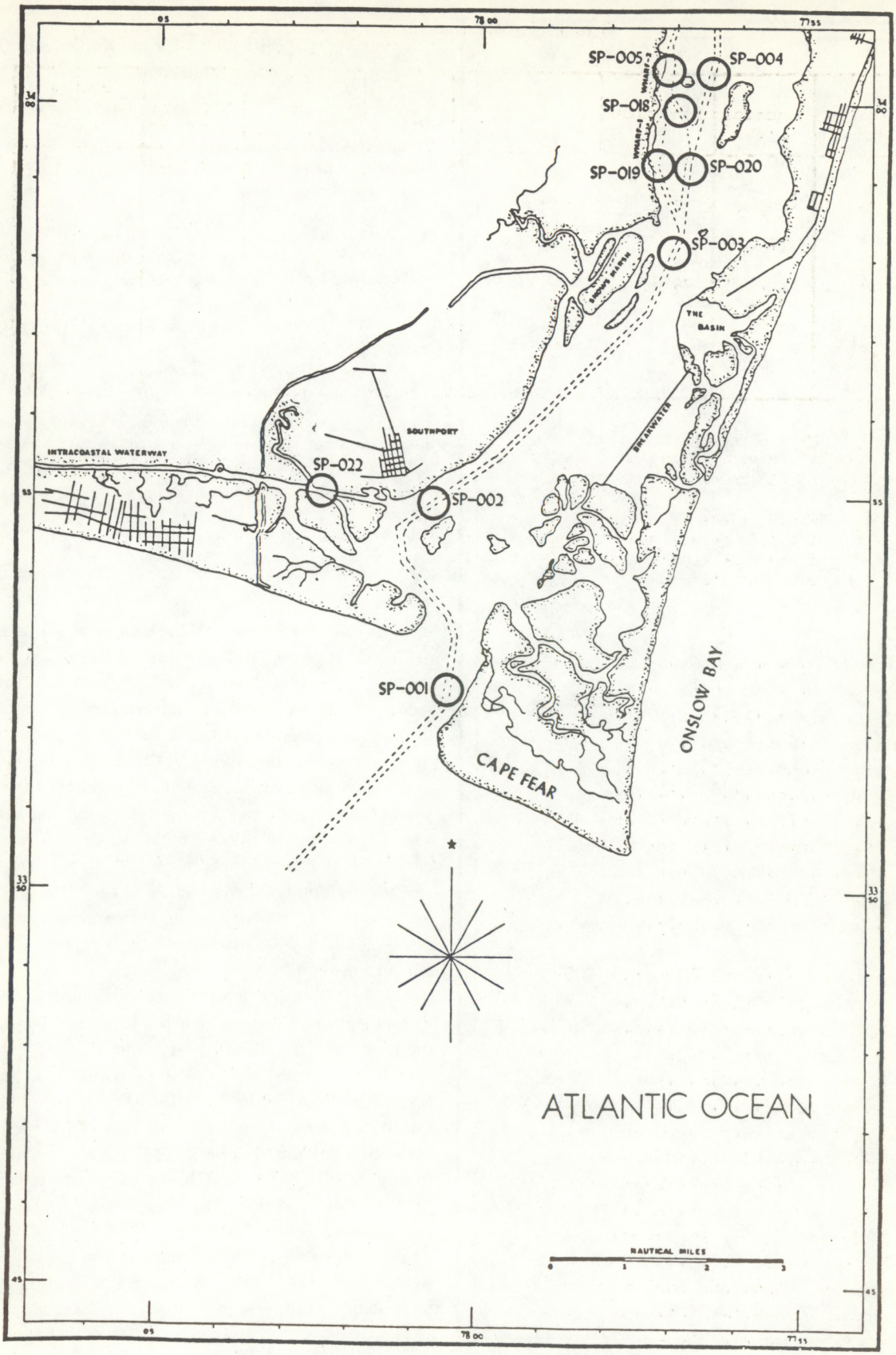

FIGURE 26.—Salinity and temperature (STD) station locations.

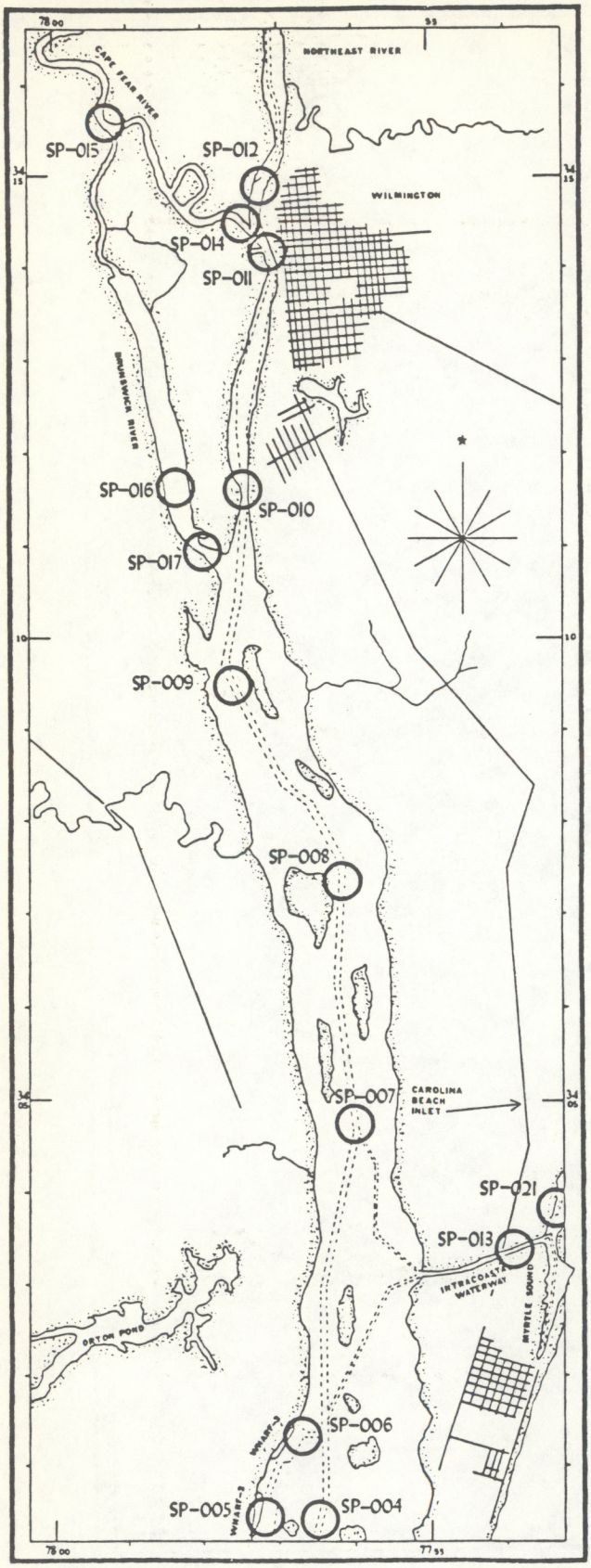

FIGURE 26.—Continued.

TABLE 16.—Specifications for the Kahlsico RS5–3 salinometer

Specifications

Salinity Range: 0–40 ppt ± 0.3 ppt*
Temperature Range: 0–40°C ± 0.5°C*
Conductivity Range: 0–60 millimhos/cm
±0.5 millimhos/cm*

Depth: The above accuracies hold to 400 feet.
Standard cable length is 50 feet with lengths to 400 feet available in 50 foot increments.

Dimensions: Instrument: 6 in by 7 in by 9 in
Transducer: 4 in diameter by 2 in long

Weight: Instrument: 10.9 lb
Transducer: 2.5 lb
Cable: 0.112 lb/ft

* Owing to the stable nature of the bridge circuits used in this instrument, error curves may be plotted and the readings corrected to the following accuracies:

Salinity: ±0.05 ppt
Temperature: ±0.05°C
Conductivity: ±0.05 millimhos/cm

through 27g are plots of the longitudinal transects recorded at slack water before flood; figures 28a through 29e are plots of the longitudinal transects recorded at slack water before ebb. Figures 29a through 31b are the plots of the three 13-hour time series stations. Program CONTPR allows one to choose the contour differentials. A salinity spacing of 0.5 parts per thousand (ppt) and a temperature spacing of 0.2°C were chosen for all plots except 31a and 31b, which have spacings of 0.1 ppt and 0.1°C respectively. The smaller differentials were chosen for 31a and 31b, because they contain the time series plots for station SP–012, which has little variability in its salinity and temperature data.

The headings for the transects include the distance in nautical miles over which the transects were taken, the number of levels of observation, the year and the Julian day of the year, the station numbers, and the time of the cast for each station. The station numbers for the transects do not have the leading zeros in the three-digit station numbers, and the station numbers in figures 29b, 31a, and 31b are preceded by the letter "P" instead of "SP." The time series stations have similar headings except for the distance parameter. As with the tide and tidal current data for the Cape Fear River, any STD data requests or information should be sent to the address given in section 2.2.

5.3. Results of Analysis

Ippen (1966) states that there are four distinct dy-

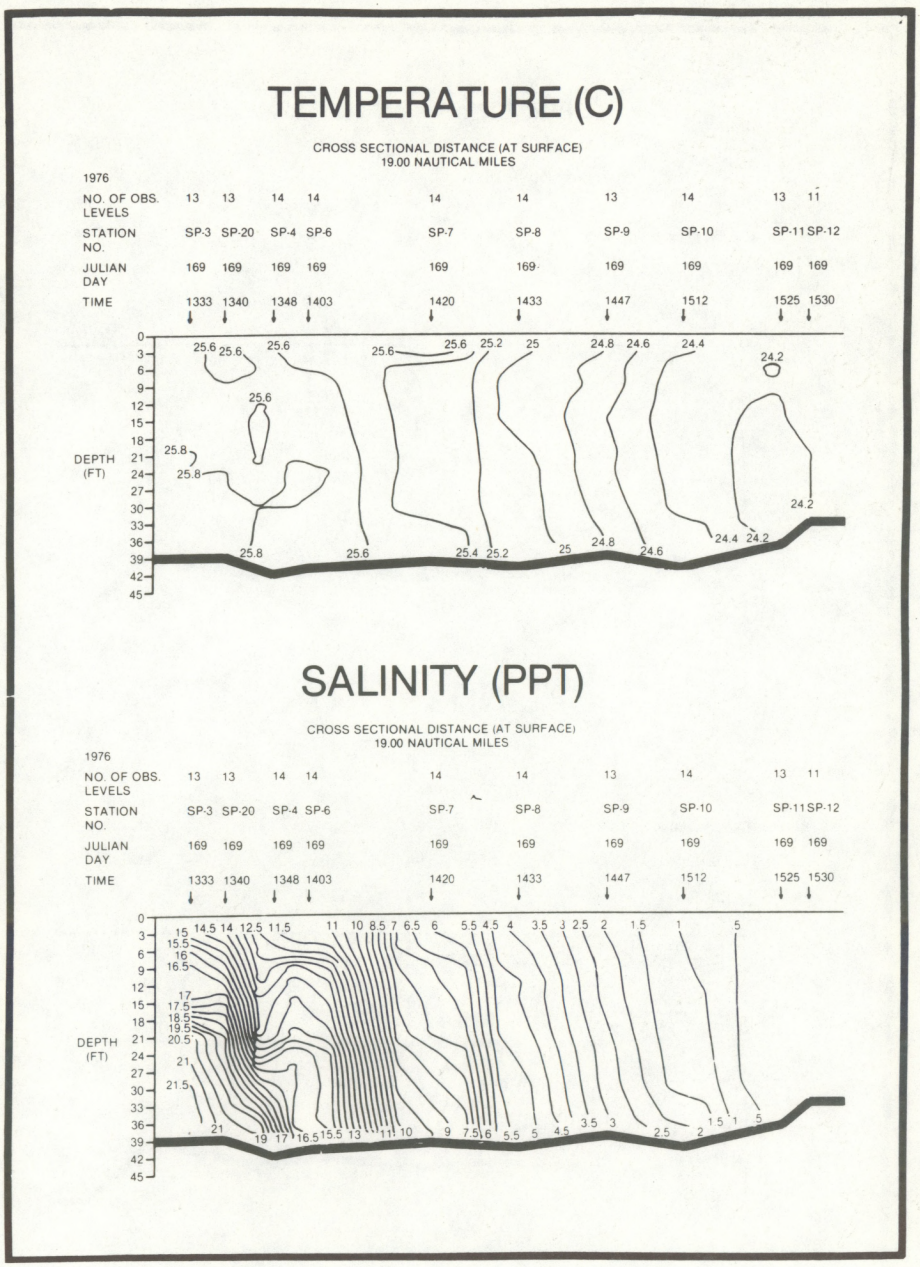

FIGURE 27a.—Temperature and salinity longitudinal transects, slack before flood.

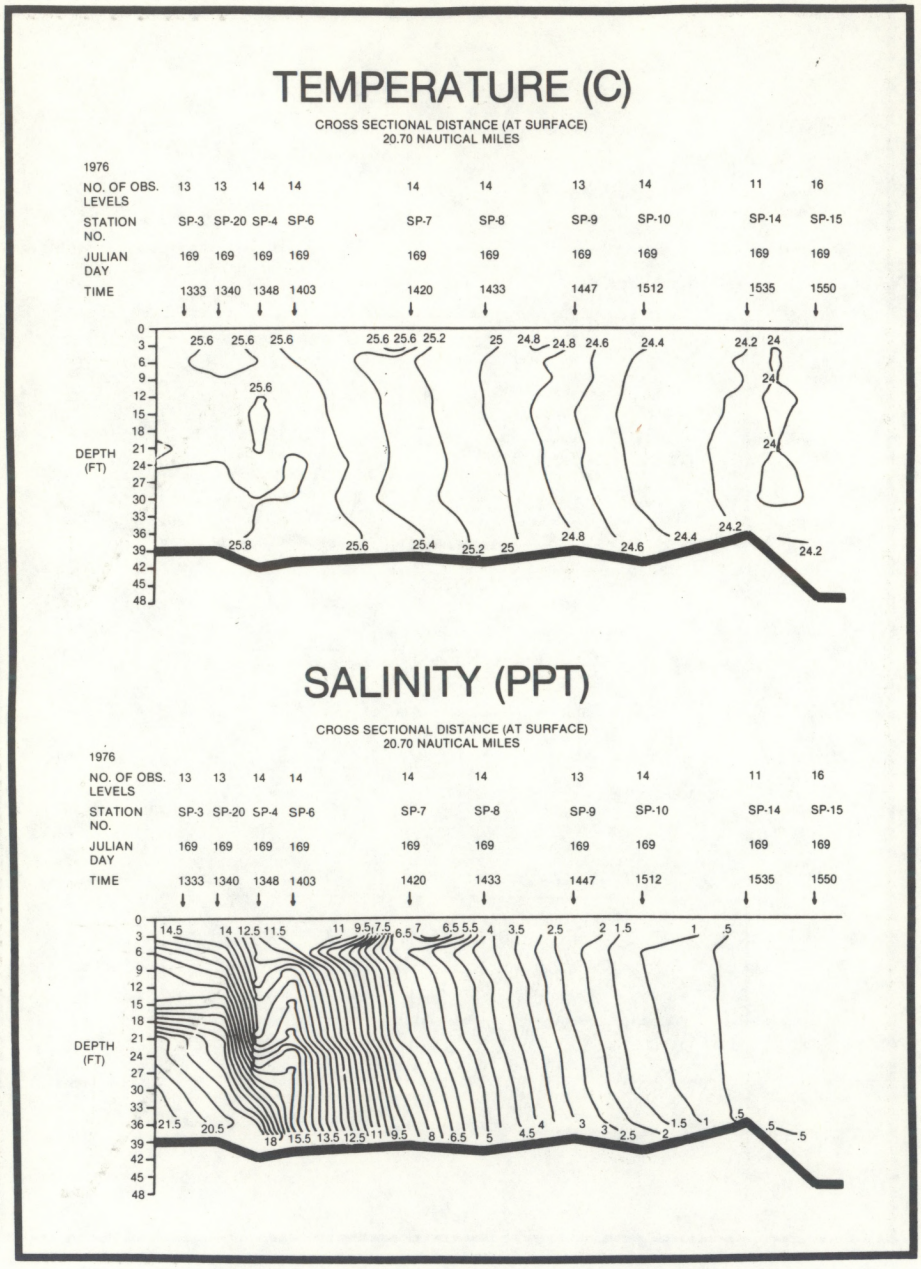

FIGURE 27b.—Temperature and salinity longitudinal transects, slack before flood.

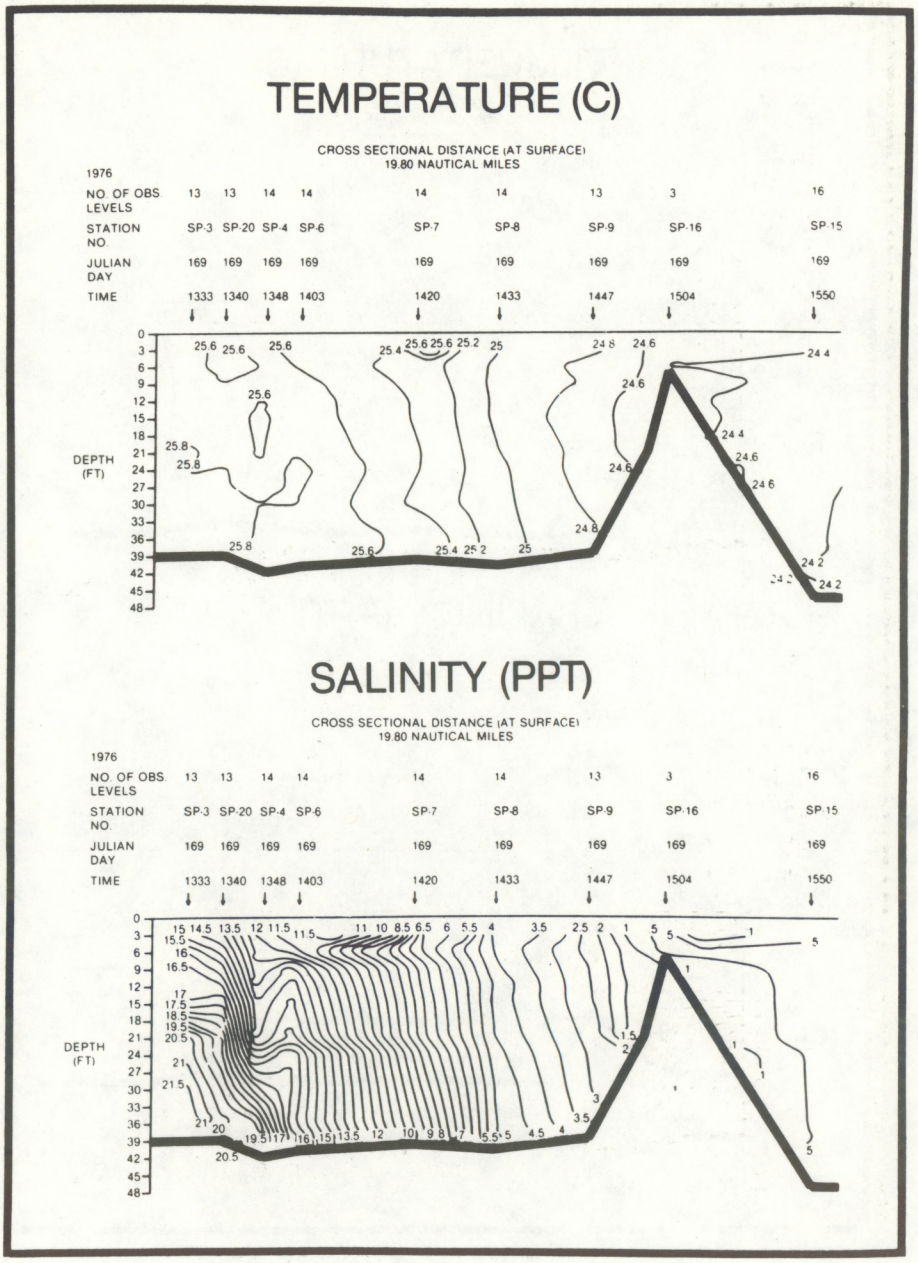

FIGURE 27c.—Temperature and salinity longitudinal transects, slack before flood.

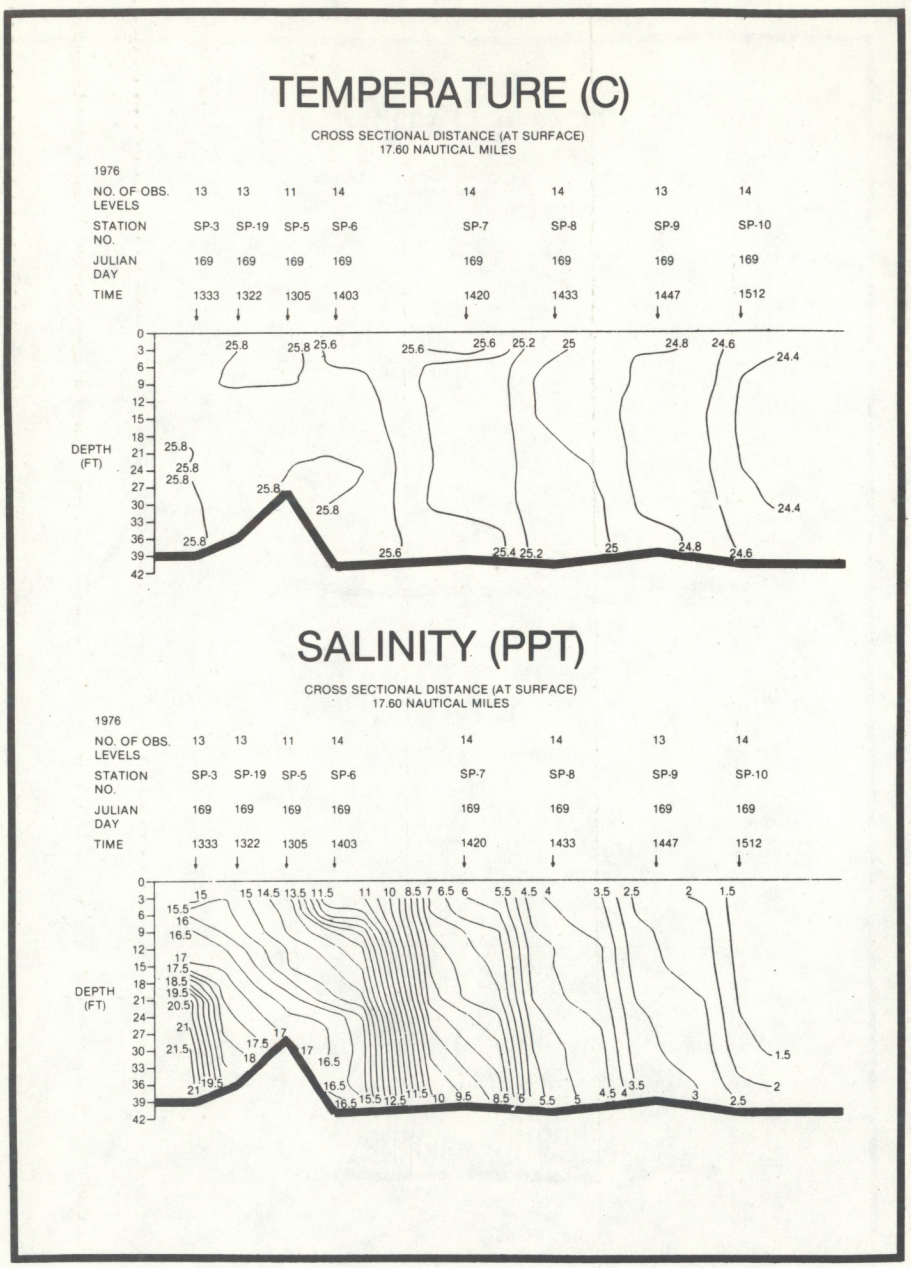

FIGURE 27d.—Temperature and salinity longitudinal transects, slack before flood.

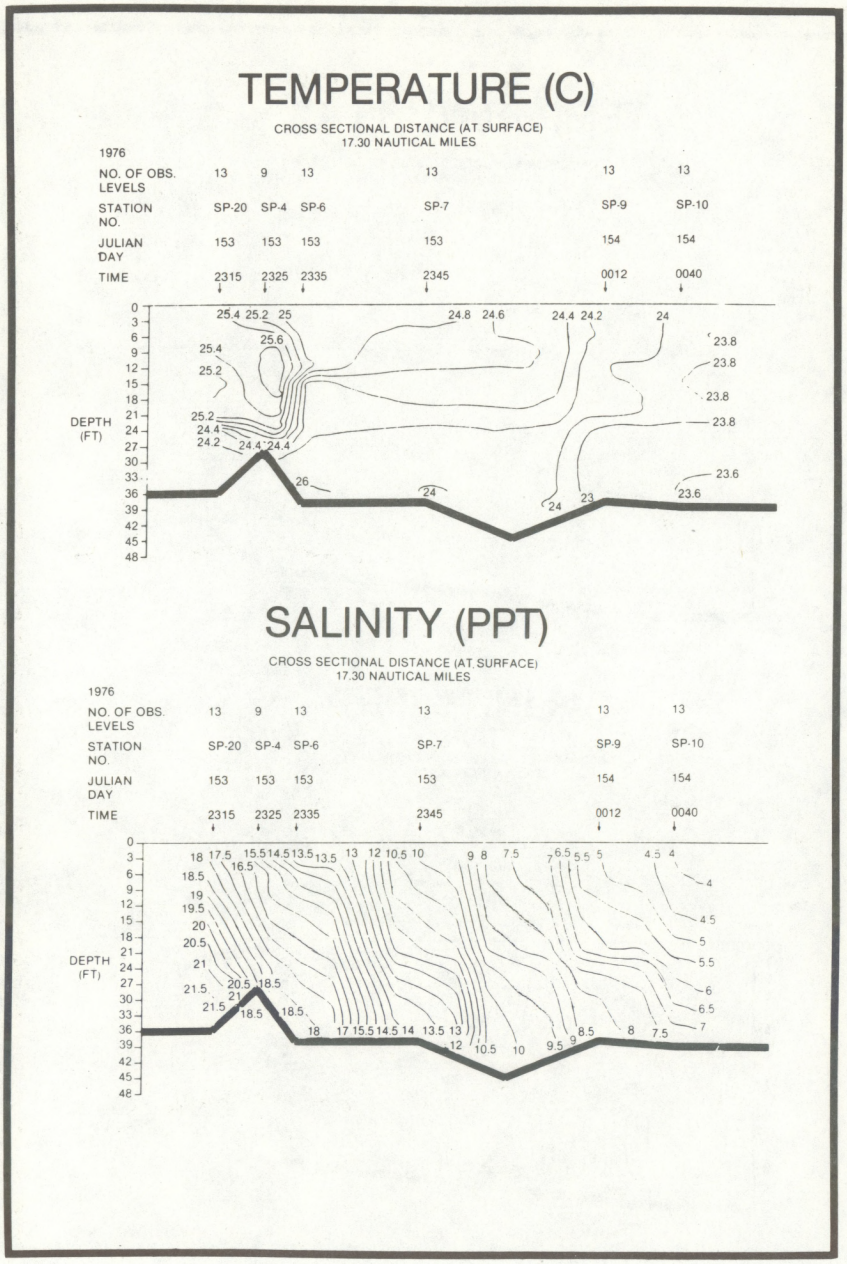

FIGURE 27e.—Temperature and salinity longitudinal transects, slack before flood.

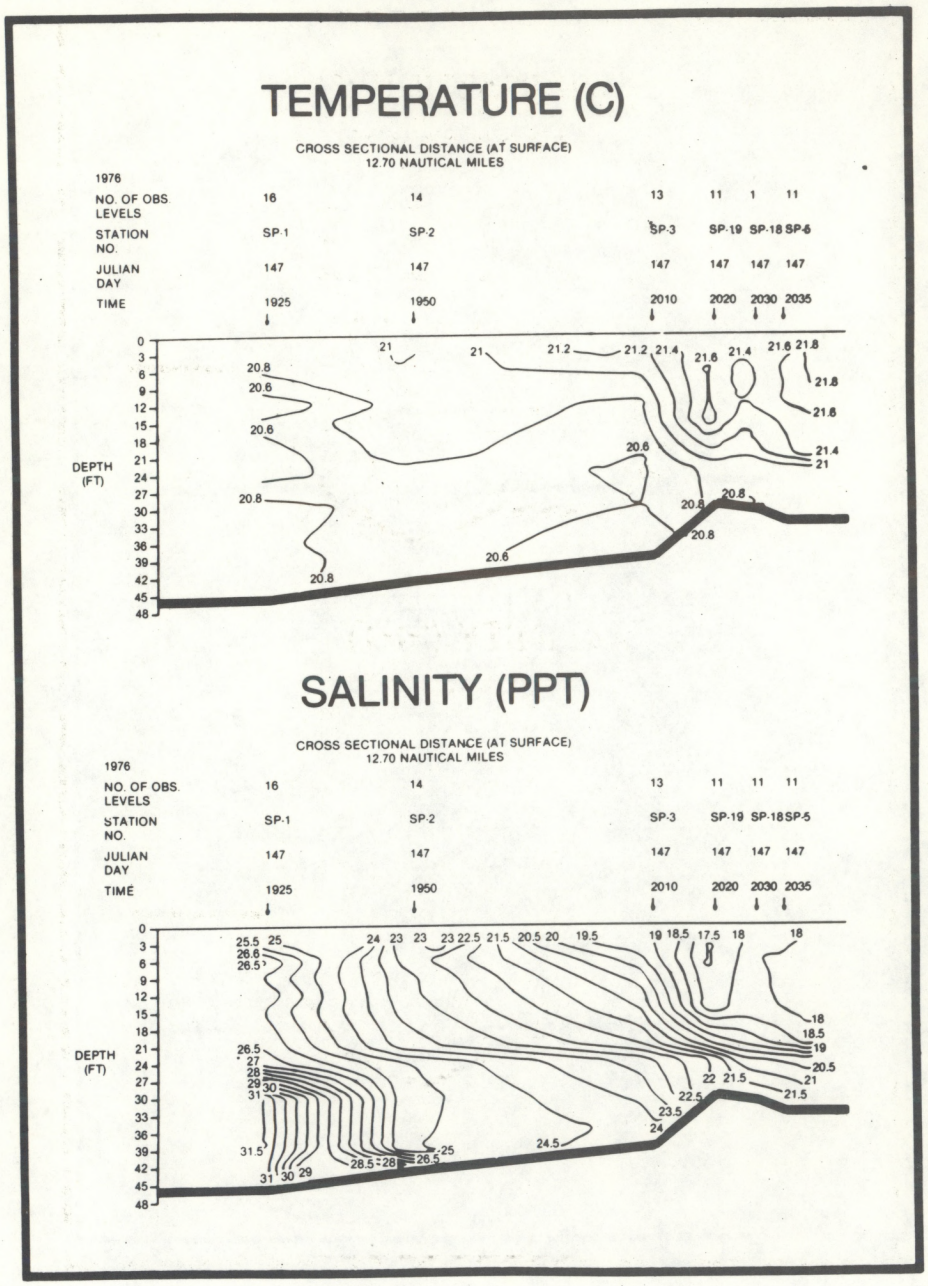

FIGURE 27f.—Temperature and salinity longitudinal transects, slack before flood.

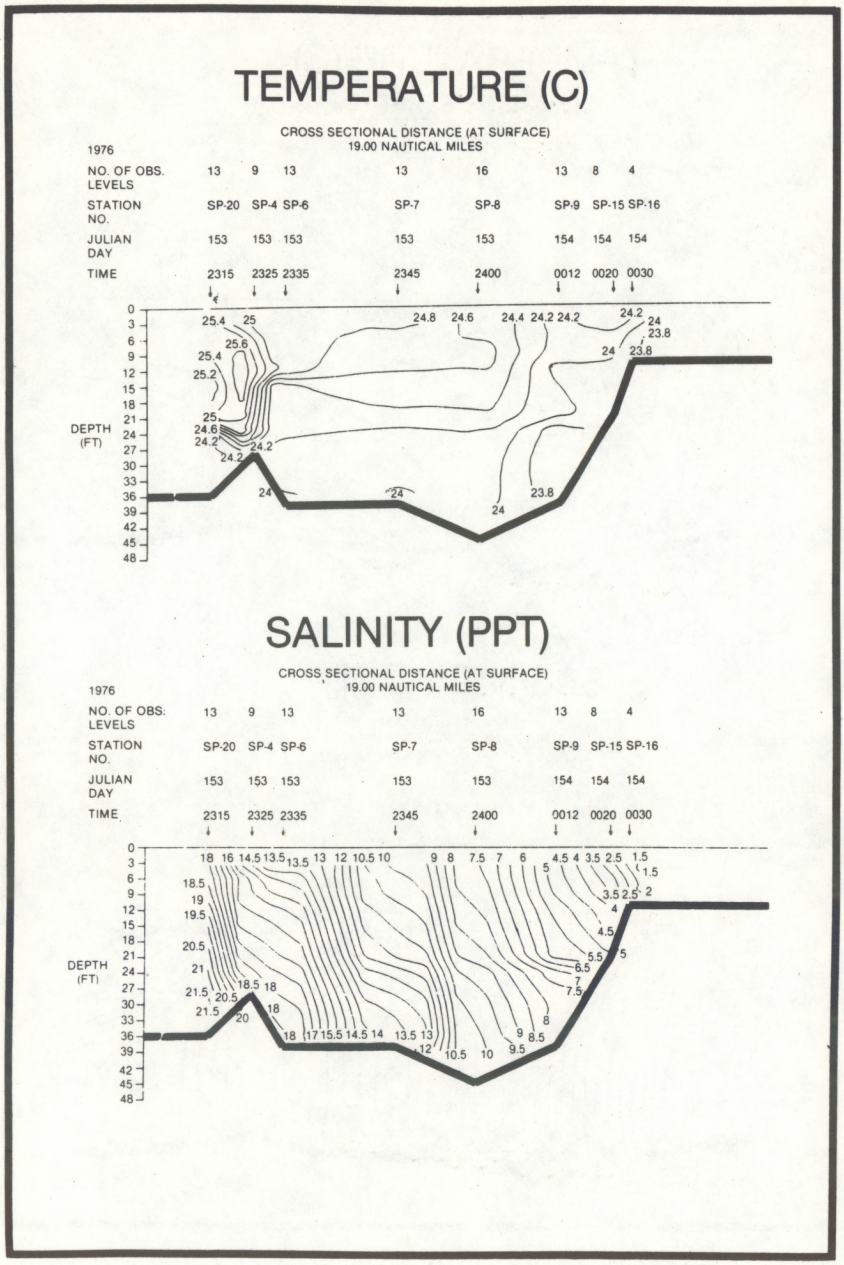

FIGURE 27g.—Temperature and salinity longitudinal transects, slack before flood.

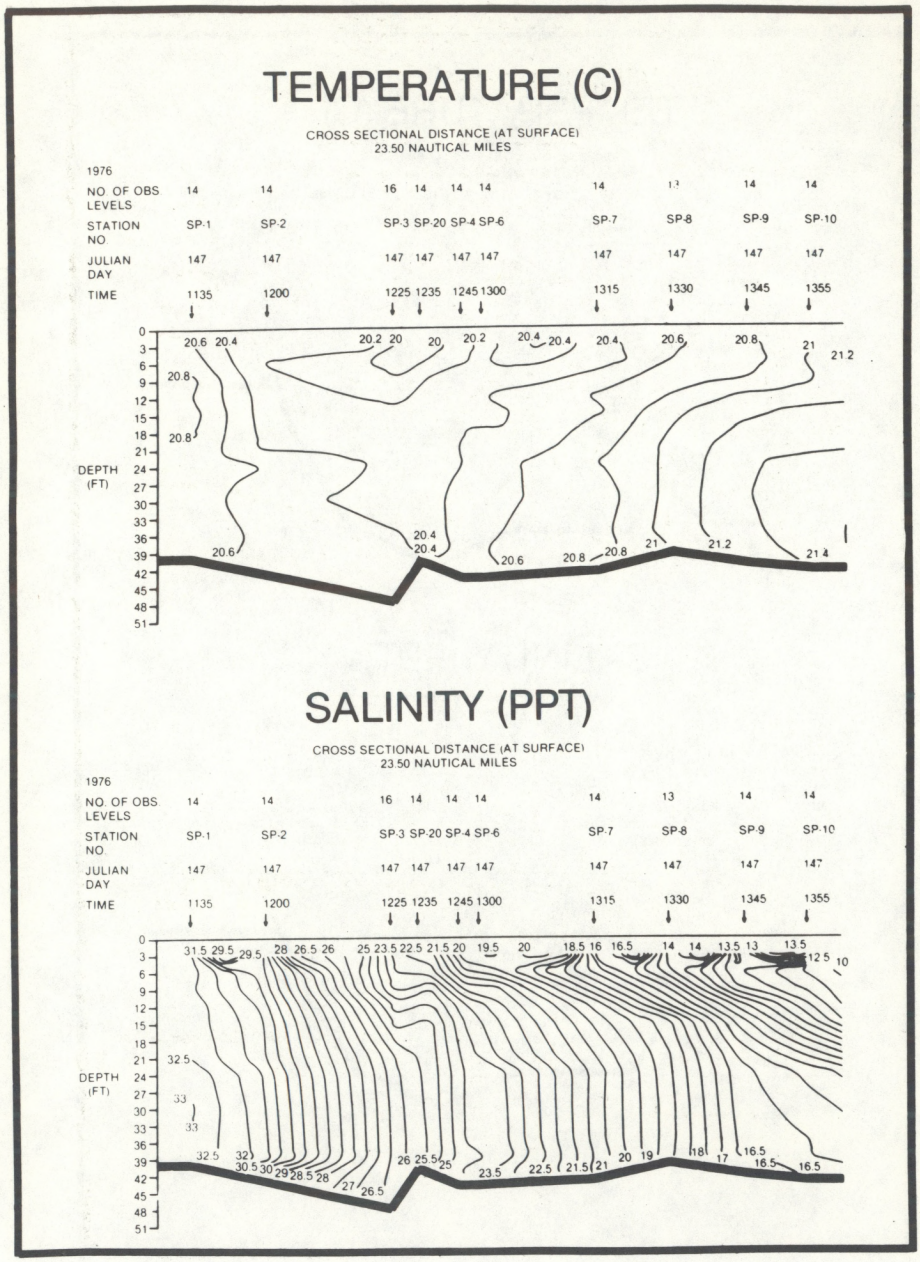

FIGURE 28a.—Temperature and salinity longitudinal transects, slack before ebb.

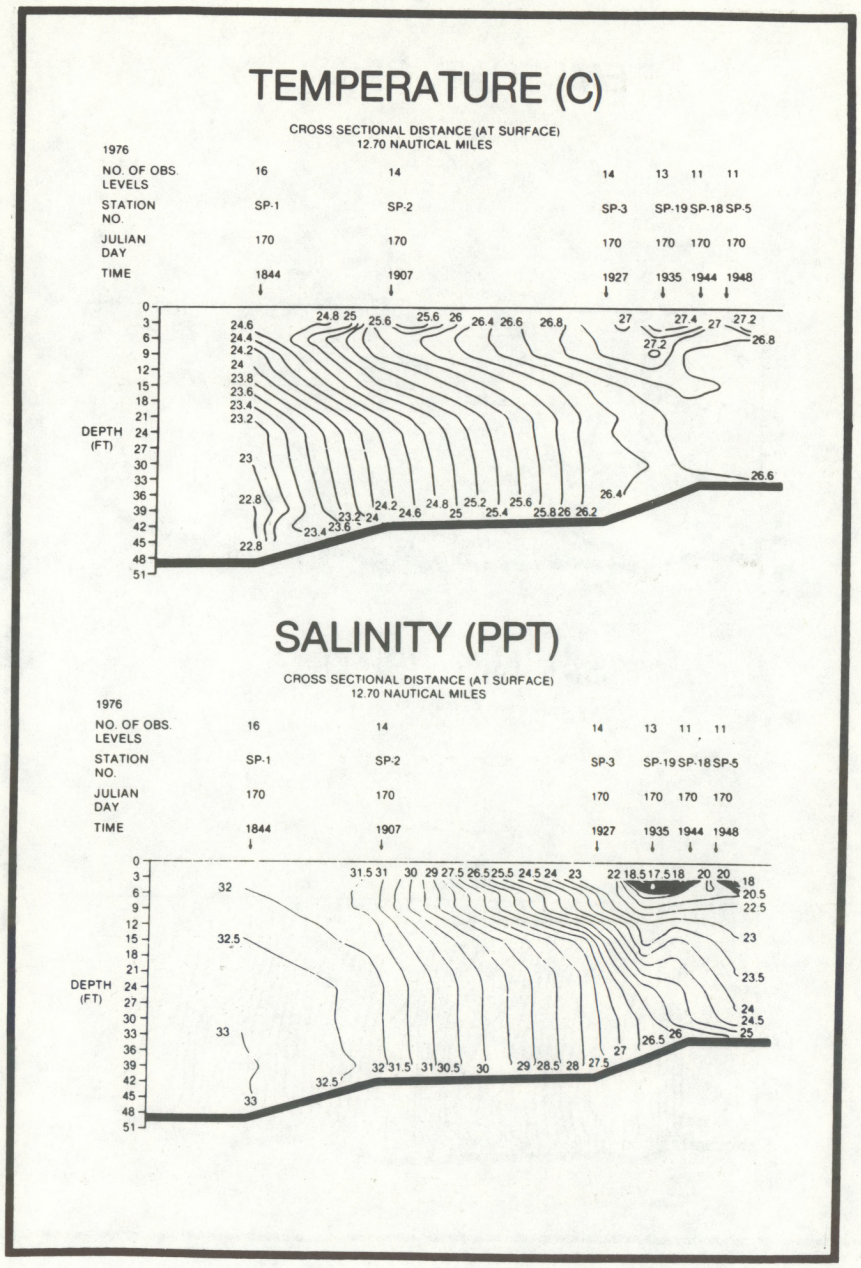

FIGURE 28b.—Temperature and salinity longitudinal transects, slack before ebb.

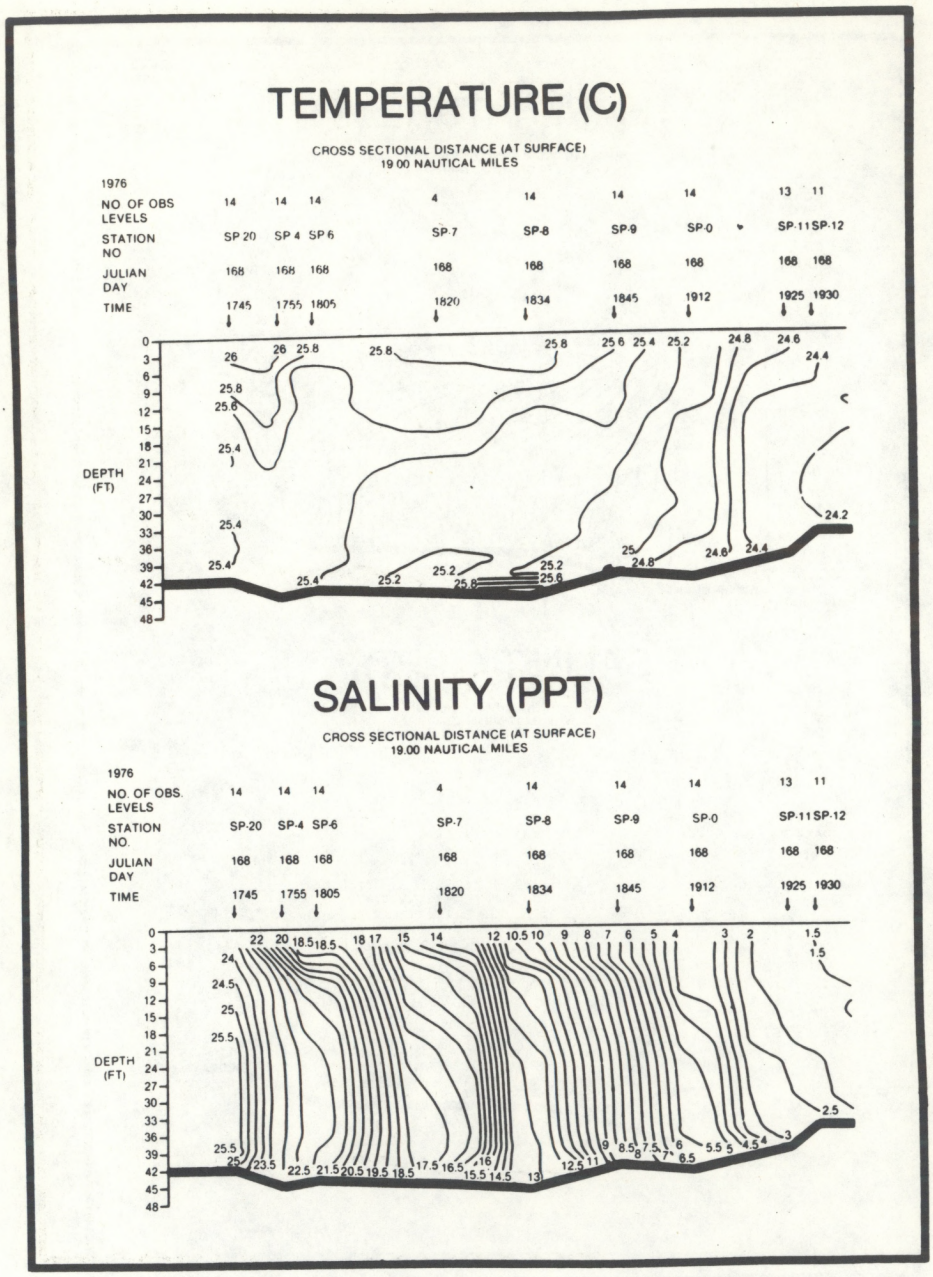

FIGURE 28c.—Temperature and salinity longitudinal transects, slack before ebb.

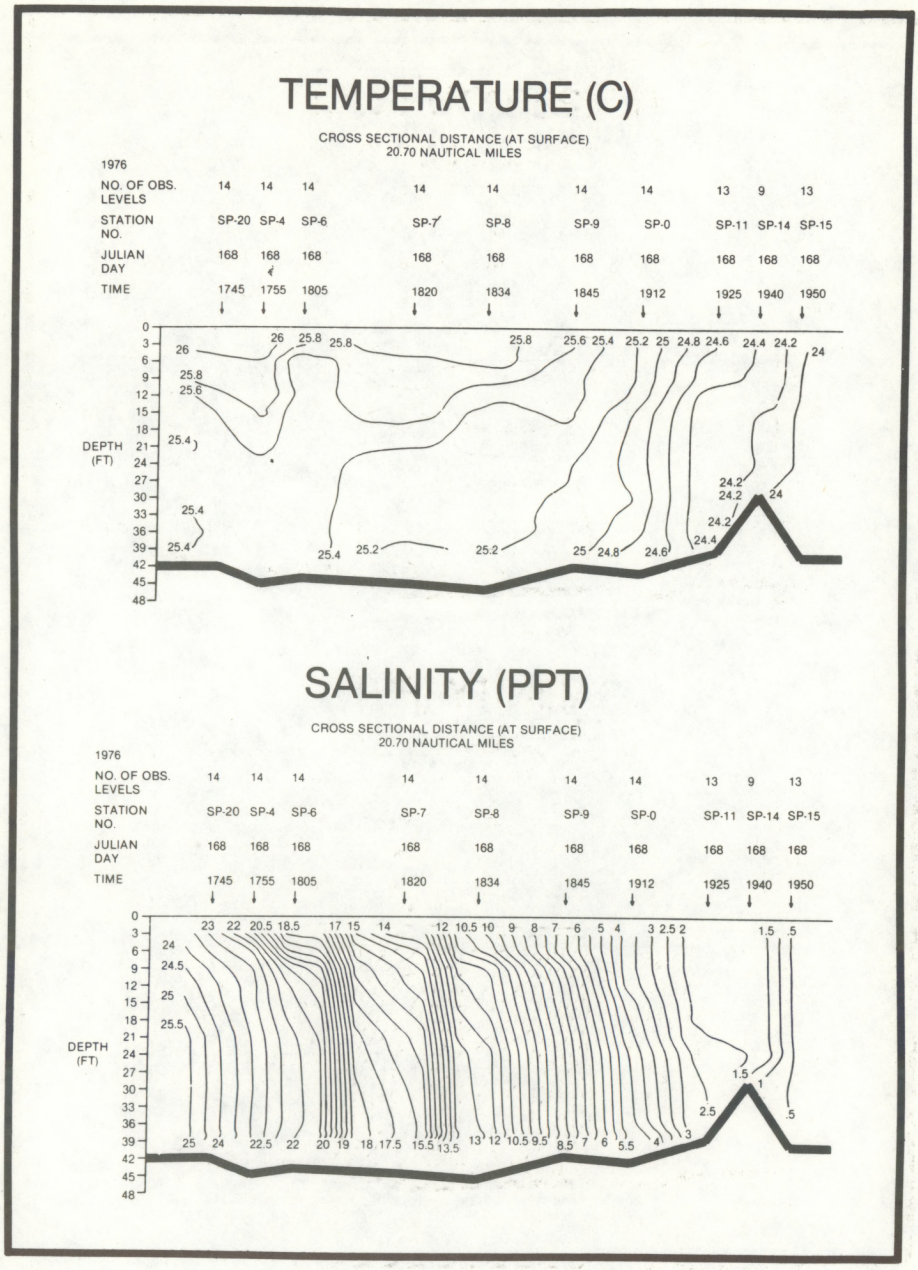

FIGURE 28d.—Temperature and salinity longitudinal transects, slack before ebb.

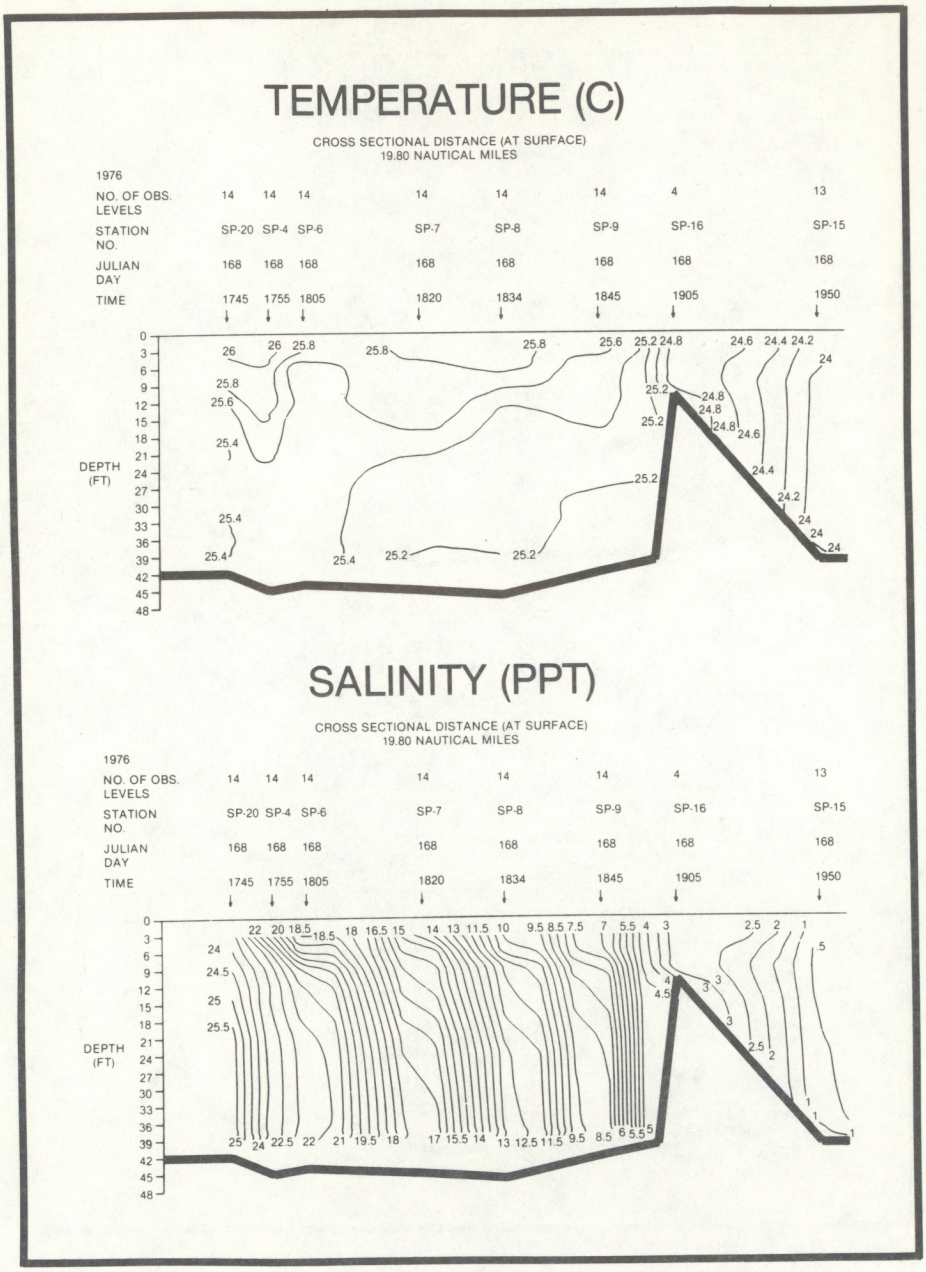

FIGURE 28e.—Temperature and salinity longitudinal transects, slack before ebb.

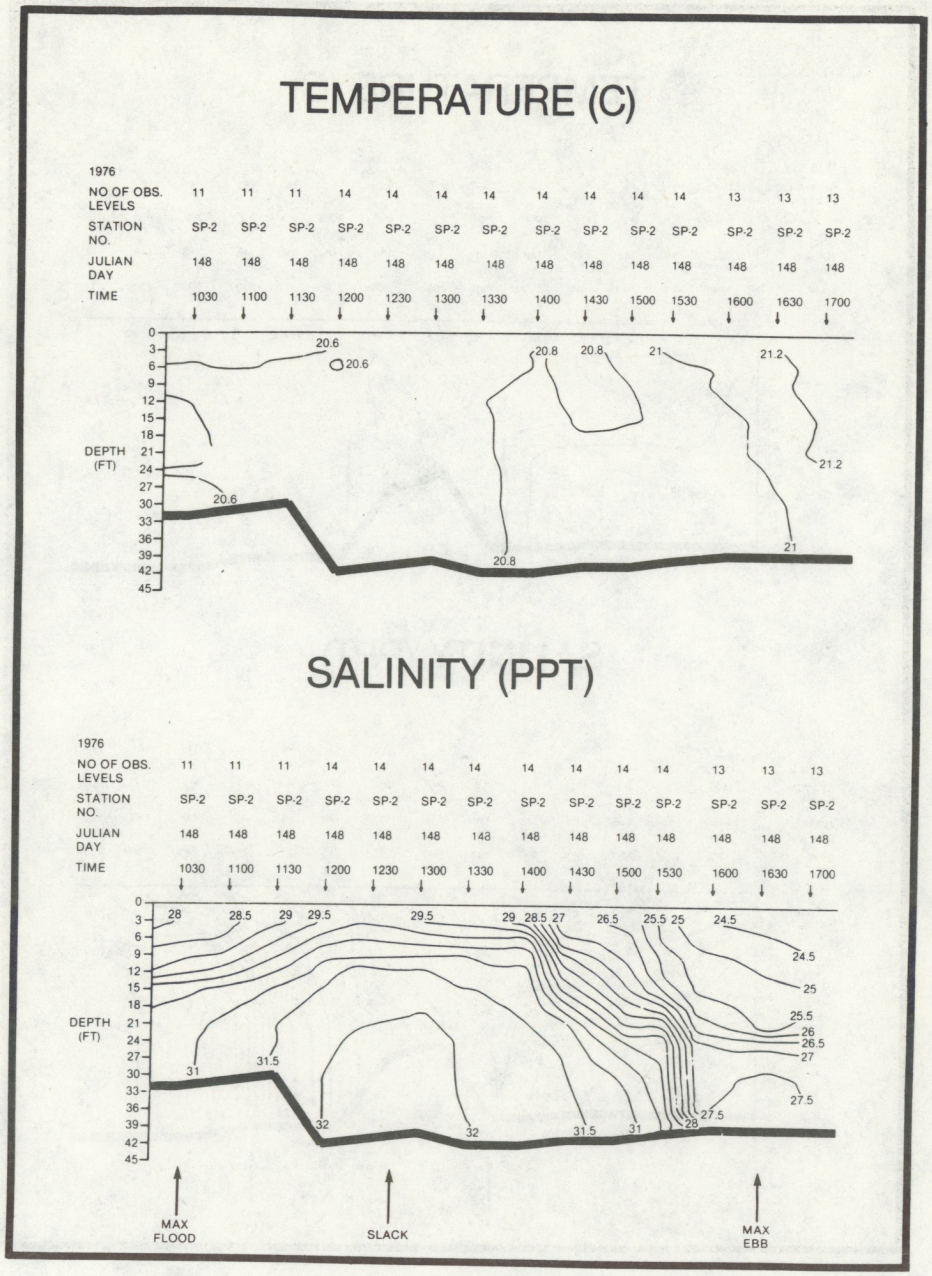

FIGURE 29a.—Temperature and salinity time series, station SP–002.

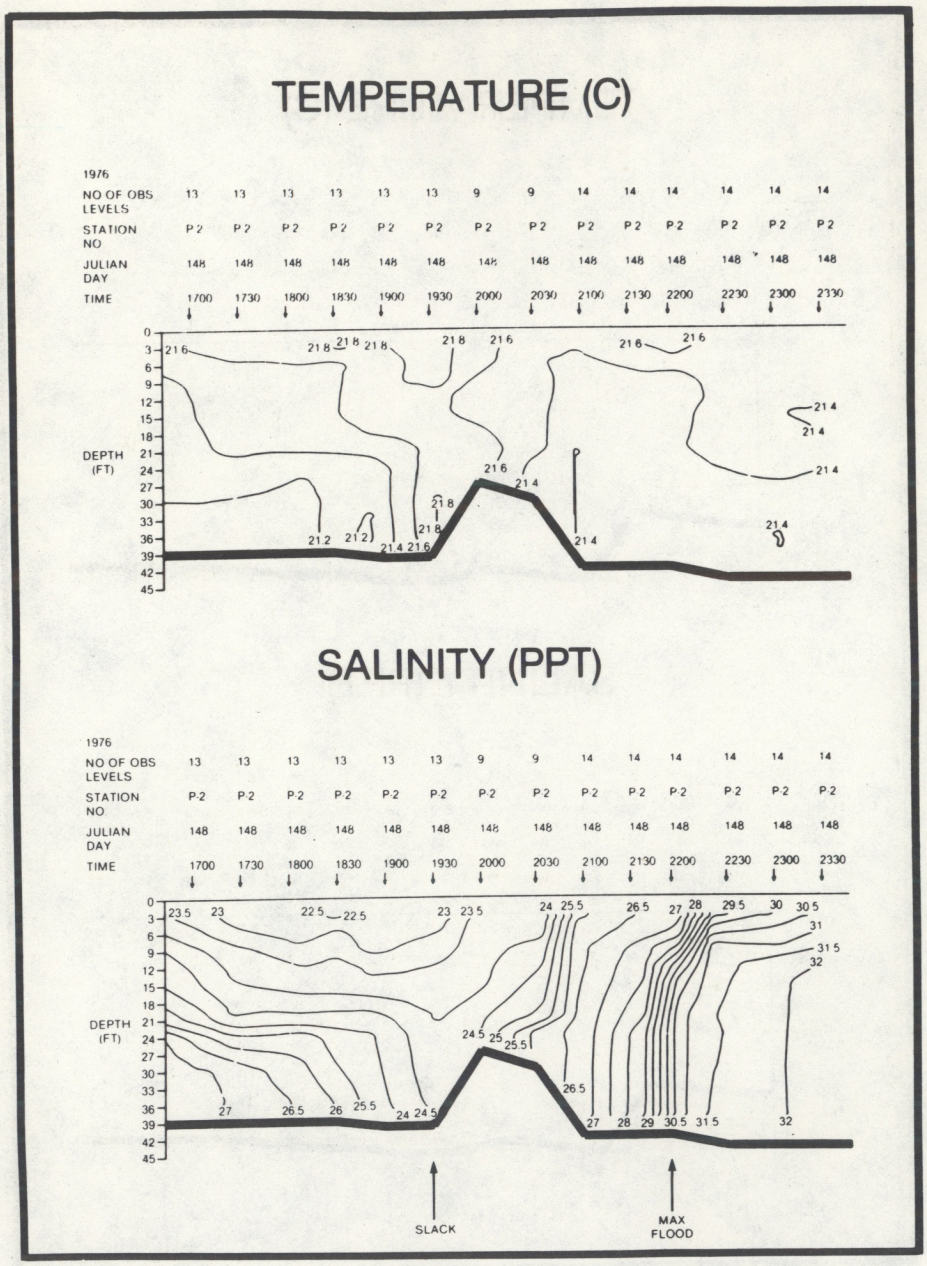

FIGURE 29b.—Temperature and salinity time series, station SP-002.

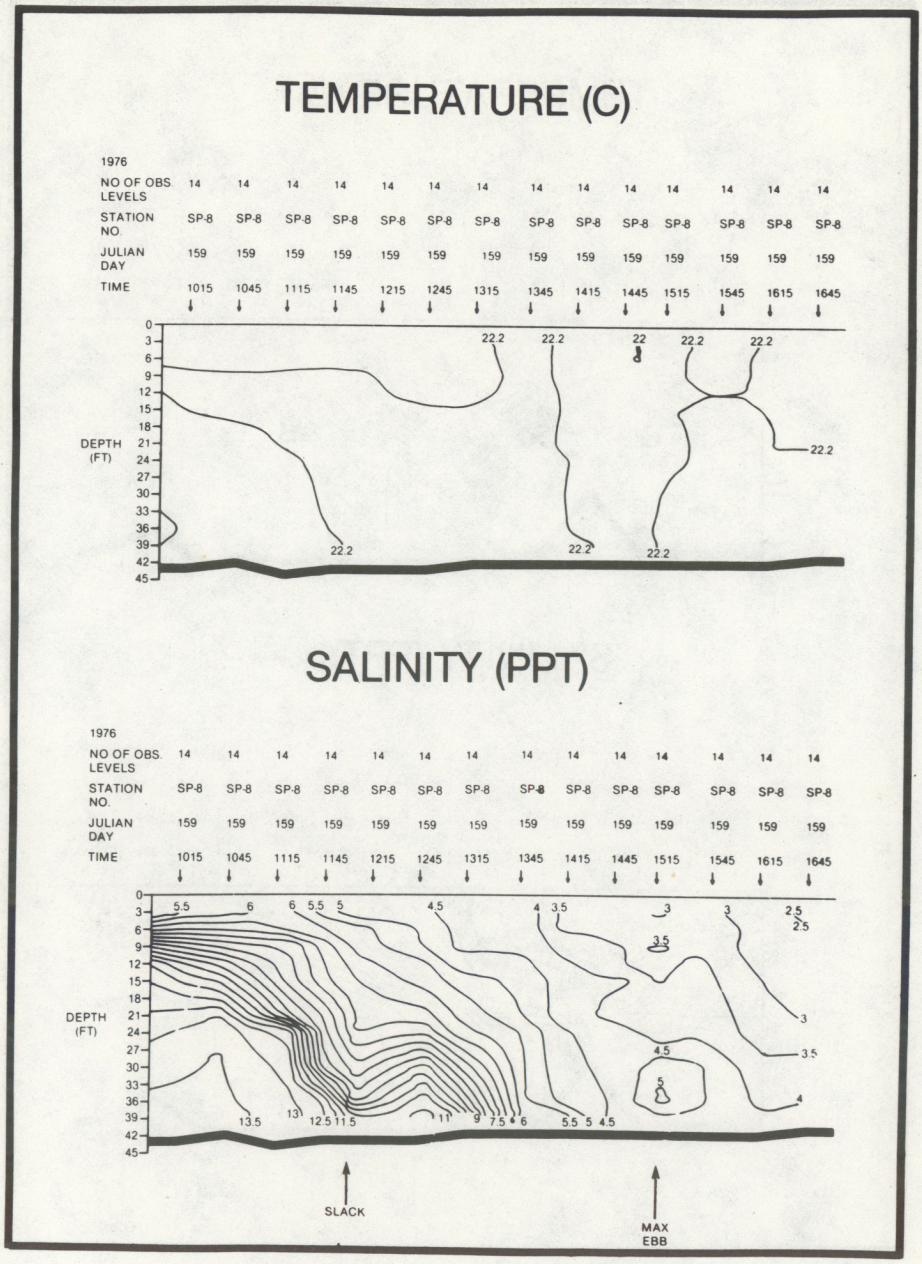

FIGURE 30a.—Temperature and salinity time series, station SP–008.

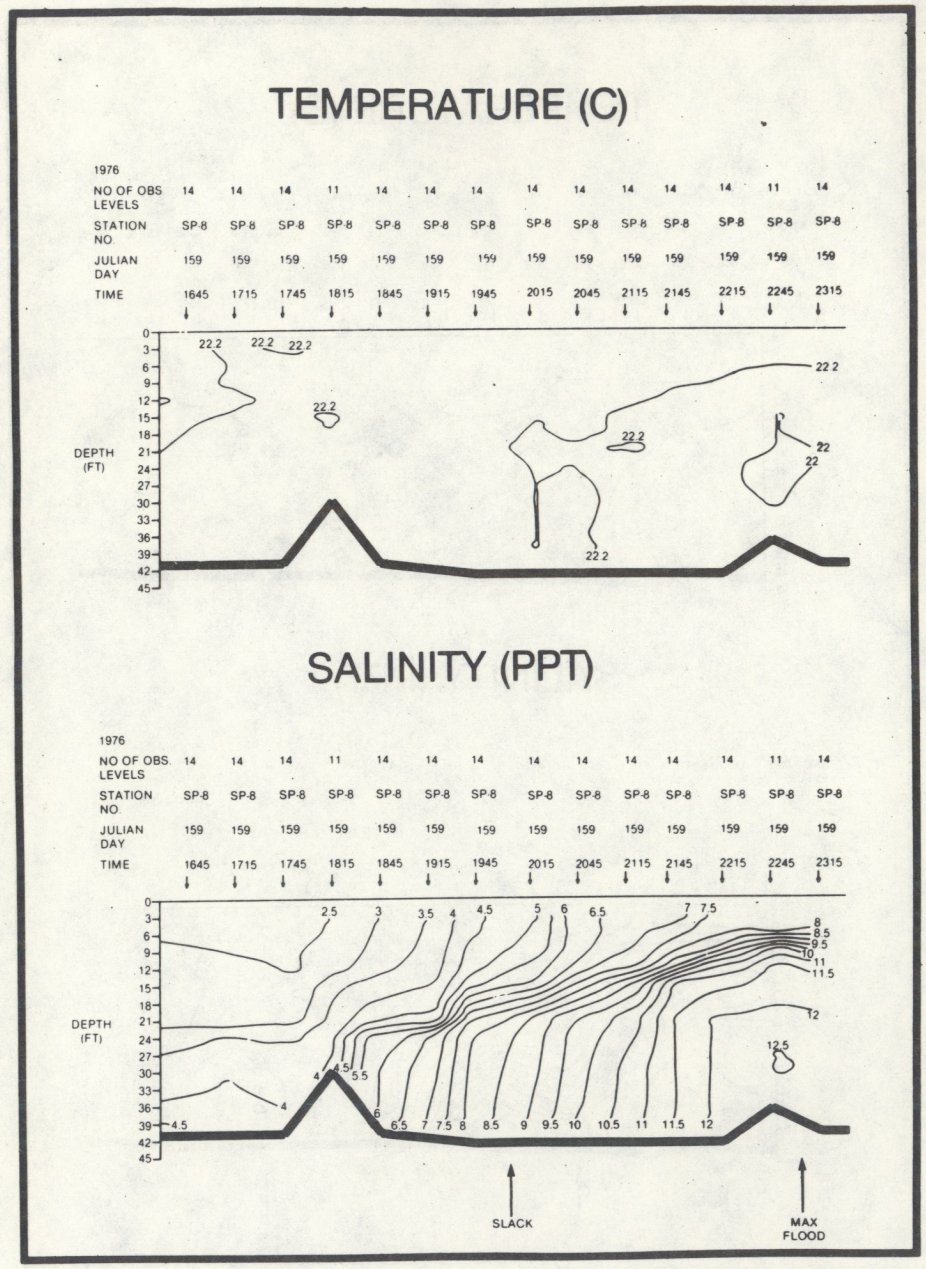

FIGURE 30b.—Temperature and salinity time series, station SP–008.

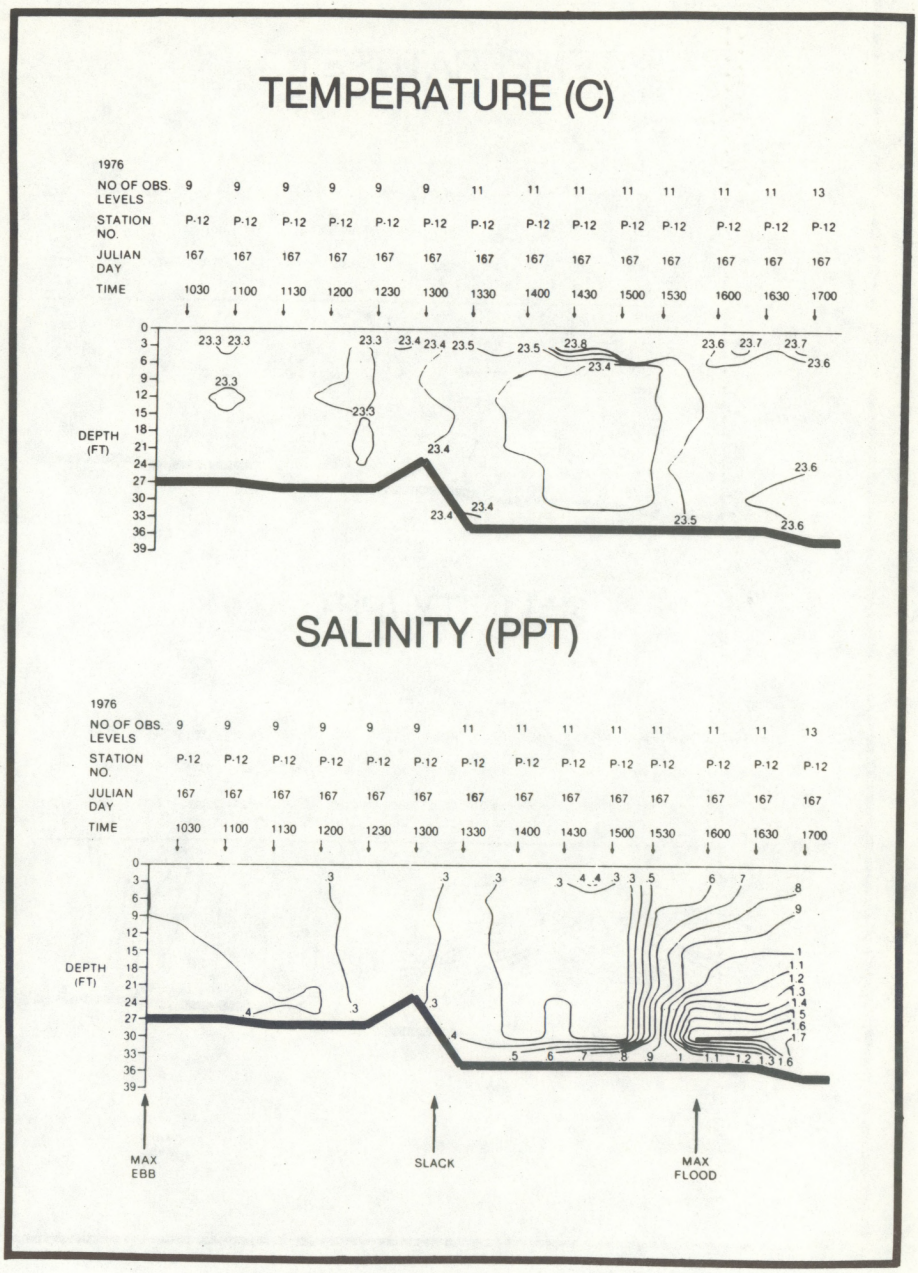

FIGURE 31a.—Temperature and salinity time series, station SP–012.

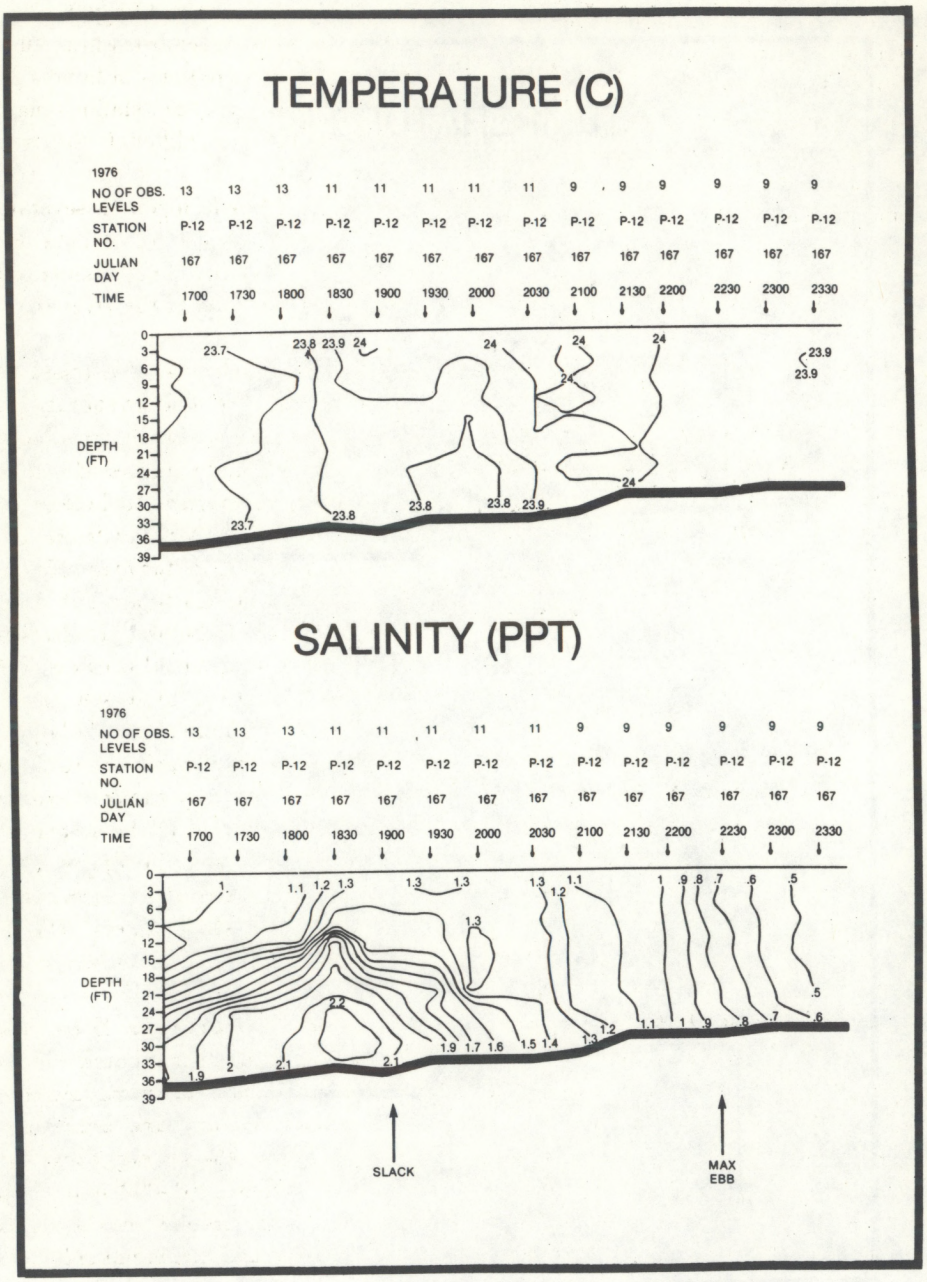

FIGURE 31b.—Temperature and salinity time series, station SP–012.

namic influences governing the flow regime in estuaries. These four influences are as follows:

1. Effect of the tide throughout the salinity intrusion length as a function of the forcing tide at the entrance.

2. Effect of gravitational forces due to density variations between freshwater from upland sources and saline water entering from the sea.

3. Gravitational forces needed to produce a net seaward transport of freshwater.

4. Coriolis forces and centrifugal forces inducing transverse fluid motion due to rotation of the Earth and due to the curvature of the estuary channel, respectively.

The Cape Fear River is narrow enough that the Coriolis forces are negligible. The river bathymetry and its geographic complexity do influence the tidal currents that will in turn affect the salinity regime.

The interaction of the freshwater and saltwater results in mixing processes that are driven by the density differences between the two waters. The density of seawater is dependent on both salinity and temperature. In estuaries with substantial river flow, the density of seawater is very dependent on the salinity regime and influenced to a lesser degree by the temperature.

Dyer (1973) states that an overmixing process is likely to be prevalent in estuaries with constricted mouths and intense tidal mixing. Intense tidal movements result in velocities that are larger than would occur in an ideal saltwedge estuary. The turbulence will mix saltwater from the lower layer into the fresh layer above and freshwater downwards. The energy for this mixing is derived from the frictional energy dissipated by the water moving across a rigid bottom.

This information concerning tidal mixing is necessary to understand the processes that influence the salinity distribution in the Cape Fear River. The river flow and tidal forces result in a vertically well-mixed estuary north of SP–003 most of the time and a partially mixed estuary south of SP–003. The recorded salinity extremes were 32.98 ppt at SP–001 (river mouth) down to 0.12 ppt at SP–015 (most northern station), and the recorded temperature extremes were 27.77°C down to 19.65°C at SP–021 (Myrtle Sound). Temperature extremes in the river itself ranged from a low of 20.66°C at SP–009 to a high of 27.56°C at SP–019. There is very little variability in the temperatures and considerable variability in the salinities for the Cape Fear River.

Station SP–009 was chosen as the seasonal station for the Cape Fear River Circulatory Survey. The salinity profiles were plotted to see if a trend did exist for the duration of the survey. As stated in section 5.1, the 10 profiles did not show any consistent trend for the 3 weeks that they covered. The casts, which were taken at slack before flood, show a top to bottom gradient variation of 1.0 ppt to 5.5 ppt and a surface variation of 1.5 ppt to 16.5 ppt.

Two facts to remember while studying the salinity and temperature contours in figures 27 and 28 are that a large distance between stations may result in unreliable contours, and although the transects were supposed to be run at slack water, it often took up to 2 hours to complete them. In several of the transects, there is some duplication of data as a result of displaying the salinity and temperature distributions over several sections of the river that have stations in common.

In figures 27a through 27g (slack before flood), the maximum surface to bottom salinity gradients occurred at the lower stations in the river and never exceeded values of 6.5 ppt. In figures 28a through 28e (slack before ebb), the surface to bottom salinity gradients were generally smaller and more uniform than the values in figures 27a through 27g, but did reach a value around 8 ppt in figure 28b around station SP–019. The surface to bottom gradients for both salinity and temperature are small because of the partially and well-mixed conditions discussed above. The salinities at slack before ebb are generally larger throughout the system than those at slack before flood. Although the water temperature may change from day to day, there is very little variation in the system at any one time.

The time series plots in figures 29 through 31 contain arrows indicating times of maximum floods, maximum ebbs, and slack waters. The plots show that maximum salinities occur either at slack water after maximum flood or within several hours preceding slack water after maximum flood. Minimum salinity values occur between maximum ebb and slack water after maximum ebb. Maximum salinities are associated with concave contours, and minimum salinities have convex contours. The salinity contours in figures 29a and 29b for station SP–002 indicate that well-mixed conditions occur around maximum flood and to a lesser extent around maximum ebb. In figures 30a and 30b, the salinity contours indicate well-mixed conditions for station SP–008 just prior to maximum ebb and partially mixed to well-mixed conditions for the remainder of the tidal cycle. The time series salinity contours for station SP–012 in figures 31a and 31b show the low salinity values and well-mixed conditions that exist north of Wilmington. Further implications of the STD results will be discussed in section 7.

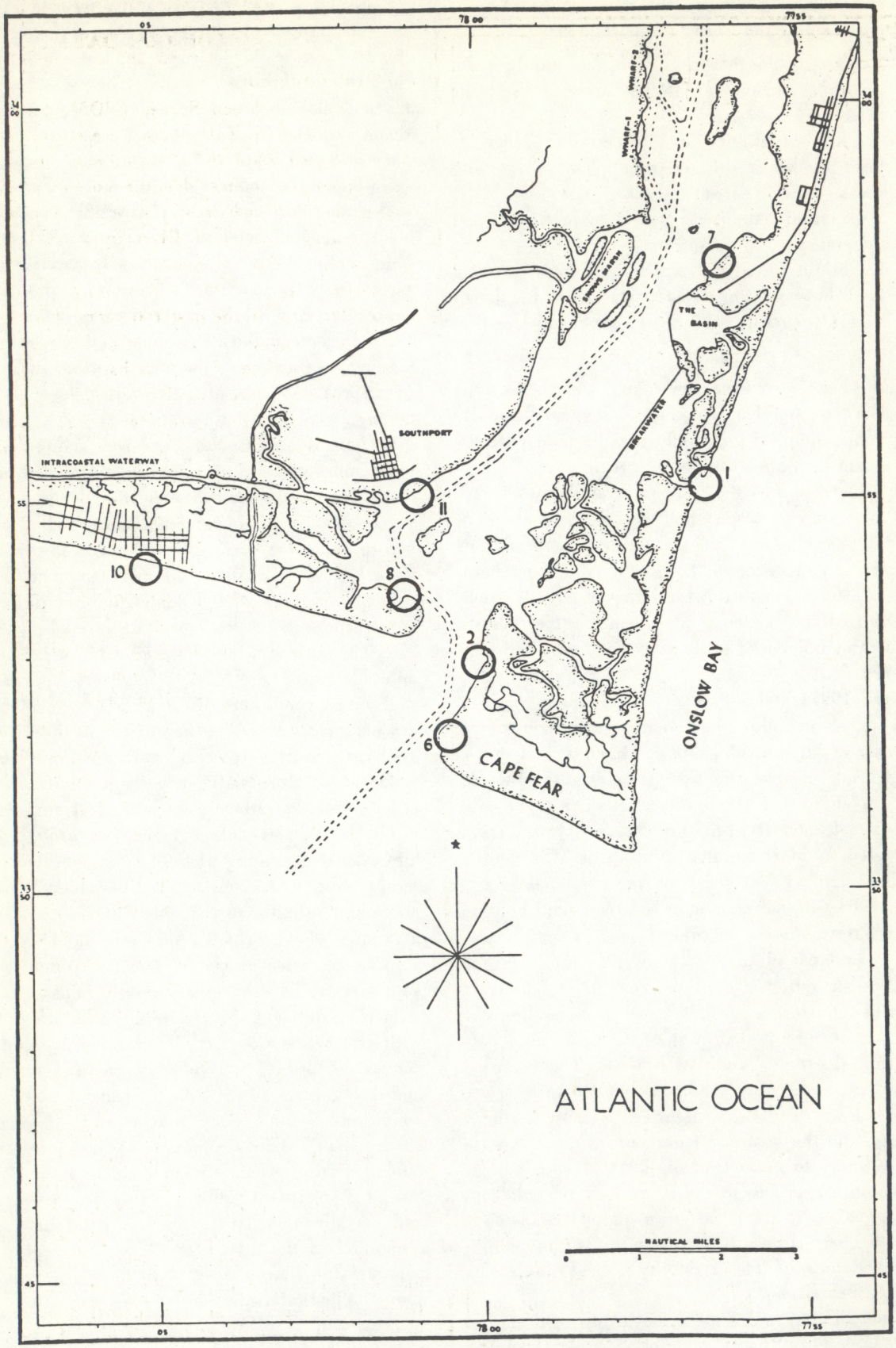

FIGURE 32.—NOS historical tide station locations.

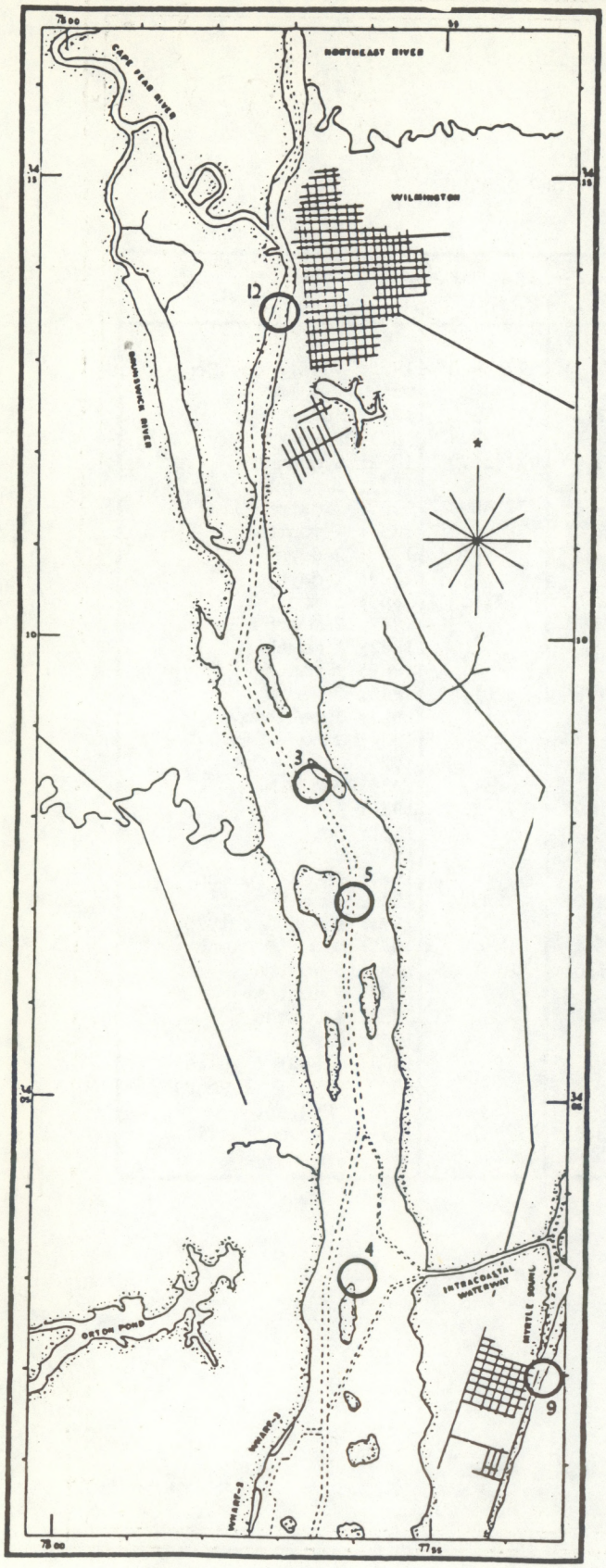

FIGURE 32.—Continued.

6. HISTORICAL DATA

6.1. Introduction

The National Ocean Survey (NOS), formerly the U.S. Coast and Geodetic Survey, created in 1807, has been responsible for the acquisition of current, tide, temperature, and salinity data for more than 170 years. This section will include what data have been collected for the lower Cape Fear River by NOS during this time period. NOS has more than 100 years of tide data, some current data, a little temperature data, and no salinity data. In the past 100 years, there has been a significant amount of dredging and channel deepening in the Cape Fear River that has resulted in physical parameter changes which will be discussed in section 7. In comparing the historical data to present data, one must consider the constantly improving state of the art of data acquisition and analysis over the past 100 years. Details concerning these historical data will be presented throughout the remainder of section 6.

6.2. Tide Data

Figure 32 shows the locations of the historical tide stations, and table 17 presents information concerning these stations. The dates of observation in table 17 may contain a few discrepancies, particularly for those data collected before 1900. The tide stations at both Wilmington and Southport have data series in excess of 19 years, which makes both stations valuable when comparing present to historical data. The various types of measuring devices used to collect the historical tide data may be found in the *Manual of Tide Observations*, Publication 30–1, 1965, or in *Tidal Datum Planes*, Special Publication 135, 1951. Predictions and mean ranges for some of these historical stations can be found in *Tide Tables, East Coast of North and South America*, published by NOS. Information concerning the availability of historical tide data may be obtained by writing to the address given in section 2.2.

6.3. Current Data

Figure 33 shows the NOS historical current station locations, and table 18 presents pertinent information concerning these locations. The data taken from the 22 stations between the years 1850 and 1853 may be of questionable quality and are therefore not included. The data from the 22 stations were probably recorded by means of Price current meters or current pole measurements. The data collected in table 18 are from a 1959 survey and were gathered by means of Roberts Radio Current Meters. None of the data series in table 18 are more than 5 days long; therefore, the

TABLE 17.—NOS historical tide data

Reference Number	Station	Latitude (N)	Longitude (W)	Dates of Observation
1	Corncake Inlet	33°55.0'	77°56.0'	1923; June, Aug, Sept, Oct
2	Baldhead Creek Ent.	33°52.7'	77°59.8'	1934; Aug - Sept
3	Lower Western Jetty	34°08.4'	77°56.8'	1873; 2 weeks
4	Orton Pt. Post Light	34°03.0'	77°56.0'	1852; 1 month 1873; 1 month
5	Campbell Is. Post Light	34°07.0'	77°56.0'	1853; 3 days
6	Baldhead, Cape Light	33°52.0'	78°00.0'	1854; 4 months 1906; 2 days 1923; 2 days
7	Federal Point	33°58.0'	77°56.0'	1865; 1 month 1879; 2 months 1882; 1 month 1889; 1 month
8	Fort Caswell	33°54.0'	78°01.0'	1865; 2 weeks 1923; June - Nov 1924; June - Dec 1925; July - Oct 1926; Jan - Mar
9	Wilmington Beach	34°01.9'	77°53.6'	1956; Aug 1972; Sept 1975; ? 1977; Feb - Present
10	Yaupon Beach	33°54.0'	78°05.0'	1973; June - Dec 1974; Jan - Apr 1975 1977; Nov - Present
11	Southport	33°55.0'	78°01.0'	1881; 5 months 1882; 4 months 1853; 4 months 1865; 2 weeks 1878 - 1883; 6 years 1933 - 1953; 21 years 1976 - Present
12	Wilmington	34°13.6'	77°57.2'	1883 - Present

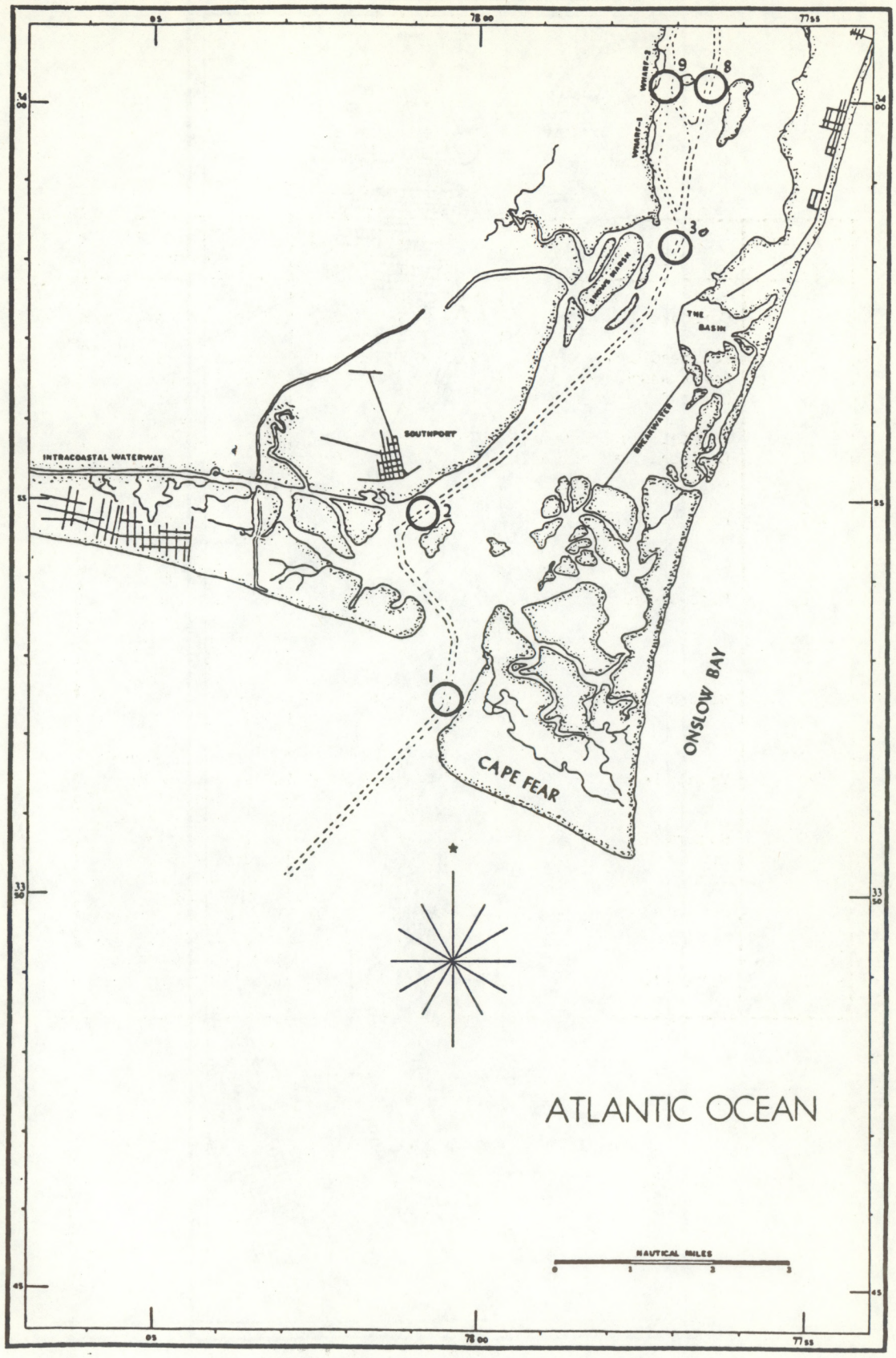

FIGURE 33.—NOS historical tidal current station locations.

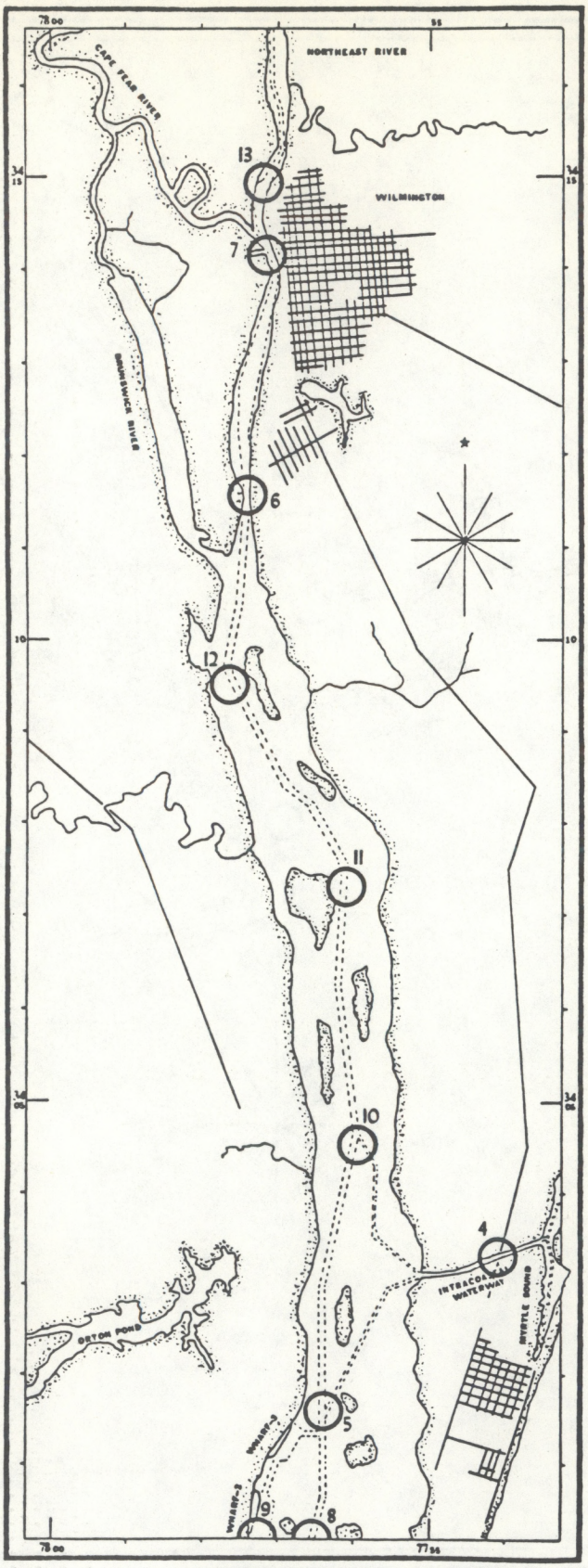

FIGURE 33.—Continued.

TABLE 18.—NOS historical tidal current data

Ref. No.	Station	Latitude (N)	Longitude (W)	Dates of Observation	Days Data	Depths[2] (Feet)	Method of Observation
1	Baldhead	33°52.4'	78°00.4'	May 1959	5	6,16,26	RRCM[3]
2	Southport	33°55.1'	78°00.6'	May 1959	5	6,16,26	RRCM
3	Horseshoe Shoal	33°58.1'	77°57.0'	May 1959	5	6,16,26	RRCM
4	Snows Cut Bridge	34°03.3'	77°54.1'	May 1959	3	+10	RRCM
5	Upper Midnight Channel	34°01.7'	77°56.4'	May 1959	5	6,16,26	RRCM
6	Forth East Jetty Channel 0.5 miles SSE of Dram Tree Pt.	34°11.5'	77°57.4'	May 1959	5	6,16,26	RRCM
7	Wilmington	34°14.2'	77°57.1'	May 1959	5	6,22,36	RRCM
8	Lower Midnight Channel 0.6 miles E. of Reaves Pt.	34°00.3'	77°56.6'	May 1959	5	6,16,26	RRCM
9	Reaves Pt, 0.3 miles N. of	34°00.3'	77°57.2'	May 1959	5	6,16,26	RRCM
10	Lower Lilliput Channel 0.5 miles NW. of Doctor Pt.	34°04.4'	77°56.0'	May 1959	5	6,16,26	RRCM
11	Keg Island Channel East of Campbell Island	34°07.3'	77°56.2'	May 1959	5	6,16,26	RRCM
12	Lower Brunswick Channel	34°09.4'	77°57.6'	May 1959	5	6,16,26	RRCM
13	Turning Basin	34°15.0'	77°57.1'	May 1959	5	6,16,25	RRCM
-	22 Stations[1]	-	-	1850-1853	-	-	-

[1]There were 22 short-term current stations between 1850 and 1853.

[2]The depths are in feet below surface except for reference number 4 which is feet above bottom.

[3]RRCM stands for Roberts Radio Current Meter.

data cannot be harmonically analyzed. The data were analyzed by nonharmonic rotary reductions. Information concerning these methods of current measurement is available in the *Manual of Current Observations*, Special Publication 215, 1950. Predictions and mean values for some of these historical current stations can be found in *Tidal Current Tables, Atlantic Coast of North America*, published by NOS. The data in table 18 are available from the address listed in section 2.2.

6.4. Temperature and Density Data

No salinity observations have been made by NOS in the Cape Fear River prior to this survey, but surface temperature and density measurements were made at the tide station at Southport between 1946 and 1954. The measurements were made once each weekday with a thermometer and several hydrometers. The results of the measurements can be found in *Surface Water Temperature and Density, Atlantic Coast, North and South America*, NOS Publication 31–1, 1972. The publication provides the average mean, maximum, minimum, mean maximum, and mean minimum temperatures and densities of the surface water for each month and for the duration of the data series. These data do provide valuable information concerning the seasonal variations in temperature and density.

7. CONCLUSIONS AND IMPLICATIONS OF RESULTS

The historical tide data reflect the significant changes that have taken place in the tidal regime as a result of the navigational improvements outlined in table 1. By comparing the historical tide data from Southport and Wilmington to the present data, one can see the increase in the mean tidal range (*Mn*) as a result of the increased channel depths. By increasing the depth, more water is allowed to enter the estuary, resulting in less energy being lost owing to bottom friction, thus allowing for a greater tidal range. By increasing the depth, there is less wave damping. The same phenomenon has taken place in the Delaware River. The mean range increased at Wilmington from 2.55 ft in 1908 to 4.20 ft in 1976, and the mean range increased at Southport from 4.12 ft in 1933 to 4.26 ft in 1976. Further evidence of the increase in tidal range is the increase in the M_2 amplitudes at the two stations. The M_2 amplitude at Wilmington increased from 1.12 ft in 1887 to 1.96 ft in 1976, and increased at Southport from 1.96 ft in 1940 to 2.02 ft in 1976. In 1938, the epoch differences between Southport and Wilmington for M_2 was 69° compared to 55° in 1976. The increase in depth resulted in an increase in rate of travel of the tidal wave, the rate of travel being directly proportional to the water depth.

A pure progressive tidal wave is one whose tide and tidal current epochs are identical. This would indicate that maximum current velocities occur at high and low tides. The tidal wave in the Cape Fear River is close to a pure damped progressive wave, not a pure progressive wave. The tidal wave cannot be classified as a pure damped progressive wave because of the partial reflection in the narrowing channel around Wilmington which results in some modification south of Wilmington. Common harmonic constituents for the tide and tidal currents for 1976 exist only at Southport (T–02, C–002) and Wilmington (T–11, C–011). The distance between these two locations is 21.2 nmi or about 90 percent of the study area. The tide station at Wilmington is about 0.5 nmi south of the current station, and the two stations at Southport are at the same location.

At Southport, the average M_2 tidal current epoch precedes the M_2 tidal epoch by 38°, and at Wilmington the same tidal current epoch precedes the tidal epoch by 37°. The average K_1 tidal current epoch precedes the K_1 tidal epoch by 64° at Southport and 48° at Wilmington. At Southport, the M_2 tidal current is preceding (leading) the M_2 tide by 1.3 hours, and at Wilmington the value is 1.3 hours. The K_1 tidal current is leading the K_1 tide by 4.2 hours at Southport and 3.2 hours at Wilmington.

In 1976, the M_2 tidal epoch difference between Southport and Wilmington was 55°, and the corresponding average tidal current epoch difference was 57°. The K_1 tidal epoch difference was 29°, and the average K_1 tidal current epoch difference was 44°. The M_2 epoch rate of change is very similar for the tide and tidal current, 2.6°/nmi and 2.7°/nmi respectively. The K_1 epoch rate of change is greater for the tidal current than for the tide, 2.1°/nmi compared to 1.4°/nmi.

Another method used to investigate the relationship between the tides and tidal currents was comparing the time differences between the high water intervals and low water intervals in table 7 to the corresponding surface flood strength times and ebb strength times in table 13. The flood strength times preceded the tidal high water times by an average of 1.9 hours, and the ebb strength times preceded the tidal low water times by an average of 1.7 hours. The only areas where the tide preceded the tidal current were Snows Cut and Myrtle Sound, which shows the influence of the tidal flow through Carolina Beach Inlet.

The results of the harmonic constituent epoch differences between Southport and Wilmington, and the differences between the tidal high and low water intervals and the times of maximum floods and ebbs indicate that the tidal wave in the Cape Fear River is much closer to being a pure damped progressive wave than a standing wave, with maximum tidal current velocity times preceding the times of high and low waters by less than 2 hours. The differences in time between the tidal currents and tides are not uniform over the river. Geographic features, river bathmetry, and adjacent bodies of water affect the tides and tidal currents differently.

A simple model used to explain the tidal hydrodynamics of the Cape Fear River system, based on incident and reflected tidal waves undergoing exponential damping, provided some insight as to why the mean tidal range decreases from the mouth of the river preceding north to a point around MOTSU Wharf No. 1 (T–19) and then increases going up the river to Wilmington (T–11). The model developed by Redfield (1950) and others, and modified by Parker (1979) to include the effects of a percentage energy loss at the point of reflection, is valuable in the study of long narrow estuaries, because geographical dimensions are eliminated by specifying distance in terms of fractions of a tidal wavelength. This model requires prior knowledge of the tidal harmonic constituents (M_2 for the Cape Fear River) for they are used as data input into the computer program.

Figure 20 shows the results of the model with 80 percent of the damped progressive incident tidal wave being reflected in the vicinity of Wilmington back down the river. The high damping coefficient indicates that the reflected wave amplitude decreases rapidly relative to the incident wave amplitude. There are no nodal points in the river, because only 20 percent of the M_2 tidal wave and 10 percent of the K_1 tidal wave can fit into the Cape Fear River.

The tide and tidal current data indicate that the flow regime in the Cape Fear River is dependent on the maintained main navigational channel. The cross sections in figure 4 show that outside of the main channel the river depths rarely exceed 4 to 8 ft. The results from program ROTARY in table 13 indicate that the flood and ebb directions at each station generally coincide with the channel orientation at each station. An interesting flow situation exists because of the complex channel configuration around MOTSU (Wharfs No. 1, 2, and 3). Flow through the main channel is diverted through three smaller connecting channels to the area contiguous to the wharfs. The decreased velocities in the secondary channels combined with their orientation have resulted in major siltation and shoaling problems that are presently under investigation by the U.S. Army Corps of Engineers. The Intracoastal Waterway at both Southport and Snows Cut is influenced not only by the river flows but also by the adjacent bodies of water. The power spectrum plots of the original tidal current data series in figure 25c show how the narrow shallow Intracoastal Waterway enhances the shallow water higher harmonic constituents.

Although the values are rather rough, the volume transport figures in table 14 indicate the relative magnitudes of the flow volumes during average flood and ebb cycles at several points in the Cape Fear River. The six cross sections are at Southport (C–002), 0.6 miles north of Doctor Point (C–007), the mouth of the Brunswick River (C–017), Wilmington (C–011), 1.1 mi west of Southport in the Intracoastal Waterway (C–021), and Snows Cut (C–013). The flood volume at Wilmington is 15 percent of that at Southport, and the ebb volume is about 13 percent of that at Southport. The Brunswick River which does not have a maintained channel and is relatively shallow, has a flood volume that is 35 percent of that at Wilmington, and an ebb volume that is 50 percent of that at Wilmington. The volume transport through Snows Cut and the Intracoastal Waterway at Southport is similar during the ebb cycle, but the volume transport during the flood cycle at the Intracoastal Waterway at Southport is only about 62 percent of that at Snows Cut.

When discussing the harmonic constituents, "ages" of the tides and currents, power spectrum plots, and the various ratios of the constituent amplitudes, the single most important factor is the strength of the M_2 constituent. The M_2 constitutent dominates both the tides and currents, but particularly the tides where the M_2 amplitude is generally about five times that of the next largest constituent, N_2, and six to eight times the value of the largest diurnal constituent, K_1. The morphology of the river basin has a greater effect on the tidal currents than on the tides which results in more variability in the tidal current parameters than in the tidal parameters.

The K_1 to M_2 ratio for the tides is about 0.13 over the river; the corresponding ratio for the tidal currents varies from 0.08 at Southport to 0.12 at Wilmington. The ratio of the (K_1+O_1) range to the (M_2+S_2) range is used by NOS to define the

"type of tide," and the ratio is less than 0.25 for both the tides and tidal currents indicating that the system is semidiurnal with two cycles a day, with both high waters and both low waters (and corresponding tidal currents) having about the same values. The (K_1+O_1) to (M_2+S_2) ratio values for Snows Cut and Myrtle Sound are slightly larger than the ratio values for the rest of the study area. The S_2 to M_2 ratio for the tides decreases going up the river, and the S_2 to M_2 ratio for the tidal currents decreases going down the river with the tidal current ratio undergoing a greater change than the tidal ratio. The N_2 to M_2 ratio is reasonably steady for both the tides and tidal currents with values ranging from 0.19 to 0.21 for both parameters. The O_1 to K_1 ratio for the tides does not show any positive trend; for the tidal currents, the ratio is larger at Wilmington than at Southport. The "ages of the tide" (phase, parallax, and diurnal) do not appear to contain any significant trends except for the phase age, which increases going up the river. As pointed out in section 4, the lack of a sufficient number of long-term tidal current stations means that there are not enough stations for which harmonic constituents could be computed to establish definite conclusions (trends) concerning the changing tidal current characteristics over the study area.

The shallow water constituents, M_4 and M_6, have increased amplitudes as a result of the crest of the tidal wave moving faster than the trough of the wave in shallow water. When the M_4 and M_6 amplitudes become sufficiently large with respect to the M_2 amplitude, the cosine form of the tidal wave will become distorted. Both the M_4 and M_6 tidal amplitudes increase going up the river, but it is only in the upper portion of the study area that the higher harmonic amplitudes are of sufficient size with respect to the M_2 amplitude to cause any significant distortion of the tidal curve.

Interesting results were obtained by comparing the nontidal time series derived from the Doodson-filtered original data series for Wilmington (T–11) and Southport (T–02) to wind and barometric pressure data collected during the same period. The meteorological data show that wind shifts generally occur during periods of pressure transitions from high to low or low to high. The wind data in figure 18 show that the wind is blowing principally in either a northerly or southerly direction for the time period covering the circulatory survey. From 14 May 1976 to 8 June 1976, the nontidal flow direction corresponded extremely well with the predominant wind direction. Each time the wind shifted during that time period, the direction of nontidal flow shifted accordingly. When the winds were from the south, the nontidal direction of flow was to the north (a nontidal rise in water surface elevation), and when the winds were from the north, the nontidal direction of flow was to the south. The length of the time interval that the wind would blow in a principal direction does not appear to be related to the rate of travel of the nontidal flow. Results in table 8 show that the nontidal rate of travel varied from a minimum of 0.9 kn during the time period, 14 to 23 May, to a maximum of 3.5 kn during the time period, 23 to 29 May. No effort has been made to correlate the magnitude of the wind speed and the barometric pressure to the nontidal wave parameters. The largest recorded nontidal amplitude for Wilmington was 0.66 ft below the mean water level on 22 May, and for Southport was 0.75 ft below the mean water level on 21 May.

The salinity and temperature contours presented in figures 27 through 31 are for longitudinal transects and time series stations. The contours permit the analysis of the flow regime in the Cape Fear River estuary, which is dependent upon several dynamic influences. The dynamic influences include salinity intrusion as a result of the tidal forcing function, density variations between the salinity intrusion and the river freshwater runoff, and the gravitational forces that produce a net seaward transport of freshwater. The mixing process at any one time is therefore a result of the tidal forcing function and the river freshwater runoff. The meteorological forces of wind and barometric pressure will also influence mixing to a lesser degree.

The salinity and temperature data collected in May and June of 1976 indicate that the portion of the Cape Fear River north of station SP–003 covered by the circulatory survey is vertically well mixed most of the time with little variability in the water temperature and progressively decreasing salinity values going up the river. South of station SP–003, the river is generally partially mixed. The salinity values range from around 33 ppt at the river mouth down to less than 1 ppt north of Wilmington. The time series plots in figures 29 through 31 indicate a maximum surface to bottom salinity gradient of around 5 ppt at Southport, 8 ppt at Campbell Island, and 1 ppt at those stations north of Wilmington.

ACKNOWLEDGMENTS

The authors wish to extend their gratitude to the personnel of the Tides and Water Levels Division and the Circulatory Surveys Branch for their participation in the processing of the 1976 NOS tide, current, salinity, and temperature data used in this report. The NOAA Ship FERREL under the command of NOAA Corps Officer, Cdr. Roy Matsushige, collected all of the current, salinity, and temperature data and most of the tide data. Personnel from the Wilmington District of the U.S. Army Corps of Engineers were responsible for the installation of the tide gages around MOTSU. The Carolina Power and Light Company in Raleigh, N.C., furnished the wind and barometric pressure data. Gina Stoney typed the original manuscript and all of the tables for this report.

REFERENCES

ANONYMOUS.
1957. Cape Fear River basin pollution survey report. N.C. State Stream Sanitat. Comm., Rep. No. 6, 613 p.

CAROLINA POWER AND LIGHT COMPANY.
1976. Environmental monitoring system. Carolina Power and Light Co., Raleigh, N.C., Unpubl. data, 16 p.

DEFANT, ALBERT.
1961. Physical oceanography, Vol. 2. MacMillan Co., N.Y., 598 p.

DENNIS, R. E., AND E. E. LONG.
1971. A user's guide to a computer program for harmonic analysis of data at tidal frequencies. U.S. Dep. Commer., NOAA Tech. Rep. NOS 41, 31 p.

DOODSON, A. T., AND H. D. WARBURG.
1941. Admiralty manual of tides. Hydrographic Dep., Admiralty, London, p. 176–182.

GROVES, G. W.
1955. Numerical filters for discrimination against tidal periodicities. Trans. Am. Geophy. Union 36(6):1073–1084.

HARRIS, D. L., N. A. PORE, AND R. CUMMINGS.
1963. The application of high speed computers to practical tidal problems. *In* Abstracts of papers, p. 16 Internatl. Union Geodesy Geophy., 13th Gen. Assembly, Vol. 6, Berkeley.

HICKS, STEACY D.
1964. Tidal wave characteristics of Chesapeake Bay. Chesap. Sci. 5(3):103–113.

IPPEN, A. T.
1966. Salinity intrusion in estuaries. *In* Arthur T. Ippen (editor), Estuary and coastline hydrodynamics, p. 599. McGraw-Hill Book Co., Inc., N.Y.

JACOBSON, STEPHEN R., AND ALAN HERMAN.
1972. FESTSA, a system for time series analysis. U.S. Dep. Commer., NOAA, Natl. Ocean Surv., 256 p.

MARMER, H. A.
1951. Tidal datum planes, U.S. Coast and Geodetic Surv. Spec. Publ. No. 135, 142 p.

PARKER, BRUCE B.
1975. CURNT. U.S. Dep. Commer., NOAA, Natl. Ocean Surv., Oceanogr. Div., Rockville, Md., Unpubl. manuscr.
1977a. Tidal hydrodynamics in the Strait of Juan de Fuca–Strait of Georgia. U.S. Dep. Commer., NOAA Tech. Rep. NOS 69, 56 p.
1977b. ROTARY. U.S. Dep. Commer., NOAA, Natl. Ocean Surv., Oceanogr. Div., Rockville, Md., Unpubl. manuscr.
1979. Investigative analytical models for tidal hydrodynamics in a long narrow deep bay. U.S. Dep. Commer., NOAA, Natl. Ocean Surv., Rockville, Md., Unpubl. manuscr.

PATCHEN, RICHARD C.
1975. CONTPR. U.S. Dep. Commer., NOAA, Natl. Ocean Surv., Oceanogr. Div., Rockville, Md., Unpubl. manuscr.

REDFIELD, ALFRED.
1950. The analysis of tidal phenomena in narrow embayments. Pap. Phys. Oceanogr. Meteorol. 11(4):2–37.

SCHUREMAN, PAUL.
1958. Manual of harmonic analysis and prediction of tides. U.S. Coast and Geodetic Surv., Spec. Publ. No. 98, 317 p.

U.S. ARMY CORPS OF ENGINEERS.
1976. A feasibility study on reducing maintenance dredging costs at the Military Ocean Terminal, Sunny Point. Unpubl. manuscr., p.1–16.

U.S. COAST AND GEODETIC SURVEY.
1950. Manual of current observations, *Its* Spec. Publ. No. 215, 87 p.
1952. Manual of harmonic constant reductions. *Its* Spec. Publ. No. 260, 74 p.
1965. Manual of tide observations. *Its* Publ. 30–1, 72 p.

U.S. DEPARTMENT OF COMMERCE
1853–1976. Tide tables, east coast of North and South America. NOAA, Natl. Ocean Surv., various issues.
1890–1976. Tidal current tables, Atlantic coast of North America. NOAA, Natl. Ocean Surv., various issues.

1972. Surface water temperature and density, Atlantic coast, North and South America. NOS Publ. 31–1, 109 p.
1976. Cape Fear River. NOAA, NOS nautical chart 11537.

ZETLER, BERNARD D.
1959. Tidal characteristics from harmonic constants. J. Hydraulics Div. 85 (HY12):77–87.

☆ U.S. GOVERNMENT PRINTING OFFICE: 1979 –281–067/247

(Continued from inside front cover)

NOS 55 A mathematical model for the simulation of a photogrammetric camera using stellar control. Chester C. Slama, December 1972. (COM-73-50171)

NOS 56 Cholesky factorization and matrix inversion. Erwin Schmid, March 1973. (COM-73-50486)

NOS 57 Complete comparator calibration. Lawrence W. Fritz, July 1973. (COM-74-50229)

NOS 58 Telemetering hydrographic tide gauge. Charles W. Iseley, July 1973. (COM-74-50001)

NOS 59 Gravity gradients at satellite altitudes. B. Chovitz, J. Lucas, and F. Morrison, November 1973. (COM-74-50231)

NOS 60 The reduction of photographic plate measurements for satellite triangulation. Anna-Mary Bush, June 1973. (COM-73-50749)

NOS 61 Radiation pressure on a spheroidal satellite. James R. Lucas, July 1974. (COM-74-51195/AS)

NOS 62 Earth's gravity field and station coordinates from Doppler Data, Satellite Triangulation, and Gravity Anomalies. Karl-Rudolf Koch, February 1974. (COM-74-50490/AS)

NOS 63 World maps on the August epicycloidal conformal projection. Erwin Schmid, May 1974. (COM-74-11746/AS)

NOS 64 Variability of tidal datums and accuracy in determining datums from short series of observations. Robert Lawrence Swanson, October 1974. (COM-75-10275)

NOS 65 NGS-1. The statistics of residuals and the detection of outliers. Allen J. Pope, May 1976, 133 pp. (PB258428)

NOS 66 NGS-2. Effect of geoceiver observations upon the classical triangulation network. Robert E. Moose, and Soren W. Henriksen, June 1976, 65 pp. (PB260921)

NOS 67 NGS-3. Algorithms for computing the geopotential using a simple-layer density model. Foster Morrison, March 1977, 41 pp. (PB266967)

NOS 68 NGS-4. Test results of first-order class III leveling. Charles T. Whalen and Emery Balazs, November 1976, 30 pp. (PB265421)

NOS 69 Tidal hydrodynamics in the Strait Juan de Fuca - Strait of Georgia. Bruce B. Parker, January 1977, 56 pp. (PB270191)

NOS 70 NGS-5. Selenocentric geodetic reference system. Frederick J. Doyle, A. A. Elassal, and J. R. Lucas, February 1977, 53 pp. (PB266046)

NOS 71 NGS-6. Application of digital filtering to satellite geodesy. C. C. Goad, May 1977, 73 pp. (PB270192)

NOS 72 NGS-7. Systems for the determination of polar motion. Soren W. Henriksen, May 1977, 55 pp. (PB274698/AS)

NOS 73 NGS-8. Control leveling. Charles T. Whalen, May 1978, 23 pp. (PB286838)

NOS 74 NGS-9. Survey of the McDonald Observatory radial line scheme by relative lateration techniques. William E. Carter and T. Vincenty, June 1978, 33 pp. (PB287427)

NOS 75 NGS-10. An algorithm to compute the eigenvectors of a symmetric matrix. E. Schmid, August 1978, 5 pp. (PB287923)

NOS 76 NGS-11. The application of multiquadric equations and point mass anomaly models to crustal movement studies. Rolland L. Hardy, November 1978, 63 pp. (PB293544)

NOS 77 Numerical simulation of sedimentation and circulation in rectangular marina basins. David R. Askren, January 1979, 137 pp. (PB294107)

NOS 78 Wave sensors survey. Richard L. Ribe, July 1979.

NOS 79 NGS-12. Optimization of horizontal control networks by nonlinear programming. Dennis Milbert, August 1979.

NOAA SCIENTIFIC AND TECHNICAL PUBLICATIONS

The National Oceanic and Atmospheric Administration was established as part of the Department of Commerce on October 3, 1970. The mission responsibilities of NOAA are to assess the socioeconomic impact of natural and technological changes in the environment and to monitor and predict the state of the solid Earth, the oceans and their living resources, the atmosphere, and the space environment of the Earth.

The major components of NOAA regularly produce various types of scientific and technical information in the following kinds of publications:

PROFESSIONAL PAPERS — Important definitive research results, major techniques, and special investigations.

CONTRACT AND GRANT REPORTS — Reports prepared by contractors or grantees under NOAA sponsorship.

ATLAS — Presentation of analyzed data generally in the form of maps showing distribution of rainfall, chemical and physical conditions of oceans and atmosphere, distribution of fishes and marine mammals, ionospheric conditions, etc.

TECHNICAL SERVICE PUBLICATIONS — Reports containing data, observations, instructions, etc. A partial listing includes data serials; prediction and outlook periodicals; technical manuals, training papers, planning reports, and information serials; and miscellaneous technical publications.

TECHNICAL REPORTS — Journal quality with extensive details, mathematical developments, or data listings.

TECHNICAL MEMORANDUMS — Reports of preliminary, partial, or negative research or technology results, interim instructions, and the like.

Information on availability of NOAA publications can be obtained from:

ENVIRONMENTAL SCIENCE INFORMATION CENTER (D822)
ENVIRONMENTAL DATA AND INFORMATION SERVICE
NATIONAL OCEANIC AND ATMOSPHERIC ADMINISTRATION
U.S. DEPARTMENT OF COMMERCE

6009 Executive Boulevard
Rockville, MD 20852

NOAA--S/T 78-418